FOR OFFICIAL USE ONLY

JPRS L/8321

8 March 1979

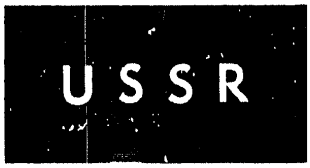

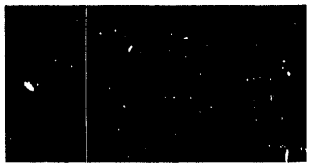

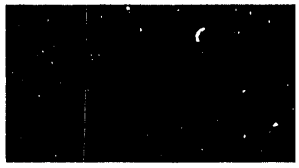

TRANSLATIONS ON USSR SCIENCE AND TECHNOLOGY
PHYSICAL SCIENCES AND TECHNOLOGY
(FOUO 14/79)

U. S. JOINT PUBLICATIONS RESEARCH SERVICE

FOR OFFICIAL USE ONLY

APPROVED FOR RELEASE: 2007/02/08: CIA-RDP82-00850R000100030024-1

NOTE

JPRS publications contain information primarily from foreign newspapers, periodicals and books, but also from news agency transmissions and broadcasts. Materials from foreign-language sources are translated; those from English-language sources are transcribed or reprinted, with the original phrasing and other characteristics retained.

Headlines, editorial reports, and material enclosed in brackets [] are supplied by JPRS. Processing indicators such as [Text] or [Excerpt] in the first line of each item, or following the last line of a brief, indicate how the original information was processed. Where no processing indicator is given, the information was summarized or extracted.

Unfamiliar names rendered phonetically or transliterated are enclosed in parentheses. Words or names preceded by a question mark and enclosed in parentheses were not clear in the original but have been supplied as appropriate in context. Other unattributed parenthetical notes within the body of an item originate with the source. Times within items are as given by source.

The contents of this publication in no way represent the policies, views or attitudes of the U.S. Government.

APPROVED FOR RELEASE: 2007/02/08: CIA-RDP82-00850R000100030024-1

BIBLIOGRAPHIC DATA SHEET	1. Report No. JPRS L/ 8321	2.	3. Recipient's Accession No.
4. Title and Subtitle TRANSLATIONS ON USSR SCIENCE AND TECHNOLOGY - PHYSICAL SCIENCES AND TECHNOLOGY, (FOUO 14/79)			5. Report Date 8 March 1979 6.
7. Author(s)			8. Performing Organization Rept. No.
9. Performing Organization Name and Address Joint Publications Research Service 1000 North Glebe Road Arlington, Virginia 22201			10. Project/Task/Work Unit No. 11. Contract/Grant No.
12. Sponsoring Organization Name and Address As above			13. Type of Report & Period Covered 14.

15. Supplementary Notes

16. Abstract

The report contains information on aeronautics; astronomy and astrophysics; atmospheric sciences; chemistry; earth sciences and oceanography; electronics and electrical engineering; energy conversion; materials; mathematical sciences; cybernetics, computers; mechanical, industrial, civil, and marine engineering; methods and equipment; missile technology; navigation, communications, detection, and countermeasures, nuclear science and technology; ordnance; physics; propulsion and fuels; space technology; and scientists and scientific organization in the physical sciences.

17. Key Words and Document Analysis. 17a. Descriptors

USSR
Aeronautics
Astronomy
Astrophysics
Atmospheric Sciences
Chemistry
Computers
Cybernetics
Earth Sciences
Oceanography
Electronics
Electrical Engineering
Energy Conversion
Materials
Mathematics
Mechanical Engineering
Civil Engineering
Industrial Engineering
Marine Engineering
Methods
Equipment
Missile Technology
Navigation and Communications
Detection and Countermeasures
Nuclear Science and Technology
Ordnance
Physics
Propulsion and Fuels
Space Technology

17b. Identifiers/Open-Ended Terms

17c. COSATI Field/Group 01,03,04,07,08,09,10,11,12,13,14,16,17,18,19,20,21,22

18. Availability Statement	19. Security Class (This Report)	21. No. of Pages
For Official Use Only. Limited Number of Copies Available From JPRS	UNCLASSIFIED	116
	20. Security Class (This Page) UNCLASSIFIED	22. Price

THIS FORM MAY BE REPRODUCED

USCOMM-DC 14952-P72

JPRS L/8321

8 March 1979

TRANSLATIONS ON USSR SCIENCE AND TECHNOLOGY
PHYSICAL SCIENCES AND TECHNOLOGY

(FOUO 14/79)

CONTENTS

PAGE

ELECTRONICS AND ELECTRICAL ENGINEERING

Nuclear Power Generating Units With RBMK-1000 Reactors Described, Evaluated
(L. M. Voronin; ELEKTRICHESKIYE STANTSII, No 1, 1979) 1

A Method of Interchannel Synchronization in the Playback of a Multichannel Recording of a Wideband Signal With Frequency Division
(A. I. Grechikhin; RADIOTEKHNIKA, Nov 78) 13

Filtering Discrete Multifrequency Signals in Nongaussian Interference
(I. M. Pyshkin, et al.; RADIOTEKHNIKA, Nov 78) 20

A Shield in the Shape of a Double Ring To Shield Antennas Against Interference
(Yu. M. Mel'nikov; RADIOTEKHNIKA, Nov 78) 31

The Structure of a Receiver and the Optimum Detection Characteristics for Signals With a Random Initial Phase, Amplitude and Duration
(G. D. Filin; RADIOTEKHNIKA, Nov 78) 38

The Application of the Methods of Games Theory to the Recognition of the Signals of a Source Where Transforming Type Interference Is Present in the Channel
(Yu. P. Kuznetsov; RADIOTEKHNIKA, Nov 78) 43

A Quantitative Evaluation of the Economic Engineering Efficiency of Discontinuous Communications Service
(F. F. Yurlov, L. A. Roshdestvenskaya; RADIOTEKHNIKA, Nov 78) 49

CONTENTS (Continued)

Page

Equivalent Parameters of Gunn Diode in Two-Frequency Mode
(A. S. Kosov, I. A. Strukov; RADIOTEKHNIKA I ELEKTRONIKA, No 10, 1978) 57

Principles of Miniaturization of Passive Microwave Strip Elements
(Ye. L. Bachinina, et al.; RADIOTEKHNIKA I ELEKTRONIKA, Aug 78) 63

GEOPHYSICS, ASTRONOMY AND SPACE

Fundamentals of the Theory and Technique for Neutron Activation Element and Salt Analysis of Sea Water Under Full-Scale Conditions
(Ye. M. Filippov, I. A. Lamanova; MORSKIYE GIDROFIZICHESKIYE ISSLEDOVANIYA, No 1, 1978) 68

Possibility of Determining Sea Water Salinity and Density From Gamma-Radiation Attenuation
(Ye. M. Filippov; MORSKIYE GIDROFIZICHESKIYE ISSLEDOVANIYA, No 1, 1978) 81

Experimental Check of a Baseless Method for Measuring the Electrical Field in the Sea
(Yu. P. Butrov, et al.; MORSKIYE GIDROFIZICHESKIYE ISSLEDOVANIYA, No 1, 1978) 89

Calculation of an Equivalent Base for a Measuring System With Current Fairing of a Rectangular Form
(V. I. Lopatnikov, et al.; MORSKIYE GIDROFIZICHESKIYE ISSLEDOVANIYA, No 1, 1978) 96

PUBLICATIONS

Information Networks and Their Analysis
(A. D. Kharkevich, V. A. Germash; INFORMATSIONNYYE SETI I IKH ANALIZ, 1978) 101

List of Soviet Articles Dealing With Composite Materials
(GOSUDARSTVENNYY KOMITET SOVETA MINISTROV SSSR PO NAUKE I TEKHNIKE. AKADEMIYA NAUK SSSR. SIGNAL'NAYA INFORMATSIYA. KOMPOZITSIONNYYE MATERIALY, No 21, 1978) 110

List of Soviet Articles Dealing With Composite Materials
(GOSUDARSTVENNYY KOMITET SOVETA MINISTROV SSSR PO NAUKE I TEKHNIKE. AKADEMIYA NAUK SSSR. SIGNAL'NAYA INFORMATSIYA. KOMPOZITSIONNYYE MATERIALY, No 23, 1978) 112

ELECTRONICS AND ELECTRICAL ENGINEERING

NUCLEAR POWER GENERATING UNITS WITH RBMK-1000 REACTORS DESCRIBED, EVALUATED

Moscow ELEKTRICHESKIYE STANTSII in Russian No 1, 1979 pp 10-15

[Article by L.M. Voronin, candidate in technical sciences, Scyuzatomenergo [Nuclear Power Alliance]: "Experience in Starting up and Mastering the Rated Capacity of Power Generating Units with RBMK-1000 Reactors"]

[Text] In keeping with the "Main Guidelines for the Development of the National Economy of the USSR for 1976-1980," adopted by the 25th CPSU Congress, there has been an unprecedented advance in nuclear power in the European sector of our country. During the years of the 10th Five-Year Plan period alone, the plan is to add 13.7 million kW of capacity at nuclear power plants.

At the present time extensive construction is under way on nuclear power generating units at the sites of the Novovoronezhskiy, Kola, Kursk, Chernobyl', Leningrad, Smolensk, Armenian, Beloyarsk, Rovno, Southern Ukrainian, Kalinin, Ignalina and other AES's.

At nuclear power plants whose construction is planned for the next five to 10 years will be installed chiefly large power generating units with nuclear reactors with an electrical capacity of one million to 1.5 million kW and turbogenerator sets with a capacity of 500,000, 750,000 and one million kW.

An important contribution to the development of nuclear power in the 10th and following five-year plan periods will be power generating units with type RBMK-1000 and RBMK-1500 channel-type uranium-graphite boiling water reactors. Each power generating unit of an AES with an RBMK-1000 is furnished with two 500,000-kW turbines, and in units with an RBMK-1500 will be installed two turbines with a capacity of 750,000 kW each.

The installation in a power generating unit of two turbogenerator sets operating from a single nuclear reactor noticeably facilitates the mastery of complex AES equipment and promotes better utilization of installed capacities and efficient organization of repair servicing of turbines and auxiliary equipment in turbine rooms.

At the end of 1978 in operation were four power generating units with RBMK-1000 reactors (two at the Leningrad AES and one each at the Kursk and Chernobyl'

AES's). The total electrical capacity of power generating units with type RBMK reactors in operation and under construction at the present time is 20 million kW. About one half of all the electric power which will be generated at nuclear power plants in the 10th Five-Year Plan period is planned for production at AES's with RBMK-1000 reactors.

The first prototype power generating unit with an RBMK-1000 at the Leningrad AES was put into industrial service in December 1973 and reached its rated capacity of one million kW by the end of November 1974. A second similar unit at this AES was put into service in the middle of 1975. Both power generating units at the Leningrad AES have been operating reliably and stably in the Lenenergo [Leningrad Power] System in the basic load mode.

In 1974-1978 about 45 billion kWh of electric power were generated with them.

Broad utilization of the know-how gained in starting up and mastering the prototype power generating units at the Leningrad AES has made it possible to master successfully similar units at other nuclear power plants. For example, in December 1976 the first power generating unit at the Kursk AES began to produce power, and its rated capacity was reached in the first half of October 1977. At the end of September 1977 the first power generating unit went into industrial service at the Chernobyl' AES, and its rated capacity was mastered as early as in the second half of May 1978.

The first phases of the Kursk and Chernobyl' AES's differ little from one another with regard to design solutions. They consist of two power generating units with an electrical output of one million kW each. The basic equipment of each of these units is an RBMK-1000 reactor, two K-500-65/3000 turbogenerator sets and two type TVV-500-2 generators. The basic technological layout of a power generating unit with an RBMK-1000 is shown in fig 1.

A distinctive feature of AES's with type RBMK reactors is the fact that the technological layout of each power generating unit is of the single-circuit type and differs little in this respect from the traditional layouts used in thermal electric power plants. Serving as the source of thermal power are channel-type uranium-graphite reactors of the boiling water type with water as the heat transfer agent.

The water heat transfer agent, at a temperature of 270°C with a total flow rate through the reactor of 45,000 to 50,000 m^3/h, is supplied through individual pipelines to the reactor's fuel channels (TK's), where it is heated to the saturation point and is partly evaporated (the mean vapor content at the outlet of a TK is approximately 15 percent). Then the steam-water mixture through individual pipelines from each TK enters a drum-type steam trap. After separation, the steam, at a rate of about 5.4 million tons per hour at 284°C and a pressure of 70 kg/cm^2, is sent to the turbines, and the condensate from the turbogenerator sets, passing through feed-water heaters, is mixed with the water from the drum-type steam traps and is supplied to the TK's by means of the main circulation pumps (GTsN's).

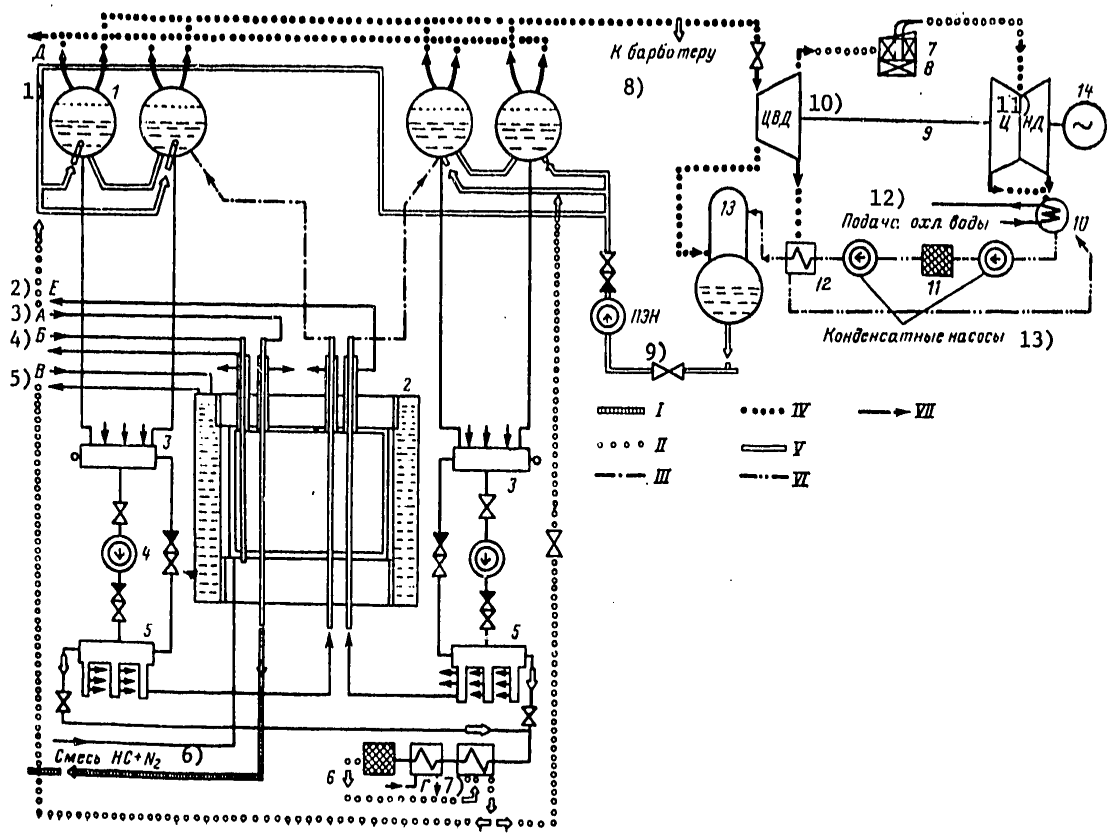

Figure 1. Basic Technological Layout of Power Generating Unit of an AES with an RBMK-1000 Reactor:
I--heat transfer agent; II--decontamination loop water; III--steam-water mixture; IV--steam; V--feed water; VI--condensate; VII--gas loop; 1--steam trap; 2--reactor; 3--induction manifold; 4--GTsN pump; 5--pressure header; 6--heat transfer agent decontamination system; 7--intermediate steam trap; 8--intermediate steam heater; 9--turbine; 10--condenser; 11--condensate decontamination system; 12--feed-water heater; 13--deaerator; 14--generator; A--water to SUZ [control and protection system] channels; B--cooling of deflector; C--cooling of SKh"L" system; D--water from washing system; E--to second turbine loop; F--to KTsTK [fuel channel circulation loop] system

[Key on following page]

Key:

1. E
2. F
3. A
4. B
5. C
6. Mixture HC + N_2
7. D
8. To bubbler
9. PEN [delivery pump]
10. TsVD [high-pressure cylinder]
11. TsND [low-pressure cylinder]
12. Cooling water delivery
13. Condensate pumps

The repeated forced circulation loop (KMPTs) for the heat transfer agent consists of two independent parts, each of which contains two drum-type steam traps connected by connectors for steam and water, downcomers from the drum-type steam traps, the intake and pressure manifolds of the GTsN's, four GTsN's (three active and one standby), group distributing manifolds, and also circulation pipes and the necessary stop and regulating fittings. A circuit water ion exchange decontamination system with a capacity of 200 t/h is provided for both parts of the KMPTs.

The steam partly used up in the turbines, at a temperature of 140°C and a pressure of 3.5 kg/cm^2, after the high-pressure cylinder (TsVD), is sent to steam superheater traps. Steam superheated to 263°C at a pressure of 3 kg/cm^2 enters the low-pressure cylinders (TsND's) of the turbines, and then the condensers. The major condensate from the turbines, after the condensers, undergoes total decontamination in ion exchange filters and is heated in the recovery system to 155°C, and is then sent to the deaerators, whence it is delivered to drum-type steam traps by means of delivery pumps.

The key reactor and turbine equipment is remote controlled from a unit control console. All technological monitoring at the AES is performed by means of the "Skala" totally automated computing and information system, making it possible to monitor the state of equipment, make measurements and record parameters, warn of deviations in parameters from established limit values, and to calculate the major conditions and technical and economic indicators for operation of the power generating unit.

At the Kursk and Chernobyl' AES's a recycling water supply system has been used which employs open artificial reservoirs. From the reservoir, through an open delivery channel, the cooling water is delivered to the pumping station and then by means of circulation pumps with a flowrate of approximately 105 m^3/s is delivered to a delivery tank with a capacity of 20,000 m^3, whence the water by gravity flow enters to cool the turbines' condensers. This arrangement improves the reliability of the AES's operation, since it makes possible normal cooling of turbine condensers even with a brief interruption (3 min maximum) in power in the circulation pump motors.

The electric power of the first phases of the Kursk and Chernobyl' AES's is being released into the united power system through three 330-kV overhead lines, originating at each of these electric power plants. With further expansion of these AES's, power will be released also through 750-kV overhead lines.

Each RBMK-1000 reactor is supplied with a loading-and-unloading machine (RZM), designed for removing spent fuel elements from the reactor's core and installing fresh elements there. The design of the RZM makes it possible to perform these important operations in a reactor without reducing the output of the AES.

Based on the experience of constructing and putting into service existing AES's, there has been further elucidation of the main aspects of and steps in starting up and mastering power generating units with RBMK-1000 type boiling water channel reactors.

The specific features of the technological process at an AES, the presence of a considerable amount of complex special equipment, and the need to ensure nuclear and radiation safety impose special stipulations and requirements on the quality of performance of building and erection work and startup operations and tests, especially of tests which determine the extended capacity for work of equipment and pipelines in the process of operation.

One of the major conditions having a favorable influence on the quality and duration of startup and adjustment operations, as well as on progress in the mastery of the rated capacity of AES power generating units with an RBMK-1000, is a high degree of readiness, from the construction and erection standpoint, to begin startup, on the part of all equipment, key and secondary systems, and buildings and space of the AES, since the appearance of ionizing radiation and radioactive contamination after startup of the reactor unit considerably hinders and at times makes impossible the performance of startup and adjustment work.

The technological sequence, extent and structure of startup and adjustment operations at nuclear power plants depend to a considerable extent on the type of reactor unit used at these AES's.

On the basis of know-how gained in constructing and putting into operation the first power generating units at the Kursk and Chernobyl' AES's, as well as at other nuclear power plants, it is possible to single out the following major steps in starting up and mastering the rated capacity of power generating units with RBMK-1000 reactors.

1. Testing, adjusting and putting into service secondary equipment, systems and units enabling the startup and normal operation of key technological equipment (under this heading come chemical water treatment systems, electrical equipment and electrical service equipment of the power system for the AES's internal needs, lubrication maintenance, nitrogen and air compressor units, industrial water supply systems, and the like).

2. Post-assembly individual and systemic cleaning ("shooting through" or blasting), as well as hydraulic testing of the equipment and pipelines of the KMPTs and all other systems enabling the operation of the reactor and turbine units.

3. Cold and hot circulating flushing of the KMPTs.

4. A hot running test of key reactor equipment and thorough adjustment of technological systems under conditions approximating to a maximum operation at rated parameters.

5. Inspection and examination of the condition of key equipment of the KMPTs and individual units of the reactor after the hot running test.

6. Thorough check and final adjustment of equipment of the regular and startup systems for controlling and protecting the reactor (SUZ's).

7. Initial loading of nuclear fuel into the reactor's core.

8. Physical startup of the reactor (checking neutron physics characteristics and the effectiveness of the SUZ's absorbers, organizing initial loading of the core, and also bringing the reactor to the capacity level, on the order of one percent of the rated, which is minimally controllable by the regular SUZ).

9. Power startup of the reactor unit.

10. Thorough testing of equipment and all technological systems of the startup power generating unit when operating at the assigned electric power in parallel with the power system.

11. Step-by-step mastery of the rated capacity of the power generating unit.

Experience has demonstrated that for the purpose of improving the quality of and shortening the time required for startup and adjustment operations at an AES it is advisable to perform all key startup operations according to regular systems and to refrain to a maximum extent from using temporary technological and electrical systems for testing individual equipment or systems.

A typical feature of the startup of an AES with RBMK-1000 reactors is the considerable amount of work involving post-assembly decontamination and flushing of reactor equipment and pipelines. Post-assembly flushing of the KMPTs and secondary technological systems serving the reactor unit represents essentially the beginning of startup operations at power generating units under construction.

Flushing of KMPTs equipment and pipelines is performed in two stages: First high-speed water flushing is performed on individual elements or sections of pipeline mains and technological systems according to an open system, with discharge of the flush water into the waste water system or into special containers, and then hot and cold circulating flushing is performed on the KMPTs as a whole.

In high-speed flushing of individual pipelines and systems it is necessary to ensure the required rate of flushing water (as a rule, water rates are set 1.5 times higher than design rates). Flushing of pipelines and KMPTs

equipment it is a good idea to begin with individual rapid flushing ("shooting through"), with chemically desalted water, of each fuel channel for 3 to 5 min at a rate of flow of about 150 m^3/h. After individual flushing of all key and secondary pipelines and equipment, cold (maximum water temperature of 50°C) and then hot circulating flushing are performed in each separate half of the KMPTs.

Hot closed-cycle flushing of the KMPTs is performed for the purpose of guaranteeing the necessary cleanliness of the inside spaces of equipment and pipelines. The water is heated in the KMPTs on account of the heat released during the operation of the GTsN's. Experience has demonstrated that in hot closed-cycle flushing it is advisable to turn on two GTsN's apiece alternately in each half of the KMPTs. Then the temperature of the water in the circulation loop is held steadily at 150 to 155°C with a total rate of flow of approximately 30,000 m^3/h, and continuous cleaning of the water is performed by means of mechanical regular bypass decontamination filters and special sieve-type filters temporarily installed in the group distributing headers.

Closed-cycle flushing of the KMPTs is terminated upon achieving the required quality of the flushing water.

For example, upon conclusion of hot closed-cycle flushing of the KMPTs in the first power generating unit of the Kursk AES, the quality of the water in the loop was characterized by the following figures: iron content--approximately 0.1 mg/kg; chloride content--not greater than 0.05 mg/kg; hardness--about 5 μg-equiv./kg; and presence of oil--less than 0.2 mg/kg.

An important feature of single-circuit AES's with RBMK-1000 reactors is that the major amount (up to 90 percent) of iron corrosion products enters the reactor's KMPTs from the turbine room along with the feed water. Therefore, the condensate delivery channel and other secondary loops of the turbine room especially made out of stainless steel should be subjected to a thorough cleaning and washing, both for post-assembly contaminants and corrosion products.

At the Kursk and Chernobyl' AES's, for these purposes extensive use is made of manual and mechanical cleaning and of rapid water flushing, as well as of chemical flushing of the most contaminated sections of equipment and pipelines. For the purpose of making possible acid flushing of the condensate delivery line, circulation of a chemical washing solution has been created at a rate of 800 to 1000 m^3/h by means of special acid-resistant pumps, containers for chemical reactants, and temporary pipelines provided for in the planned technological system for post-assembly flushing.

As a principal washing solution for acid flushing, recommended is a composition consisting of "Trilon B" (3 g/l), citric acid (3 g/l) and a moderate amount of a special inhibitor. Acid flushing of the condensate delivery line takes about 20 h. After its conclusion special ammonia passivation has been carried out--the loop is flushed for not less than 8 h with a water and ammonia solution (pH higher than 10) at about 50°C.

Acid flushing of loops made of stainless steel gives good results. At the same time the experience of starting up the first power generating unit at the Kursk AES demonstrated that in individual cases at an AES with an RBMK-1000 it is possible to refrain completely from acid flushing of the condensate delivery line, limiting oneself to thorough pre-startup washing of it and all steam pipes with water, as well as to blasting through with steam the main steam pipes in the regular system leading from the reactor operating at low output.

A quite important and critical step in operations at an AES is the physical startup of the reactor. The main objectives of a physical startup of an RBMK-1000 reactor are the formation of the composition of the initial load of the core and an experimental check of the key physical characteristics of the reactor.

At AES's with RBMK-1000 reactors fuel assemblies (TVS's) are loaded into the reactor in several stages. At first so-called minimal loading of the reactor is carried out, whereby only 23 or 24 TVS's are loaded (with initial 1.8-percent fuel enrichment and without water in the fuel channels and SUZ channels). Then the number of TVS's loaded is increased step-by-step, while at the same time installing additional absorbing rods (DP's) in the core.

From the know-how gained in starting up the Kursk and Chernobyl' AES's, the initial load for the core of an RBMK-1000 reactor is approximately 1445 to 1455 TVS's and 230 to 240 DP's. In the process of step-by-step formation of the composition of the initial load for the core, the critical state was approached at a very low power level (on the order of 10^{-5} to 10^{-4} percent of the nominal) and a precise determination was made of neutron physics characteristics of the reactor, the effectiveness of the SUZ rods, and of other characteristics of the core.

Physical startup of an RBMK-1000 reactor concludes with bringing it up to the minimum power level controllable by the regular SUZ (to the MKU), which is maintained steadily by an automatic control and equals about one percent of its nominal thermal capacity.

After the completion of operations relating to the procedure for physical startup of the reactor, all key and secondary equipment and systems of the power generating unit are readied for the power startup, when the unit is brought up to a power level greater than one percent of the nominal.

Experience in constructing an AES with RBMK-1000 reactors has demonstrated that it is advisable to perform the power startup of a power generating unit also in several stages, constantly broadening the amount of checks and tests, as well as the makeup of technological equipment and systems taking part in the power startup.

The first step (stage) in the power startup for a power generating unit with an RBMK-1000 is customarily considered blasting the main steam pipes with the steam of the reactor when operating at an output of eight to 10 percent

of the nominal. For proper cleaning of the main steam pipes of an AES, it is necessary to provide a steam flowrate of up to 350 t/h, with a pressure in the drum-type steam traps of 12 to 14 kg/cm^2. Blasting of the steam pipes should be performed according to the regular system, using an insignificant number of temporary pipelines to enable exhausting the blasting steam into the atmosphere above the roof of the turbine room building. The total blasting period for all steam pipes is about 15 to 20 h. During blasting of the main steam pipes into the atmosphere, it is necessary to arrange for careful monitoring of the radiation situation in the area of and in areas in the AES, as well as around it within a radius of a few kilometers. The experience of starting up the Kursk and Chernobyl' AES's demonstrated that performance of this blasting practically does not exert an influence on the radiation state of the environment.

The second stage in the power startup includes adjusting and mastering the operating modes of the key and secondary equipment of the power generating unit at a thermal capacity of a maximum of 10 percent of the nominal. During this time safety valves and rapid-response reducers are adjusted, emergency steam admission systems are tested, and other startup and adjustment work is performed. The time required for the second stage of the power startup depends on the level of readiness of reactor unit and turbine room equipment and systems. At the Kursk and Chernobyl' AES's this stage took not more than three to five 24-hour periods.

The third stage in the power startup can be either a trial startup of the power generating unit lasting up to 8 h, with alternate testing of turbogenerator sets in operation with a relatively moderate power load (50,000 to 70,000 kW), or a 72-hour thorough test of the power generating unit when operating with a specified load.

A thorough test of the power generating unit's equipment and systems is the concluding stage in the power startup of an AES. The main objective of this test is to test the working capacity of the power generating unit's equipment when operating under a load with parameters close to the rated. The load level, procedure and conditions for the thorough test of the power generating unit are selected on the basis of the representativeness of this test for the purpose of confirming the reliability and working capacity of the key equipment and all systems of the AES.

The following are the key parameters of the thorough test cycle used in the startup of the first power generating units at the Kursk and Chernobyl' AES's:

	Parameter	
	Rated	With combined equipment
Thermal capacity of reactor, thousand kW	3140	650-900
Electrical output of a single (or of each) turbogenerator, thousand kW	500	150-220

Pressure in drum-type steam traps, kg/cm^2	70	65-70
Feed water temperature, °C	168	155-164
Flowrate of water in KMPTs, thousand tons per hour	36	24
Temperature of water in KMPTs, °C	284	275-280
Number of operating GTsN's	6	4
Mean steam content in fuel channel, %	15	4.5-5.5

After a successfully performed thorough test of power generating units, further mastery of the rated capacity is carried out in stages at the following levels: 20 to 35 percent, 40 to 50 percent, 55 to 70 percent, 80 to 90 percent and 100 percent of the nominal (thermal) capacity of the reactor. At each stage in mastery of the rated capacity, a large amount of work is done relating to studying and adjusting operating modes and optimizing the distribution of energy release in the reactor's core, along with other work relating to ensuring reliable operation of the power generating unit at various power levels.

In single-circuit AES's of especially great importance are high-quality adjustment and maintenance of the required water chemistry in the KMPTs, in the condensate delivery line and in other loops of the AES. For the purpose of running power generating units with an RBMK-1000, a correction-free neutral water chemistry is used for the KMPTs and condensate delivery line. The standards for water quality are the following:

Index	For KMPTs water	For feed water
pH indicator	6.5-8.0	6.8-7.2
Iron content, µg/kg	$\leq$ 50	$\leq$ 10
Copper content, µg/kg	$\leq$ 50	$\leq$ 2
Chloride content, µg/kg	$\leq$ 100	-
Oil content, µg/kg	$\leq$ 200	-
Hardness, µg-equiv./kg	$\leq$ 5	$\leq$ 0.5
Electrical conductivity, µΩ/cm	$\leq$ 1.0	$\leq$ 0.2
Radioactivity of water, curies/l	$2 \cdot 10^{-3}$	-

The time required for mastery of individual stages in the rated capacity of the first power generating units of the Kursk and Chernobyl' AES's is shown in table 1.

In the process of mastering capacities at the Kursk and Chernobyl' AES's, individual defects and maladjustments were discovered in the operation of heat exchange and pumping equipment, fittings and secondary systems.

For example, during the initial period of operation there occurred increased vibration of feed water equipment and pipelines. This required additional

unfastening of pipelines and reinforcement of supports, which made it possible to reduce vibration to the normal level.

Table 1.

Stage	Capacity, thousand kW	Time required for mastery, 24-hour periods: First unit of Kursk AES	First unit of Chernobyl' AES
1	350	53	27
2	500	89	65
3	650	100	83
4	800	210	85
5	1000	272	238

For the purpose of improving the separation of moisture in drum-type steam traps with different loads, the internal equipment in the drums was modernized. Improvements were made in the planned systems for additional feeding of the KMPTs from emergency delivery pumps, in circuits for electrical powering of pulsed safety valves, and in other systems.

In the course of mastering the first power generating units of the Kursk and Chernobyl' AES's, new progressive measures were also introduced, such as, for example, the employment of absorbing rods (SP's) for the purpose of equalizing the distribution of energy in the reactor's core and extending the length of the operating period, the improvement of gas purification systems, and the like. All this made it possible in a relatively short time to ensure reaching the rated level of capacity and the stable operation of the power generating units of the Kursk and Chernobyl' AES's in the united power system.

The key operating figures achieved by the first power generating units of the Kursk and Chernobyl' AES's are given in table 2.

Table 2.

Indicator	Rated	Figures achieved: Kursk AES	Chernobyl' AES
Thermal capacity of reactor, thousand kW	3140	3140	3140
Electrical load of turbogenerators, thousand kW	2 X 500	2 X 500	2 X 500
Maximum capacity of reactor's fuel channel, kW	2990	2700	2650
Maximum bulk steam content in TK, %	20.1	20.0	17.0
Reactor's nonuniform heat release factor:			
In terms of radius	1.27	1.27	1.18
In terms of height	1.2	1.33	1.26

[Continued on following page]

Minimum safety factor prior to heat removal crisis	1.0	1.05	1.10
Rate of flow of heat transfer agent through reactor, thousand m^3/h	49.0	48.3	49.4
Pressure in drum-type steam traps, kg/cm^2	70	70	70
Rate of flow of steam to turbines, t/h	5400	5470	5450
Live steam pressure, kg/cm^2	65.9	65.9	65.8
Live steam temperature, °C	280.4	280.4	280.0
Feed water temperature, °C	168	164	165
Efficiency of power generating unit, %			
Net	29.9	29.8	29.8
Gross	31.84	31.84	31.8

Conclusion

The operation of two power generating units with RBMK-1000 reactors at the Leningrad AES, as well as the experience of starting up and mastering the rated capacity of the first power generating units of this kind at the Kursk and Chernobyl' AES's, have demonstrated that the key equipment of these nuclear power plants operates completely reliably under all rated conditions.

8831
CSO: 8144/0756

ELECTRONICS AND ELECTRICAL ENGINEERING

A METHOD OF INTERCHANNEL SYNCHRONIZATION IN THE PLAYBACK OF A MULTICHANNEL RECORDING OF A WIDEBAND SIGNAL WITH FREQUENCY DIVISION

Moscow RADIOTEKHNIKA in Russian No 11, Nov 78 pp 48-52

[Article by A.I. Grechikhin, manuscript received 24 Oct, 77]

[Text] When the volume of a signal in which there is no redundancy exceeds the capacity of one transmission channel, which cannot be increased, one resorts to multichannel transmission of this signal. A special case of such transmission is the multichannel recording of wideband signals.

A block diagram of a signal conversion device is shown in Figure 1 for N-channel recording with frequency division. The signal spectrum which occupies a bandwidth (0, f), is split by frequency filters Φ_k ($1 \leq k \leq N$) into N adjacent sections, the width of which is F. Then using record converters, PZ, the spectra of each of the high frequency sections ($2 \leq \leq N$) are converted to the low frequency range (0, F), corresponding to the passband of one record-playback channel. The record carrier synthesizer, SZ, is synchronized by a pilot signal (PF), fed from the GPS generator [pilot signal generator]. The pilot signal can be recirded in any of the channels. During playback, the pilot signal is segregated from the information signal, back conversion is accomplished in the high frequency channels, as well as the combining of the individual signals into a composite signal.

We shall assume that the components of the signal conversion devices, within the limits of the corresponding frequency bands, are nondistorting, and assume that the recording and playback in the K-th channel reduce only to the time delay $\tau_k(t)$ of the reproduced signal, where $d\tau_k(t)/dt << 1$. It is then not difficult to show that a component of the spectrum of the input signal which appears following division in one of the high frequency channels, $u_k(t) = A_k \cos \omega_k t$ ($2 \leq k \leq N$), and following playback and back conversion of the spectrum has the form:

$$u_k^*(t) = B_k \cos \{\omega_k [t - \tau_k(t)] + \omega_{0k} [\tau_k(t) - \tau_{0k}(t)]\}, \quad (1)$$

where ω_{0k} is the frequency of the carrier for the playback converter of the k-th channel (it is assumed that $\omega_{0k} = 2\pi kF$ for simplicity); $\tau_{0k}(t)$ is the delay of this signal, which is identical to the delay in that channel where the pilot signal is recirded, which is used for its generation.

As follows from (1), for the precise restoration of the composite signal during playback, it is necessary to meet three conditions:

1. $\tau_k(t) \equiv \tau_{0k}(t)$, i.e., to generate the carrier for the back conversion from the pilot signal, rec rded in "its own" channel; in this case, the k-th section of the signal is reproduced within the precision of the group delay $\tau_k(t)$ and the phase shift $\omega_{0k}(\tau_k - \tau_{0k})$ is eliminated in (1).

2. $\tau_k(t) \equiv \tau_m(t)$; $k \neq m$. This means the elimination of the mutual interchannel time shifts, and the complete restored composite signal differs from the original one only in the delay, i.e., $u_{out}(t) = \text{const}\, u_{in}[t - \tau_k(t)]$.

3. The elimination of time scale distortion in the composite signal, for example, by means of a delay block with a delay function $\tau(t) = \tau_c - \tau_k(t)$; $\tau_c = \text{const}$.

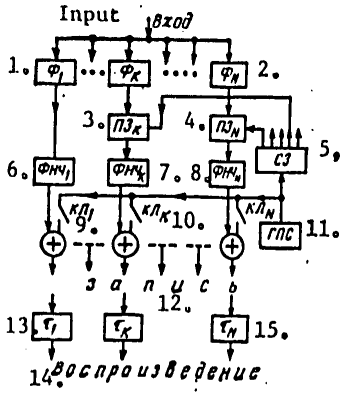

Figure 1.

Key:
1. F_1 [frequency filter 1];
2. F_N [frequency filter N];
3. PZ_K [record converter K];
4. PZ_N [record converter N];
5. SZ [record carrier synthesizer];
6. $FNCh_1$ [low pass filter 1];
7. Low pass filter K;
8. Low pass filter N;
9. KL_1 [switch 1];
10. KL_K [switch K];
11. GPS [pilot signal generator];
12. Record;
13. τ_1 [time delay 1];
14. Playback;
15. Time delay N.

For the case of multichannel recording on a moving vehicle, for example, on magnetic tape, one of the most serious causes of distortions in the waveform of the composite, reproduced signal is interchannel time shits $\Delta\tau_{mk}(t) = \tau_m(t) - \tau_k(t)$.

The classical timeswise procedure for correcting interchannel shifts using delay blocks, which are controlled by

the output voltages of pilot signal phase detectors [1], has a number of drawbacks. Controlled delay blocks are required with a wide passband (up to the frequency f). It is necessary to record the pilot signal in each channel, something which makes it difficult to mutually decouple the information signal and the pilot signal. Phase detectors are required as well as individual playback synthesizers for each of the high frequency channels.

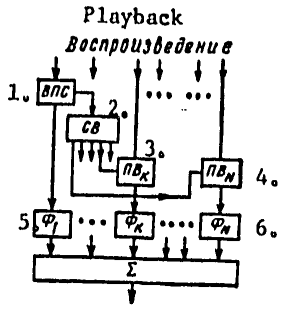

Figure 2.

Key: 1. VPS pilot signal separator;
2. SV [playback carrier synthesyzer];
3. PV_K [playback converter K];
4. Playback converter N;
5. F_1 [frequency filter 1];
6. Frequency filter N.

The distortions of the reproduced signal can be substantially reduced using phase equalization [2] with considerably simpler means, without resorting to reducing the physical sizes of the interchannel shifts. Depicted in Figure 2 is a signal conversion channel for playback with phase equalization. The back conversion carriers for all the high frequency channels are generated from one pilot signal, recorded only on the track of one low frequency channel (only the key KL_1 [9] is closed during recording). It follows from (1), that in this case, the signal in the k-th channel will receive phase distortions in the form of a phase shift which does not depend on the frequency, $\Delta\phi_k(t) = \omega_{0k}[\tau_k(t) - \tau_1(t)]$. By representing (1) in the following form

$$u_k^*(t) = B_k \cos\{\omega_k[t - \tau_k(t) - \Delta\tau_{k1}^*(t)]\},$$

Following some simple transformations, we derive an expression for the equivalent time shift of the spectral component of the reproduced signal having a frequency ω_k in the k-th channel with respect to the signal in the first channel (the low frequency one, where the pilot signal is recprded):

$$\Delta\tau_{k1}^*(t) = \Delta\tau_{k1}(t)\left(1 - \frac{\omega_{0k}}{\omega_k}\right) \qquad (2)$$

It can be seen from (2) that the most complete equalization is obtained at the upper frequencies of the channel passband, and at the lower passband frequencies, there is the greatest uncompensated residue (more accurately, an over-compensated one). We will note that equalization is possible only with respect to the "duty factor", but not with respect to the envelope,

since changes in the carrier phase can influence only the phase of the converted components of the signal and no way influence the group delay in the channel. Thus, the method is based on the partial correction of the time shift (delay) in the passband by a phase shift of the components of the spectrum in this passband, which does not depend on the signal frequency. The distortion in the signal waveform which results in the channel (in a portion of the wideband signal) nonetheless has less influence, as shown below, on the distortion of the reproduced signal as a whole than the absence of equalization with the combining of the undistorted portions of the signal, while the record and playback unit proves to be significantly simpler. Only one pilot signal detector, VPS (Figure 2), is required, and a synthesizer converters and record filterssare sutiable for playback (see Figure 1).

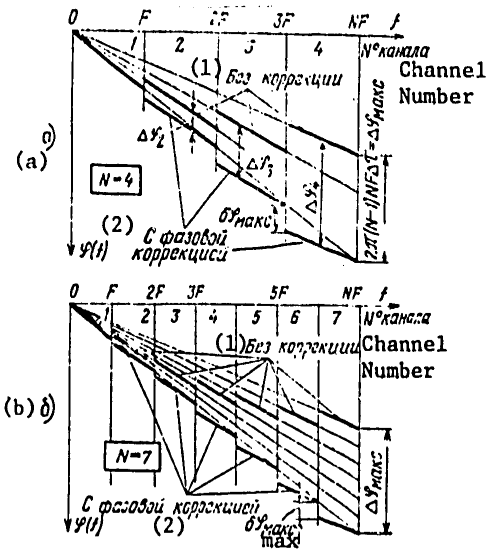

Figure 3.

Key: 1. Without correction;
2. With phase correction.

We shall assess the capabilities of the phase equalization method from the viewpoint of signal distortion. Shown in Figure 3a is an idealized phase-frequency response characteristic (FChKh) of the through channel of a four channel record-playback system with phase equalization for the case where the shifts between signals reproduce from adjacent tracks are identical in the time interval being considered and are equal to $\Delta\tau$, so that $\Delta\tau_{mk} = \Delta\tau(m - k)$, where m and k are the numbers of channels. Such an assumption is close to reality if the major cause of interchannel shifts is the dynamic misalignment of the tape. The phase-frequency response for playback with the generation of the carriers from the pilot signal of "its own" channels, but without correction of the time shifts, is also shown here for comparison. The maximum deviation of the through phase-frequency response from the linear response representing the extension of the phase-frequency response of the first channel, without correction is equal to $\Delta\phi_{max} = 2\pi(N - 1)NF\Delta\tau$, and with phase correction is $\delta\phi_{max} = 2\pi(N - 1)F\Delta\tau$, i.e., it is N times less. It is not difficult to show that an increase in the number of channels promotes a reduction in the distortion of the reproduced signal with phase correction, since in this case, the through phase-frequency response will have overshoots which are smaller in size, although more frequent (Figure 3b). On the other hand,

in this case, one can allow a greater swing in tape misalignment (an increase in $\Delta\tau_{N1}$) while maintaining the permissible nonlinearity of the phase-frequency response.

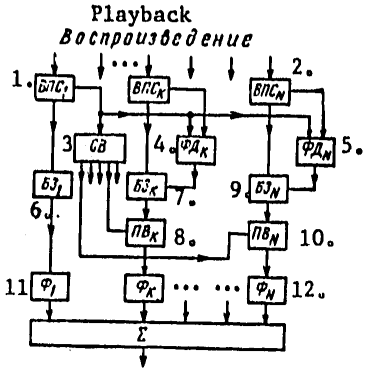

Figure 4.

Key: 1. Pilot signal separator 1;
2. Pilot signal separator N;
3. SV playback carrier synthesizer;
4. FD_K [phase detector K];
5. Phase detector N;
6. BZ_1 [delay block 1];
7. Delay block K;
8. PV_K [playback converter K];
9. BZ_N [delay block N];
10. PV_N [playback converter N];
11. F_1 [frequency filter 1];
12. Frequency filter N.

When it is undesirable to increase the number of channels, then with large values of the interchannel shifts, a combination time-phase correction proves to be extremely promising (Figure 4). Time correction is first accomplished in the low frequency passband by means of controlled delay blocks, BZ's. For this, it is necessary to record the pilot signal in each channel, and pilot signal detectors and phase detectors, FD's, are required. Then, during the back conversion of the spectra of the high frequency channels, the phase correction reduces the distortions which can arise due to the residual interchannel shifts, not eliminated by the time corrector.

A study of the time characteristics of a two-channel syst with frequency division, which was conducted both theoretically and experimentally, has confirmed the arguments presented above.

Shown in Figure 5 are the transient characteristics of a two-channel system calculated for the same conditions as above, where the system has ideal filters for cases equivalent to the recording of the pilot signal in the high frequency channel (Figure 5b) and in the low frequency channel (Figure 5a). It is not difficult to see that with identical values of the time shifts, the distortion is significantly less with phase correction. A shift of τ_0 = 5.5. nsec corresponds to an overshoot of 12% without correction, while with phase correction, τ_0 = 17 nsec.

The operation of the phase corrector is well illustrated by the oscilloscope traces of Fiugre 6 (a: with phase correction; b: without correction), recorded when testing an actual two-channel system for signal separation and addition with the same boundaries of the frequency bands as in Figure 5,

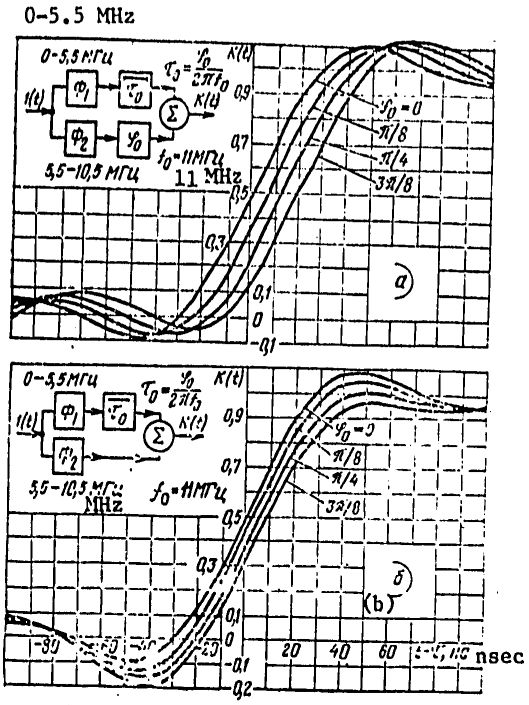

Figure 5.

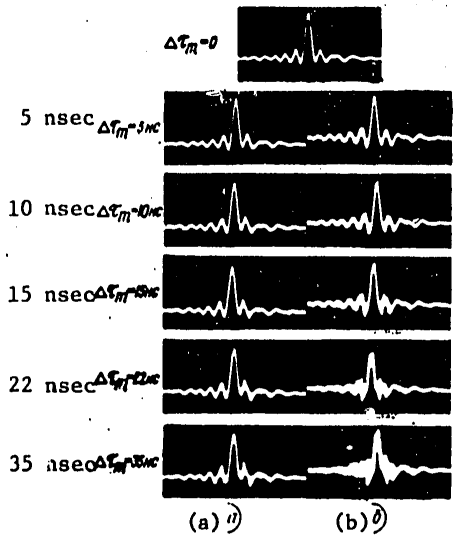

Figure 6.

for the case of a sinusoidal variation in the interchannel time shifts at a frequency of 600 Hz and amplitudes of $\Delta\tau_m$ = 5--35 nsec. A sequence of short pulses with a width of 10 nsec (δ pulse) was fed to the input. The output pulse of the first channel was used for external synchronization of the oscilloscope. The distortions in the pulse response of the through channel were hardly noticable at $\Delta\tau_m \leq 15$ nsec, which in our case corresponds to $\delta\phi \leq 0.5$ rad. This result is in complete agreement with the requirements placed on the phase characteristics of video and pulse amplifiers [3].

BIBLIOGRAPHY

1. Federal Republic of Germany Patent No. 1071754,,Class 21a1, 32/11 (H04m), 1960.

2. A.I. Grechikhin, Patent 575678 [USSR].

3. S. Gol'dman, "Garmonicheckiy analiz, modulyatsiya i shumy" ["Harmonic Analysis, Modulation and Noise"], Moscow, IIL Publishers, 1951.

8225
CSO:1870

ELECTRONICS AND ELECTRICAL ENGINEERING

UDC 621.391.019.4

FILTERING DISCRETE MULTIFREQUENCY SIGNALS IN NONGAUSSIAN INTERFERENCE

Moscow RADIOTEKHNIKA in Russian No 11, Nov 78 pp 52-60

[Article by I.M. Pyshkin, V.V. Druzhinin and R.T. Pantikyan, manuscript received 17 Feb 78]

[Text] *Introduction.* In the majority of modern radioelectronic systems, useful signals are detected and discrimated against a background of interference which differes substantially from gaussian noise. This is manifest particularly clearly in asynchronous address information transmission systems (AAS) [1], where along with the internal noise of the receiver, crosstalk interference also acts which coincides in structure with the useful signals. Subscribers to an AAS are arbitrarily distributed over a large territory, and for this reason, the interfering signals have a considerable dynamic range of amplitude variation, and because of this, the mutual interference at the input to the receiver (even for a large number of interfering signals) is not normalized. In this case, the operational characteristics of receivers which are optimized for normal noise are substantially degraded. This leads to the necessity of: in the first place, finding a system of address signals which create minimum mutual interference, and which in terms of their statistical characteristics, tend towards normal noise; in the second place, synthesizing structures which make use of the difference in the probability densities of the acting mutual interference and the gaussian noise to improve the receiver characteristics.

The best results under these conditions are given by systems of discrete, multifrequency signals [2], studies of which as applied to AAS's were started in [3, 4]. To improve the receiver characteristics for a discrete multifrequency signal (DMCh), a stiff limiter [2] which performs the useful normalizing operation on the crosstalk interference, is introduced into the device on analogy with an ShOU [? noise limiting amplifier ?] circuit [5].

A study was made in [2] of the noise immunity of a nonlinear receiver, where the processing of a discrete multichannel signal consisting of n frequency samples is performed by an n-channel filter, which differs from a matched filter by the presence in each channel of a two-way amplitude limiter.

A suboptimal circuit for the processing of such a signal is synthesized in the following on the basis of statistical decision theory, where the circuit takes the form of a matched filter, in each channel of which a nonlinear network is employed which processes in an optimal manner a signal element against a background of structural interference and noise.

The synthesis of the optimal detector of a signal element. An element $u_M(t\psi)$, of the interfering signal (structural interference) and noise act on an element $U(t,\psi)$ of the useful signal, where the noise interference is approximated by white noise, and where ϕ and ψ are the random initial phases of the elements of the useful and interfering signals, which are uniformly distributed over the range $[0, 2\pi]$:

$$\dot{\imath}_{10}=\frac{\frac{1}{4\pi^2}\int_0^{2\pi}\int_0^{2\pi}\exp\left\{-\frac{1}{N_0}\left[\int_0^{\tau_\pi}(x(t)-u(t,\varphi)-u_M(t,\psi))^2dt+\right.\right.}{\frac{1}{2\pi}\int_0^{2\pi}\exp\left\{-\frac{1}{N_0}\left[\int_0^{\tau_\pi}(x(t)-u_M(t,\psi))^2dt+\right.\right.}\rightarrow$$

$$\rightarrow\frac{\left.\left.+\int_{\tau_\pi}^{T_\Theta}(x(t)-u(t,\varphi))^2dt\right]\right\}d\varphi d\psi}{\left.\left.+\int_{\tau_\pi}^{T_\Theta}x^2(t)\,dt\right]\right\}d\psi}, \tag{1}$$

where T_Θ [T_e] is the width of the useful and interfering signal elements; the moments of appearance of the interfering elements in the range have a uniform distribution; τ_π is the overlap time of the useful and interfering elements.

If the amplitude of the interfering signals is much greater than the amplitude of the useful signal, i.e., $u_M(t,\psi) >> u(t,\phi)$, expression (1) assumes the form

$$\dot{\imath}_{10}\approx\frac{\frac{1}{2\pi}\int_0^{2\pi}\exp\left\{-\frac{1}{N_0}\int_{\tau_\pi}^{T_\Theta}[x(t)-u(t,\varphi)]^2dt\right\}d\varphi}{\exp\left\{-\frac{1}{N_0}\int_{\tau_\pi}^{T_\Theta}x^2(t)\,dt\right\}}. \tag{2}$$

It can be seen from (2) that the network for processing the signal element against a background of an interfering signal and moise element (see Figure 1) should consist of a matched filter (SF), which is cut off during the time the element of the interfering signal $u_M(t, \psi)$ acts. The circuit contains a

matched filter for the element $u(t, \phi)$ of the useful signal (SF_e), a noise detector (OP) an a switch (K) which does not pass the input signal to the filter if interference is contained in it. The interference detector for the range $\Delta t = t_{i+1} - t_i << T_e$ detects the interference against the background of noise, and in accordance with the decision which is made, controls the operation of K [the switch].

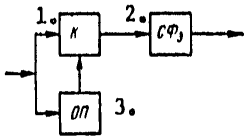

Figure 1.

Key: 1. K [switch];
2. SF_e [matched filter for the useful signal element];
3. OP. [interference detector].

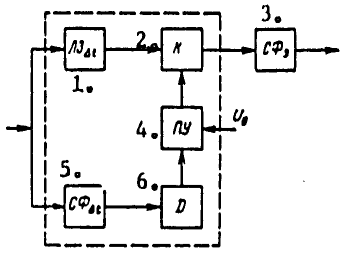

Figure 2.

Key: 1. $LZ_{\Delta t}$ [delay line];
2. K [switch];
3. SF_e [matched filter for the useful signal element];
4. PU [threshold gate];
5. $SF_{\Delta t}$ [matched filter for Δt];
6. D [envelope detector].

The probability ratio for the interference element, taking into account the action of noise, is equal to:

$$\lambda_{10}^{M} = \frac{\frac{1}{2\pi}\int_0^{2\pi} \exp\left\{-\frac{1}{N_0}\left[\int_{t_i}^{t_i+\Delta t} (x(t) - u_M(t, \psi))^2\, dt\right]\right\} d\psi}{\exp\left\{-\frac{1}{N_0}\int_{t_i}^{t_i+\Delta t} x^2(t)\, dt\right\}}. \quad (3)$$

and correspondingly, the optimal detection circuit for the interfering signal element with a random initial phase consists of the matched filter with a detector or a quadrature correlator and a threshold device.

Taking this into account, the circuit of Figure 1 assumes the form of Figure 2 and consists of the matched filter, which detects the element of the interfering signal in the range Δt ($SF_{\Delta t}$), an envelope detector (D) and the threshold device (PU) with a threshold of U_0. The voltage from the output of the threshold gate controls the opreration of switch K, to the input of which the input signal is fed through a delay line Δt ($LZ_{\Delta t}$). When an interfering signal voltage is present in the input signal, K is cut off, and there is no voltage at the output of the matched filter.

With Δt tending to zero, the portion of the block diagram in Figure 2 (see the dashed line) is replaced by a nonlinear element (NE) with the characteristic (Figure 3):

$$U_{out} = U_{вых} = \begin{cases} U_{вх} \text{ при } |U_{вх}| \leqslant U_0, \\ 0 \text{ при } |U_{вх}| > U_0 \end{cases} \quad (4)$$

$$[U_{BX} = U_{in}]$$

Such a nonlinearity form can be easily realized. Correspondingly, the optimum processing circuit (OSO_e) for the element $u(t, \phi)$ of the useful signal against the background of the element $u_M(t, \psi)$ of the interfering signal [$u_M(t, \psi) >> u(t,\phi)$] and the noise interference consists of a bandpass filter (TF), a nonlinear element with the characteristic (4), a matched filter for the useful signal element (Figure 4).

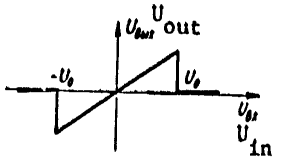

Figure 3.

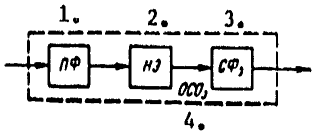

Figure 4.

Key: 1. PF [bandpass filter];
2. NE [nonlinear element];
3. SF_e [matched filter for the useful signal element];
4. OSO_e [optimal processing circuit for the useful signal element].

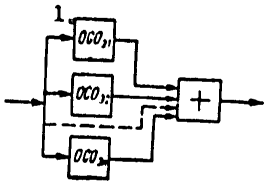

Figure 5.

Key: 1. OSO_{e1} [optimal procesing circuit for useful signal element e1].

The block diagram of a suboptimum receiver for filtering a discrete multifrequency signal against a background of mutual interference and moise (Figure 5) is ar n-channel filter, each channel of which consists of an optimal nonlinear filter for the signal element.

Noise immunity analysis. We shall consider the signal to noise ratio at the output of one of the channels of the suboptimal filter as a function of the threshold level U_0 in the absence of mutual interference. When the signal and noise pass through the nonlinear element, the power is redistributed with respect to frequency at the output as compared to the input, something which must be taken into account in calculating the error probability. For this, we shall compute the correlation function of the signal and noise mixture at the output of the nonlinear element. In accordance with [6], taking into account nonlinearity of the form of (4), we write

$$B(\tau, t) = \sum_{n=0}^{\infty} c_n(t)\, c_n(t+\tau)\, \frac{R^n(\tau)}{n!}, \qquad (5)$$

where $R(\tau) = \frac{\sin 2\pi\Delta F\tau}{2\pi\Delta F\tau}\cos\omega_0\tau$ is the noise correlation coefficient at the output of the bandpass filter;

$$c_n(t) = \frac{c}{\sqrt{2\pi}} \int_{-U_0/\sigma}^{U_0/\sigma} x H_n\left(x - \frac{U}{\sigma}\cos\theta\right) e^{-\frac{\left(x-\frac{U}{\sigma}\cos\theta\right)^2}{2}} dx;$$

σ is the mean square deviation of the noise at the output of the bandpass filter, $\sigma^2 = 2N_0\Delta F$; $\Delta F = 1/T_e$ is the bandwidth of a signal element; N_0 is the spectral noise density; $\theta = \omega_0 t + \phi$ is the total phase of the signal; U is the signal amplitude;

$H_n(x) = (-1)^n e^{\frac{x^2}{2}} \frac{d^n}{dx^n}(e^{-\frac{x^2}{2}})$ при $n = 0, 1, 2, \ldots$ is a Hermite polynomial.

When $U/\sigma << 1$, we have:

$$e^{-\frac{\left(x-\frac{U}{\sigma}\cos\theta\right)^2}{2}} \approx I_0\left(\frac{U^2}{4\sigma^2}\right) e^{-\frac{U^2}{4\sigma^2}} e^{-\frac{x^2}{2}}\left[I_0\left(\frac{U}{\sigma}x\right) + 2\sum_{k=1}^{\infty} I_k\left(\frac{U}{\sigma}x\right)\cos k\theta\right],$$

$$H_n\left(x - \frac{U}{\sigma}\cos\theta\right) e^{-\frac{\left(x-\frac{U}{\sigma}\cos\theta\right)^2}{2}} = (-1)^n \frac{d^n}{d\left(x-\frac{U}{\sigma}\cos\theta\right)^n} \times$$

$$\times\left[e^{-\frac{\left(x-\frac{U}{\sigma}\cos\theta\right)^2}{2}}\right] \approx (-1)^n I_0\left(\frac{U^2}{4\sigma^2}\right) e^{-\frac{U^2}{4\sigma^2}} \frac{d^n}{dx^n} \times$$

$$\times\left\{e^{-\frac{x^2}{2}}\left[I_0\left(\frac{U}{\sigma}x\right) + 2\sum_{k=1}^{\infty} I_k\left(\frac{U}{\sigma}x\right)\cos k\theta\right]\right\},$$

then

$$c_0(t) \approx I_0\left(\frac{U^2}{4\sigma^2}\right) e^{-\frac{U^2}{4\sigma^2}}\left[\Phi\left(\frac{U_0}{\sigma}\right) - \sqrt{\frac{2}{\pi}}\frac{U_0}{\sigma} e^{-\frac{U_0^2}{2\sigma^2}}\right] U\cos\theta,$$

$$c_1 \approx \sigma I_0\left(\frac{U^2}{4\sigma^2}\right) I_0\left(\frac{UU_0}{\sigma^2}\right) e^{-\frac{U^2}{4\sigma^2}}\left[\Phi\left(\frac{U_0}{\sigma}\right) - \sqrt{\frac{2}{\pi}}\frac{U_0}{\sigma} e^{-\frac{U_0^2}{2\sigma^2}}\right],$$

$$c_{2n+1} \approx -\sqrt{\frac{2}{\pi}}\sigma I_0\left(\frac{U^2}{4\sigma^2}\right) I_0\left(\frac{UU_0}{\sigma^2}\right) e^{-\frac{U^2}{4\sigma^2}} e^{-\frac{U_0^2}{2\sigma^2}}\left[(2n+1)\times\right.$$
$$\left.\times H_{2n-1}\left(\frac{U_0}{\sigma}\right) + H_{2n+1}\left(\frac{U_0}{\sigma}\right)\right], \quad c_{2n} \approx 0.$$

Correspondingly, expression (5) assumes the form:

$$B(\tau, t) \approx c_0(t)\, c_0(t+\tau) + \sum_{n=0}^{\infty} c_{2n+1}^2 \frac{R^{2n+1}(\tau)}{(2n+1)!}. \qquad (6)$$

From (6), we find the mathematical mean m_1 and the dispersion D at the output of the matched filter:

$$m_1 \approx I_0\left(\frac{U^2}{4\sigma^2}\right) e^{-\frac{U^2}{4\sigma^2}}\left[\Phi\left(\frac{U_0}{\sigma}\right) - \sqrt{\frac{2}{\pi}}\frac{U_0}{\sigma} e^{-\frac{U_0^2}{2\sigma^2}}\right]\frac{UT}{2}\cos\varphi \qquad (7)$$

$$D \approx \sum_{n=0}^{\infty} \frac{c_{2n+1}^2}{(2n+1)!}\int_{-T}^{T} \frac{T}{2} R^{2n+1}(\tau)\cos\omega_0\tau\, d\tau. \qquad (8)$$

We represent the integral in (8) as:

$$\int_{-T}^{T} \frac{T}{2} R^{2n+1}(\tau)\cos\omega_0\tau d\tau = \int_0^T T\left[\frac{\sin\Delta\Omega\tau}{\Delta\Omega\tau}\right]^{2n+1}\cos^{2n+2}\omega_0\tau d\tau =$$

$$= \frac{T}{\Delta\Omega}\int_0^{2\pi}\left(\frac{\sin x}{x}\right)^{2n+1}\cos^{2n+2}\frac{\omega_0}{\Delta\Omega}\,x dx,$$

where $x = \Delta\Omega\tau = \Delta\Omega;\ 2\pi\Delta F.$

Then when $\omega_0/\Delta\Omega >> 1$, considering only the constant component of the series

$$\cos^{2n+2}\frac{\omega_0}{\Delta\Omega}x = \frac{1}{2^{2n+2}}\left[\sum_{k=0}^{n} 2\binom{2n+2}{k}\times\right.$$

$$\left.\times\cos 2(n+1-k)\frac{\omega_0}{\Delta\Omega}x + \binom{2n+2}{n+1}\right].$$

We have

$$\frac{T}{\Delta\Omega}\int_0^{2\pi}\left(\frac{\sin x}{x}\right)^{2n+1}\cos^{2n+2}\frac{\omega_0}{\Delta\Omega}x dx = \frac{T}{\Delta\Omega}\frac{1}{2^{2n+2}}\times$$

$$\times\binom{2n+2}{n+1}\int_0^{2\pi}\left(\frac{\sin x}{x}\right)^{2n+1}dx = \frac{T}{2\Delta\Omega}\frac{(2n+1)!}{2^{2n}n!(n+1)!}\int_0^{2\pi}\left(\frac{\sin x}{x}\right)^{2n+1}dx \approx$$

$$\approx \frac{T}{2\Delta\Omega}\frac{(2n+1)!}{2^{2n}n!(n+1)!}\int_0^{\infty}\left(\frac{\sin x}{x}\right)^{2n+1}dx.$$

Following transformations, we finally obtain:

$$D \approx \frac{N_0 T}{4} I_0^2\left(\frac{U^2}{4\sigma^2}\right) I_0^2\left(\frac{UU_0}{\sigma^2}\right) e^{-\frac{U^2}{2\sigma^2}}\left\{\left[\Phi\left(\frac{U_0}{\sigma}\right) - \right.\right.$$

$$\left.-\sqrt{\frac{2}{\pi}}\frac{U_0}{\sigma}e^{-\frac{U_0^2}{2\sigma^2}}\right]^2 + \frac{2}{\pi}e^{-\frac{U_0^2}{\sigma^2}}\sum_{n=1}^{\infty}\frac{2}{\pi}\int_0^{\infty}\left(\frac{\sin x}{x}\right)^{2n+1}dx\times$$

$$\left.\times\frac{\left[(2n+1)H_{2n-1}\left(\frac{U_0}{\sigma}\right) + H_{\ldots}\left(\frac{U_0}{\sigma}\right)^{\ldots}\right]}{2^{2n}n!(n+1)!}\right\}. \qquad (9)$$

From (7) and (9), the signal/noise ratio is equal to

$$\frac{m_1}{\sqrt{D}} = \gamma\sqrt{\frac{U^2T}{N_0}}\cos\varphi,$$

where the coefficient γ determines the losses in the signal/noise ratio which arise as a result of the signal and noise passing through the nonlinear element.

We shall study γ^2 as a function of (U_0/σ, U/σ); and since $U/\sigma \ll 1$, we will plot the function $\gamma^2 = f(U_0/\sigma)$ (Figure 6).

It can be seen from Figure 6 that with a decrease in U_0/σ, γ^2 also falls off, i.e., the losses in the signal/noise ratio increase. This is explained by the fact with a decrease in the threshold, the input signal which has a normal distribution, exceeds the threshold for the majority of the time. Consequently, the matched filter is cut off the majority of the time and the signal/noise ratio will fall off. When $U_0/\sigma \approx 1.6$, $\gamma^2 = \pi/4$, which corresponds to the losses for a circuit with a stiff limiter. Thus, when $U_0/\sigma > 1.6$, the losses in the signal/noise ratio for the circuit studied here are less than for a circuit with a stiff limiter.

We shall consider the action of strong mutual interference ($U_M/\sigma \gg 1$) on the signal element. We shall compute the dispersion at the output of one channel of the suboptimal filter for a discrete multifrequency signal, where this dispersion is determined by the passage of the mutual interference through the channel. For simplicity in the calculation, we shall assume that the interference element completely overlaps the signal element. The voltage at the output of the channel is equal to:

$$U_{вых} = \frac{\omega_0 T}{2\pi}\left[U_M \int_{\frac{\arccos\frac{U_0}{U_M}}{\omega_0}}^{\frac{\pi-\arccos\frac{U_0}{U_M}}{\omega_0}} \cos\omega_0 t \cos(\omega_0 t + \psi)\,dt + U_M \int_{\frac{\pi+\arccos\frac{U_0}{U_M}}{\omega_0}}^{\frac{2\pi-\arccos\frac{U_0}{U_M}}{\omega_0}} \times \right.$$
$$\left. \times \cos\omega_0 t \cos(\omega_0 t + \psi)\,dt\right].$$

Following transformations, we have:

$$U_{out} = U_{вых} = \frac{U_M T}{\pi}\cos\psi\left[\arcsin\frac{U_0}{U_M} - \frac{U_0}{U_M}\sqrt{1-\left(\frac{U_0}{U_M}\right)^2}\right].$$

Averaging U^2_{out} with respect to ψ, we obtain an expression for the dispersion:

$$D_M = \overline{U}^2_{вых} = \frac{U_M^2 T^2}{8}\frac{4}{\pi^2}\left[\arcsin\frac{U_0}{U_M} - \frac{U_0}{U_M}\sqrt{1-\left(\frac{U_0}{U_M}\right)^2}\right]^2.$$

In the absence of mutual interference, the amount of dispersion determined by the noise and the system operates in a linear mode. The interference which creates a dispersion which does not exceed the dispersion due to noise does not cause a substantial degredation in the noise immunity of the circuit. Its amplitude $U_{M.ш.}$ [$U_{M.п.}$] can be computed by equating D_M to $N_0T/4$, i.e.:

$$\frac{U^2_{M.ш} T^2}{8}\frac{4}{\pi^2}\left[\arcsin\frac{U_0}{U_{M.ш}} - \frac{U_0}{U_{M.ш}}\sqrt{1-\left(\frac{U_0}{U_{M.ш}}\right)^2}\right]^2 = \frac{N_0 T}{4}. \qquad (10)$$

By designating $U_0/U_{M.n.} = z$, and taking into account the equality $2N_0/T = 2N_0\Delta F = \sigma^2$, following transformations of (10), we obtain an equation in terms of z:

$$\frac{2}{\pi}\left[\frac{1}{z}\arcsin z - \sqrt{1-z^2}\right] = \frac{\sigma}{U_0}. \qquad (11)$$

By plotting a graph of the following function in Figure 7:

$$y = \frac{2}{\pi}\left[\frac{1}{z}\arcsin z - \sqrt{1-z^2}\right],$$

We solve equation (11) graphically. The graph defines the function $\sigma/U_0 = f(U_0/U_{M.n.})$: plotting the requisite σ/U_0 ratio along the y axis, we find the value of $U_0/U_{M.n.}$ corresponding to it on the z axis. For example, when $\sigma/U_0 = 1/3$ (at a threshold three times greater than the mean square deviation of the noise), $U_0/U_{M.n.} = 0.78$, or $U_{M.n.} = 1.28\,U_0$, i.e., in this case an interference element with an amplitude of $U_M = 1.28U_0$ creates a dispersion at the channel output equal to the dispersion due to the noise $D_M = N_0T/4$. When $U_M > U_{M.n.}$, the interference element dispersion is less than the noise dispersion.

In carrying out preliminary studies of the change in the signal/noise ratio when the input signal passes through the nonlinear element, we compute the noise immunity of a suboptimal circuit for processing a discrete multi-frequency signal when transmitting discrete information with two orthogonal signals and with incoherent reception. "White" noise with a spectral density of N_0 and mutual interference, the amplitudes of the elements of which exceed $U_{M.n.}$, act on the signal. We designate $\alpha = n_M/n$, where n_M is the number of elements of the discrete multifrequency signal, where these elements are subject to the action of mutual interference; n is the overall number of elements in the signal.

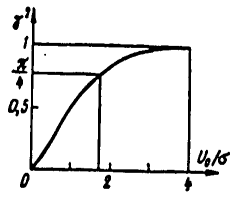

Figure 6.

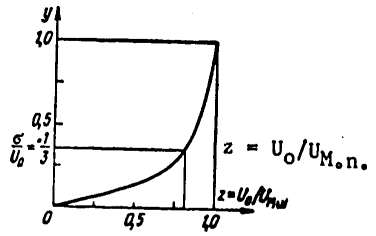

Figure 7.

Considering the fact that the voltages at the outputs of the channels of a suboptimal filter have a finite dispersion and are statistically independent, while n is large, the probability density at the output of the adder can be approximated by a normal distribution. The error probability in the case of incoherent discrimination of two orthogonal signals against a background of normal noise is equal to [9]:

$$P_{err} = P_{ош} = \frac{1}{2} e^{-\frac{(E_\Sigma/U)^2}{4D_\Sigma}}.$$

In this case $E_\Sigma = \gamma n E_1 (1-\alpha) = \gamma E (1-\alpha)$ where $E_1 = U^2T/2$ is the energy of a signal element; $E = nE_1$ is the energy of the entire signal. If the size of the dispersion from the interference elements does not exceed the size of the dispersion due to noise, then $D_\Sigma = nN_0T/4$, and

$$P_{err}\ P_{ош} < \frac{1}{2} e^{-\frac{[\gamma n E_1 (1-\alpha)/U]^2}{4n\frac{N_0 T}{4}}} = \frac{1}{2} e^{-\gamma^2 \frac{E}{2N_0}(1-\alpha)^2}.$$

When $U_M \to \infty$, the amount of dispersion from interference elements tends to zero. Then $D_\Sigma \to nN_0T/4(1-\alpha)$ and :

$$P_{err}\ P_{ош} \to \frac{1}{2} e^{-\frac{[\gamma n E_1 (1-\alpha)/U]^2}{4n\frac{N_0 T}{4}}} = \frac{1}{2} e^{-\gamma^2 \frac{E}{2N_0}(1-\alpha)}.$$

We finally obtain the inequality:

$$\frac{1}{2} e^{-\gamma^2 \frac{E}{2N_0}(1-\alpha)} < P_{ош} < \frac{1}{2} e^{-\gamma^2 \frac{E}{2N_0}(1-\alpha)^2}. \qquad (12)$$

Inequality (12) is justified for interference, the amplitude of which exceeds $U_{M.n.} = kU_0$, where k is a certain coefficient determined from the graph in Figure 7. With the action of interference with a lower amplitude, the noise immunity of the circuit will fall off.

For protection against low amplitude interference, it is necessary to reduce the threshold U_0, something which leads to a reduction in γ^2, i.e., to an increase in the losses in the signal/noise ratio and a degredation of the noise immunity. If the threshold is equal to 3σ, $\gamma^2 \approx 1$, and inequality (12) assumes the form:

$$\frac{1}{2} e^{-\frac{E}{2N_0}(1-\alpha)} < P_{ош} < \frac{1}{2} e^{-\frac{E}{2N_0}(1-\alpha)^2}. \qquad (13)$$

We shall compare the noise immunity of the synthesized suboptimal circuit with the noise immunity of a circuit with stiff limiting [2], for which the error probability under the same conditions is equal to:

$$P_{err} = P_{ош} = \frac{1}{2} e^{-\frac{\pi}{4}\frac{E}{2N_0}(1-\alpha)^2}.$$

In the absence of mutual interference ($\alpha = 0$), the losses in the signal/noise ratio of the latter circuit are 1 dB ($\gamma^2 = \pi/4$). In this case, the noise immunity of the suboptimal circuit corresponds to the noise immunity of the linear circuit, since $\gamma \approx 1$.

Shown in Figure 8 are graphs of the error probability of a function of the signal/noise ratio, E/N_0, at the input of the resolver of the receiver where $\alpha = 0.5$; curve 1 corresponds to the lower bound of inequality (13); curve 2 corresponds to the upper bound; curve 3 characterizes the error probability for a circuit with a stiff limiter. Comparing curve 2 and 3 we see that the suboptimal circuit has a gain in the noise immunity over that of a circuit with a stiff limiter, the losses of which amount to 1 dB as a result of the limiting of the input signal. When the amplitudes of the interference elements tend to infinity, the dispersions at the outputs of the channels of the suboptimal filter of such elements tend to zero, as a result of which, the overall dispersion decreases. The error probability in this case is determined by curve 1.

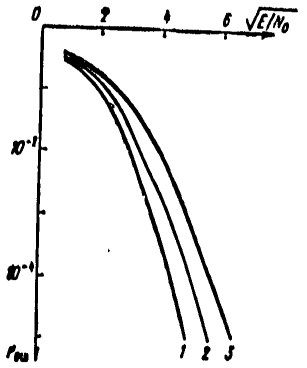

Figure 8.

Thus, the gain in the noise immunity of the structure studied here as compared to a structure with a stiff limiter is determined by the following: in the first place, by the absence of losses which arise as a result of severe limiting; in the second place, by the decrease in the overall dispersion (the increase in the signal/noise ratio) at the output of the adder as a result of the action of the interference elements having an amplitude of $U_M >> U_{M.n.}$ With the action of interference elements having lesser amplitudes, the noise immunity of the circuit studied here is degraded, however, as experimental studies have shown, it can be assumed that they will not exert a substantial influence on the noise immunity, due to their normalization at the output of the adder.

BIBLIOGRAPHY

1. L.Ye. Varakin, I.M. Pyshkin, RADIOTEKHNIKA, 1973, Vo. 28, No 11.

2. V.N. Vlasov, IZVESTIYA VUZOV SSSR [PROCEEDINGS OF THE HIGHER EDUCATIONAL INSTITUTES OF THE USSR], RADIOELEKTRONIKA Series, 1975, Vol XVIII, No 4.

3. L.Ye. Varakin, I.M. Pyshkin, Article in the book, "Trudy nauchno-tekhnicheskoy konferentsii professorsko-prepodavatel'skogo sostava MEIS" ["Proceedings of the Scientific and Engineering Conference of the Professorial and Teaching Staff of the Moscow Communications Engineering Institute"], SM SSSR, 1967.

4. L.Ye. Varakin, I.M. Pyshkin, TRUDY UCHEBNYKH INSTITUTOV SVYAZI [PROCEEDINGS OF THE COMMUNICATIONS TRAINING INSTITUTES], Leningrad, Leningrad Communications Engineering Institute imeni M.A. Bonch-Bruyevich, No 35. 1967.

5. Yu.B. Chernyak, RADIOTEKHNIKA I ELEKTRONIKA, 1962, Vol VII, No 7.

6. B.R. Levin, "Teoreticheskiye osnovy statisticheskoy radiotekhniki" ["The Theoretical Principles of Statistical Radio Engineering"], Book 1, Moscow, Sovetskoye Radio Publishers, 1974.

8225
CSO:1870

ELECTRONICS AND ELECTRICAL ENGINEERING

UDC 621.391.828:621.396.677.83

A SHIELD IN THE SHAPE OF A DOUBLE RING TO SHIELD ANTENNAS AGAINST INTERFERENCE

Moscow RADIOTEKHNIKA in Russian No 11, Nov 78 pp 68-72

[Article by Yu.M. Mel'nikov, manuscript received following revision 15 May, 1978]

[Text] One of the simplest ways of combating the interference which acts on an antenna is shielding the antenna in the direction of the incoming interference. Electromagnetic shields, which are passive and rather simple devices, permit the solution of a complex of problems related to improving the electromagnetic compatibility of various radioelectronic equipment.

The use of various shields is described in [1-3]. An analysis shows that the simplest, continuous rectangular or square shields are of little effectiveness in many cases. The comparatively high field level in the shaded region, due to the penetration of diffraction fields from the edges of the shield into the region of the geometric shadow, does not allow for a satisfactory compromise between the level of field suppression by the shield and its dimensions.

The electrical characteristics of an annular shield, described in [4], were studied in [5]. For this shield, the ratio of the size of the suppression region for a specified level to its area is maximum as compared to other shields described in [4, 6, 7].

When a plane or a spherical wave falls on the annular shield from the left (Figure 1), the field is equal to zero at the design point P on the axis of the shield, taking into account the assumptions we have made, if the dimensions of the shield are $\rho_1 = \rho_0\sqrt{1/3}$; $\rho_2 = \rho_0\sqrt{2/3}$, where ρ_0 is the radius of the first Fresnel zone, defined for the point wave source and the point P. For plane wave, $\rho_0 = \sqrt{\lambda_0 r_0}$. It is assumed in the analysis that $\rho_2 \ll r_0$; $\rho_1 \gg \gamma$; and $\rho_2 - \rho_1 \gg \gamma$, and in this case, Kirchoff's method can be used in scalar form without a great loss in precision.

The shield described here can be successfully employed to shield comparatively poorly directional microwave antennas against interference. However, for antennas with a relatively high gain (35 dB and above), its effectiveness is inadequate.

In this regard, there arises the problem of designing a shield of increased effectiveness, which would permit protecting comparatively highly directional antennas against interference (for example, radio relay link antennas).

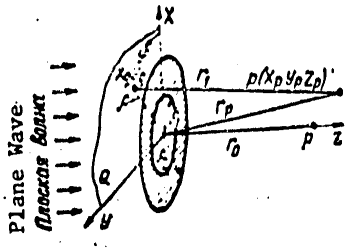

Figure 1.

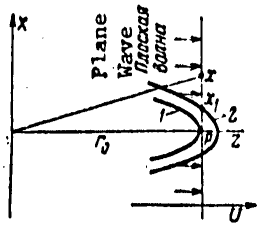

Figure 2.

To solve this problem, the field a point P can be represented in the following form [5] where an annular type shield is present:

$$U_p = U_q \exp(-ikz_p) - \frac{ikz_p U_q}{2\pi} \int_0^{2\pi} \int_{\rho_1}^{\rho_2} \frac{\exp(-ikr_1)}{r_1^2} \rho d\varphi d\rho. \qquad (1)$$

It follows from (1) that the field at point P is the difference between the field of the plane wave at this point and the field produced by the shield. The field distribution produced by the ring has a maximum at point P (Figure 2). Plotted along the U axis are values of the plane wave amplitude and the amplitude of the ring field (curve 1); the maximum of the ring field is equal in amplitude and opposite in phase to the plane wave field. For this reason, there is complete cancellation of the fields at point P. When moving from point P along the X axis, the equal amplitude and equally opposite phase conditions of the fields are violated, something which leads to a sharp increase in the resulting field. The axial symmetry of the ring easily allows for independent adjustment of the amplitude and phase of the field created by the ring at point P and in its vicinity.

By increasing the area of the ring without changing its center radius, one can provide for equality of the amplitudes of the plane wave and ring fields not at point P, but at some point x_1 (Figure 2, curve 2). Then, by changing the phase of the ring field without changing its amplitude, the precise opposite phase conditions of the fields considered here can be obtained at this point. As a result, we obtain complete cancellation of the field on a circle

of radius x_1 with a center at point P, which falls in a plane parallel to the plane of the ring. In this case, there will be a partial maximum of the field at point P.

The expressions for the inner and outer radii of the ring are [5]:

$$\rho_1 = \sqrt{\lambda_0 r_0}\sqrt{\frac{1}{2} - \beta^2 - \gamma}; \qquad \rho_2 = \sqrt{\lambda_0 r_0}\sqrt{\frac{1}{2} - \beta^2 + \gamma}. \tag{2}$$

By varying β with a constant γ, we change the phase of the field created by the ring, while its amplitude is constant. By varying γ with a constant β, we change the amplitude while the phase is constant. When $\beta = 0$ and $\gamma = 1/6$, we obtain the values of ρ_1 and ρ_2 for the usual ring, which produces complete suppression of the field at point P.

The expression for the field $F(v, \mu, \nu, \beta, \gamma)$ normalized with respect to the incident wave, where $v = \sqrt{\frac{x_p^2 + y_p^2}{\lambda_0 r_0}}$; $\mu = \lambda/\lambda_0$; $\nu = z_p/r_0$ has the form [5]:

$$F(v, \mu, \nu, \beta, \gamma) = 1 + \exp\left[-\frac{i\pi v^2}{\mu\nu}\right] \times$$
$$\times \left\{\exp\left[-\frac{i\pi\left(\frac{1}{2} - \beta^2 - \gamma\right)}{\mu\nu}\right] \sum_{n=1}^{\infty} \left[\frac{i\pi\left(\frac{1}{2} - \beta^2 - \gamma\right)}{\mu\nu}\right]^n \times \right.$$
$$\times \frac{\Lambda_n\left(\frac{2\pi}{\mu\nu}\sqrt{\frac{1}{2} - \beta^2 - \gamma}\right)}{n!} - \exp\left[-\frac{i\pi\left(\frac{1}{2} - \beta^2 + \gamma\right)}{\mu\nu}\right] \times$$
$$\left. \times \sum_{n=1}^{\infty} \left[\frac{i\pi\left(\frac{1}{2} - \beta^2 + \gamma\right)}{\mu\nu}\right]^n \frac{\Lambda_n\left(\frac{2\pi}{\mu\nu}\sqrt{\frac{1}{2} - \beta^2 + \gamma}\right)}{n!}\right\}. \tag{3}$$

It follows from the curves in Figure 3, plotted from formula (3) for different values of β and γ (curve 1: the function F(v) for $\beta = 0$, $\gamma = 1/6$, i.e., for the usual ring; 2 corresponds to $\beta = 0.1$, and $\gamma = 0.177$; 3 corresponds to $\beta = 0.2$ and $\gamma = 0.215$; and 4 corresponds to $\beta = 0.25$, $\gamma = 0.287$) that at specified ring parameters, the suppression region can be expanded with respect to a specified level. Thus, for example, the suppression region for the -24 dB level (curve 2) is 42% wider than the suppression region for the same level of an unmodified ring ($\beta = 0$; $\gamma = 1/6$). The increase in the width of the suppression region permits a reduction in the spacing between the shield and the unit being protected by 1.2--1.5 times.

It would be possible to significantly boost the effectiveness of the shield if one could suppress the partial maximum of the field at point P without substantially increasing the field at the maximum suppression circle. The

compensation of the field maximum at point P is possible by using an additional ring with a greater radius, concentric to the first one. The dimensions of the additional ring should be chosen so that its field at point P is opposite in phase to the field of the main ring. Obviously, this ring should fall in this case in the out-of-phase (second) Fresnel zone. Since the dimensions of the second ring are greater than the dimensions of the main one, its directional pattern is narrower, and for this reason, it can be assumed that its field will not substantially increase the field close to the circle of radius x_1.

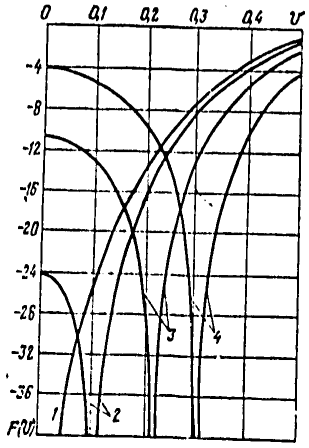

Figure 3.

To obtain a shield with the widest possible region of suppression, it is desirable to use a main ring with parameters at which the radius x_1 of the circle for complete suppression of the field is maximal. However, calculations show that even at $\beta = 0.3$, there are no values of γ at which a sufficiently deep trough can be obtained in the field distribution in the vicinity of point P. This is related to the fact that point x_1 falls in the region of the out-of-phase side lobe of the field distribution of the ring, where it is already impossible to obtain the out-of-phase condition of the ring and plane wave fields. For this reason, we shall use a ring with parameters of $\beta = 0.25$ and $\gamma = 0.287$ as the initial shield.

As an analysis and calculations for the inner and outer radii of the second ring show, we have: $\rho_3 = \xi_3\sqrt{\lambda_0 r_0} = \sqrt{\lambda_0 r_0 (d - \gamma_1)}$; $\rho_4 = \xi_4\sqrt{\lambda_0 r_0} = \sqrt{\lambda_0 r_0 (d + \gamma_1)}$, where d = 1.3353. The quality γ_1 can be determined through selection taking into account the requirements for obtaining the best suppression function F(v), from the viewpoint of effectiveness. For F(v, μ, ν), we obtain from (1):

$$F(v, \mu, \nu) = 1 - i\frac{2\pi}{\mu\nu} e^{-i\frac{\pi}{\mu\nu}v^2} \sum_{n=1}^{4} (-1)^n \int_0^{\xi_n} e^{-i\frac{\pi}{\mu\nu}\xi^2} J_0\left(\frac{2\pi}{\mu\nu} v\xi\right) \xi d\xi. \qquad (4)$$

There is no point in expanding the integrals in a series in terms of the functions Λ_n, as for the case of a single ring, since for large values of $\xi(\xi_3, \xi_4)$, the series converges slowly, something which creates inconvenience in the calculations. For this reason, we shall make use of another method. In accordance with [8]:

$$\int_0^1 e^{-i\lambda x^2} J_0(\sigma x) x dx = \frac{e^{-i\lambda}}{2\lambda} [U_1(2\lambda, \sigma) + iU_2(2\lambda, \sigma)], \qquad (5)$$

where $U_1(2\lambda, \sigma)$ and $U_2(2\lambda, \sigma)$ are the corresponding Lommel functions two variables. By using (5), (4) can be reduced to the form:

$$F(v, \mu, \nu) = 1 - 1e^{-i\frac{\pi}{\mu\nu}v^2} \sum_{n=1}^{4} (-1)^n \times$$

$$\times \left\{ e^{-i\frac{\pi\xi_n^2}{\mu\nu}} \left[U_1\left(\frac{2\pi\xi_n^2}{\mu\nu}, \frac{2\pi\xi_n v}{\mu\nu}\right) + iU_2\left(\frac{2\pi\xi_n^2}{\mu\nu}, \frac{2\pi\xi_n v}{\mu\nu}\right) \right] \right\}. \quad (6)$$

The functions $U_1(w, z)$ and $U_2(w, z)$ are tabulated in [9] for $w > 0.5$ and $z > 0.5$. In the case considered here, when $v \to 0$, and $x \to 0$, it is also impossible to use the tables. Approximate expressions are derived in [10] for the functions $U_0(ax, x)$ and $U_1(ax, x)$. By employing [11] (after correcting the misprints) and [12], we obtain:

$$U_2(y, x) = U_0\left(\frac{x^2}{y}, x\right) - \cos\frac{1}{2}\left(y + \frac{x^2}{y}\right);$$

$$U_1(y, x) = U_1\left(\frac{x^2}{y}, x\right) + \sin\frac{1}{2}\left(y + \frac{x^2}{y}\right). \quad (7)$$

In accordance with [10], we have:

$$U_0(ax, x) = \frac{1}{2}J_0(x) + \frac{a^2}{1+a^2}\cos bx + \frac{1-a^4}{4(1+a^2)} \times$$

$$\times \left[(1 + a^4 - \sqrt{2}a^2)\cos\left(x\sin\frac{\pi}{8}\right) + (1 + a^4 + \sqrt{2}a^2) \times \right.$$

$$\left. \times \cos\left(x\cos\frac{\pi}{8}\right) \right] + \operatorname{Re}\delta;$$

$$U_1(ax, x) = \frac{a^2}{1+a^2}\sin bx + \frac{a(1-a^2)}{2(1+a^2)} \times$$

$$\times \left[(1 + a^4 - \sqrt{2}a^2)\sin\frac{\pi}{8}\sin\left(x\sin\frac{\pi}{8}\right) + \right.$$

$$\left. + (1 + a^4 + \sqrt{2}a^2)\cos\frac{\pi}{8}\sin\left(x\cos\frac{\pi}{8}\right) \right] + \operatorname{Im}\delta, \quad (8)$$

where $a = x/y$; $b = \frac{1+a^2}{2a}$; $\delta = i\sqrt{(b^2-1)}e^{ibx}\int_0^x e^{-ib\xi} \sum_{n=1}^{\infty}(-1)^n J_{8n}(\xi)\,d\xi$.

In the case considered here, $x = 2\pi\xi_n v/\mu\nu$; $y = 2\pi\xi_n^2/\mu\nu$; $a = v/\xi_n$; $b = (\xi_n^2 + v^2)/2v\xi_n$.

By making use formulas (6) -- (8), the function $F(v, \mu, \nu)$ can be computed for small values of $2\pi\xi_n v/\mu\nu$. In this case, when $v = 0$ and $v = \xi_n$, formulas (8) yield the exact value of the functions $U_0(ax, x)$ and $U_1(ax, x)$ [10].

After performing the corresponding calculations, the best shape of the curve (the deepest and most uniform suppression in the wide region) for F(v, 1, 1) was obtained at $\gamma_1 = 0.1$ (the solid curve in Figure 4). Thus, we find the parameters of the double ring: $\beta = 0.25$, $\gamma = 0.287$, $d = 1.3353$, and $\gamma_1 = 0.1$. The corresponding values for ξ_n: $\xi_1 = 0.388$; $\xi_2 = 0.851$; $\xi_3 = 1.111$; $\xi_4 = 1.198$.

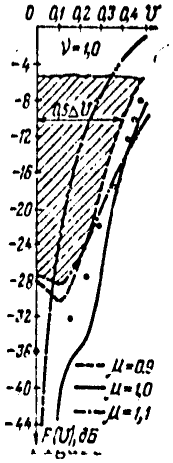

Calculations of F(v, 1, 1) were performed on a computer [by means of direct integration of (5)], and using formulas (6) --(8); the precision was good to the second decimal place for F(v) in decibels. In arange of values of $v = 0.1$--1.0, the maximum difference in the results obtained on the computer and from the formulas at the point $v = 0.1$ amounted to 1.3 dB. In this case, the average deviation for 12 points in the indicated range amounted to 0.15 dB. Thus, formulas (6), (7) and (8) can be successfully used to calculate the characteristics of a double ring throughout the range of variation in v, which is of interest in practice.

Also shown in Figure 4 are curves which characterize the coverage range of the double ring (for $\mu = 0.9$ and $\mu = 1.1$ at $v = 1.0$). The experimental curve for $\mu = 1.0$ and $v = 1.0$ is plotted with small circles. The dashed and double dotted curve of F(v, 1, 1) indicates the conventional single ring.

The effectiveness of the shield described here in the form of a double ring exceeds the effectiveness of the well known single ring by many times. Thus, for example, to produce a suppression of -18 dB at the edge of a reflector 3 m in diameter of an antenna operating at a frequency of 4 GHz, the double ring can be positioned at a distance of $r_0 = 200$ m from the antenna, i.e., six times claser than the usual ring. In this case, its maximum radius will be $\rho_4 = 4.75$ m, while its area will be 2.65 times less than the area of the conventional ring which creates the same suppression at the edge of the 3 m diameter reflector. With such a small spacing of r_0, the screen is quite effective under the actual conditions of varying atmospheric refraction.

Thus, the screen developed here in the form of a double ring exceeds well known screens by many times in terms of effectiveness and coverage, and for the first time permits the shielding of antennas with gains of 40--43 dB from directions close to the direction of the main lobe. The interference suppression in this case amounts to 20--25 dB.

BIBLIOGRAPHY

1. F.K. Preikschat, THE MICROWAVE JOURN., 1964, Vol. 7, No. 8.

2. G. Ruse, F.I. Sheftman, D.A. Cahlander, PIEEE, 1966, Vol. 54, No. 9.

3. J.E. Becker, J.-C. Sureau, IEEE, 1966, Vol. AP-14, No. 6.

4. H.E. Bussey, "Reflected Ray Eliminators", US Patent, M. Cl. 343-841, No. 2.763.001.

5. Yu.M. Mel'nikov, TRUDY NIIR [PROCEEDINGS OF THE SCIENTIFIC RESEARCH INSTITUTE FOR RADIO], 1975, No 4.

6. O.P. Frolov, TRUDY NIIR, 1974, No 3.

7. Yu.M. Mel'nikov, TRUDY NIIR, 1976, No 1.

8. G.N. Watson, "Teoriya besselevykh funktsiy" ["Bessel Function Theory"], Part I, I.L.M. Publishers, 1949.

9. Ye.N. Dekanosidze, "Tablitsy tsilindricheskikh funktsiy ot dvukh peremennykh" ["Tables of Cylindrical Functions of Two Variables"], USSR Academy of Sciences Publishers, 1956.

10. Yu.A. Yerukhimovich, Yu.V. Pimenov, ZHURNAL VYCHISLITEL'NOY MATEMATIKI I MATEMATICHESKOY FIZIKI [JOURNAL OF COMPUTER MATHEMATICS AND MATHEMATICAL PHYSICS], 1969, Vol 9, No 3.

11. A.S. Yudina, ZHURNAL VYCHISLITEL'NOY MATEMATIKI I MATEMATICHESKOY FIZIKI, 1961, Vol 1, No 6.

12. I.N. Ryzhik, I.S. Gradshteyn, "Tablitsy integralov, summ, ryadov i proizvedeniy" ["Tables of Integrals, Sums, Series and Products"], Moscow, 1962.

8225
CSO:1870

ELECTRONICS AND ELECTRICAL ENGINEERING

UDC 681.883.63

THE STRUCTURE OF A RECEIVER AND THE OPTIMUM DETECTION CHARACTERISTICS FOR SIGNALS WITH A RANDOM INITIAL PHASE, AMPLITUDE AND DURATION

Moscow RADIOTEKHNIKA in Russian No. 11, Nov 78 pp 77-80

[Article by G.D. Filin, manuscript received following revision, 27 January, 1978]

[Text] Signals with a random initial phase, amplitude and duration occur in radar, sonar and other types of range and direction finding of extensive objects (their dimensions are large as compared to the wavelength of the irradiated signals), the aspect and position of which in the search space (range, azimuth and elevation angle) are unknown before detection. The model of the useful signal in this case can be represented as:

$$x(t, \beta, B, \tau_c) = \begin{cases} BX(t)\cos[\omega_0 t + \varphi_x(t) + \beta], & t \in [t_0, t_0 + \tau_c]; \\ 0 & t \notin [t_0, t_0 + \tau_c], \end{cases}$$

where X(t) and $\phi_x(t)$ are functions which describe the amplitude and phase laws of the signal modulation; t_0, ω_0, β, B and τ_c are the moment of arrival, the carrier frequency, the initial phase, amplitude and duration of the signal respectively. In the following analysis, for the purpose of illustrating the influence on receiver structure of the indeterminacy in the knowledge of the signal width, we shall assume as in [1] that B has a Rayleigh distribution, β is uniform in a range of $(0, 2\pi)$, and t_0 and ω_0 are parameters established during detection.

The specific feature of taking τ_c into account consists in the fact that τ_c is a priori unknown (prior to the moment of detection). Thereafter, τ_c changes little from observation cycle to cycle. The minimum useful signal width is equal to the width of the counding radiation τ_0. The range of variation in τ_c is determined by the specific observation conditions [2].

We shall designate the signal energy as $\Im$ [E] when B = 1 and $\tau_c = \tau_0$. Then the signal energy for any τ_c can be represented as:

$$\Im_c(B, \tau_c) = B^2(\tau_0 + \Delta\tau) = B^2\tau_0\left(1 + \frac{\Delta\tau}{\tau_0}\right) = B^2\Im k_\tau,$$

where $k_\tau = \tau_c/\tau_0$ is the normalized signal duration.

The probability ratio for the case where B has a Rayleigh distribution, β has a uniform distribution under conditions where the interference n(t) is steady-state gaussian white noise with a mathematical mean of zero and a spectral density of N_0, taking [1] into account, can be represented in the following form:

$$l = \int_1^{\infty} \frac{N_0}{\Im k_\tau + N_0} e^{\frac{1}{N_0}\frac{z^2[y(t)/\tau_c]}{\Im k_\tau + N_0}} p(k_\tau)\, dk_\tau, \tag{1}$$

where

$$z[y(t)/\tau_c] = \int_{-\infty}^{\infty} x(t, \tau_c)\, y(t)\, dt, \tag{2}$$

$y(t) = n(t) + x(t, \tau_c)$; $p(k_\tau)$ is the probability density of the quantity k_τ. For the assumed limitations, the correlation integral (2), in being the limit of the linear combination of gaussian random quantities, is also a gaussian random quantity, the mathematical mean value and dispersion of which are respectively equal to $\bar{z} = Ek_\tau$ and $\sigma_z^2 = N_0 Ek_\tau/2$. In this case, for a uniform distribution of k_τ in a range of $[1, k_{\tau\,max}]$, the probability ratio (1) is written in the form:

$$l = \frac{1}{k_{\tau\,max} - 1} \int_1^{k_{\tau\,max}} \frac{1}{N_0 + \Im k_\tau} e^{\frac{1}{N_0}\frac{z^2(k_\tau)}{N_0 + \Im k_\tau}} dk_\tau. \tag{3}$$

Integral (3) can be solved by approximation methods [3] squares of the highest precision power. Legendre polynomials form an orthogonal system of polynomials of constant weight in the interval [1, -1]:

$$P_n(x) = \frac{1}{2^n n!} \frac{d^n (x^2 - 1)^n}{dx^n}.$$

This allows the representation of the probability ratio in form (3) in the following form:

$$l = \sum_{k=1}^{n} \frac{A_k^{(n)}}{N_0 + \Im k_{\tau k}^{(n)}} e^{\frac{1}{N_0}\frac{z^2(k_{\tau k}^{(n)})}{N_0 + \Im k_{\tau k}^{(n)}}}, \tag{4}$$

where $A_k^{(n)} = \frac{1}{[1 - (x_k^{(n)})]^2 [P_n'(x_k^{(n)})]^2}$; $k_{\tau k}^{(n)} = 1 + \frac{k_{\tau\,max} - 1}{2}(x_k^{(n)} + 1)$; $x_k^{(n)}$ are the roots of the Legendre polynomial of power n (n is determined by the precision in the solution of the problem); $P_n'(...)$ is the first derivative of the Legendre polynomial.

An analysis of expression (4) shows that the circuit for processing signals with random β, B and τ_c should take the form of a multichannel system, in each channel of which there is generated the correlation integral $z(k_{\tau k}^{(n)})$, $k = 1, \ldots, n$, the square of the absolute value of which is defined as

$$z^2(k_{\tau k}^{(n)}) = \left| \frac{1}{2} \int_0^{\tau_{ck}^{(n)}} y(t) x(t, \tau_{ck}^{(n)})\, dt \right|^2. \tag{5}$$

where $\tau_{ck}^{(n)} = \tau_0 k_{\tau k}^{(n)}$.

Expressions (4) and (5) allow for the representation of the circuit for the optimum processing of the received signals in each channel. The complete circuit (Figure 1) consists of an optimal filter OF for a single radio pulse of width $\tau_{ck}^{(n)}$, a square-law detector KD, a multiplier circuit SU using multipliers of $1/b_k^{(n)}(b_k^{(n)} = N_0 + k_{\tau k}^{(n)}E)$, a nonlinear element, NE, with a characteristic of the form $exp(u/N_0 b_k^{(n)})$, a second multiplier circuit using quadriture coefficients $A_k^{(n)}$ and an incoherent adder-store, which performs the functions of combining the video pulses which do not act simultaneously, as well as summing them.

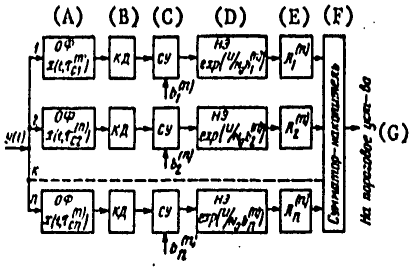

Figure 1.

Key: A. Optimal filters;
B. Square-law detector;
C. Multiplier circuit;
D. Nonlinear element;
E. Quadrature component multiplier;
F. Adder-store;
G. To the threshold gate.

With an exponential distribution of k_τ, one can employ Laguerre polynomials:

$$L_n(k_\tau) = \frac{e^{k_\tau}}{n!}\frac{d^n}{dk_\tau^n}(k_\tau^n e^{-k_\tau}),\ n = 0, 1, 2\ldots,$$

which are orthogonal with respect to the weight $exp\ (-k_\tau)$ on the half-axis $(0, \infty)$. In this case, for the signal model considered here, the probability ratio has the form:

$$l = \sum_{k=1}^{n}\frac{A_k}{N_0 + (1 + k_{\tau k}^{(n)})\Im}\, e^{\frac{1}{N_0}\frac{z^2(k_{\tau k}^{(n)})}{N_0 + (1+k_{\tau k}^{(n)})\Im}}, \qquad (6)$$

where $k_{\tau k}^{(n)}$ are roots of the Laguerre polynomials of power n.

The structure of the receiver determined by formula (6) is similar to that described above. The difference is determined by the number of channels n, the characteristics of the optimal filters at the input, and the quantities A_k and $k_{\tau k}$. This makes knowledge of the probability density $p(k_\tau)$ fundamental in the design of an optimal receiver for signals with an initial phase, amplitude and width which are random.

The probability density of the quantity z for the case of a fixed useful signal width can be represented as:

$$p_{cn}(z/k_\tau) = \frac{2z(k_\tau)}{2\sigma_x^2 + \Im^2 k_\tau^2} e^{-\frac{z^2(k_\tau)}{2\sigma_x^2 + \Im^2 k_\tau^2}}.$$

This allows the representation of the correct detection probability and the false alarm probability at the output of the processing circuitry in the form:

$$\left.\begin{aligned} D &= \int_{z_0}^{\infty} dz \int_1^{\infty} p_{\text{сп}}(z/k_\tau)\, p(k_\tau)\, dk_\tau = \int_1^{\infty} e^{-\frac{q_0^2/2k_\tau}{1+q^2k_\tau^2/2}}\, p(k_\tau)\, dk_\tau, \\ F &= \int_1^{\infty} e^{-q_0^2/2k_\tau}\, p(k_\tau)\, dk_\tau, \end{aligned}\right\} \tag{7}$$

where the following symbols are used: $q_0 = z_0/\sigma_z^\circ$, $q = \Im/\sigma_z^\circ$, $\sigma_z^\circ = N_0\Im/2$.

The structure of relationships (7) is similar to (1), and for this reason, the integrals incorporated in them can be solved by approximation [3] using the scheme adopted above, depending on the nature of the probability density $t(k_\tau)$. With an exponential distribution of k_τ, it is easy to obtain:

$$F = \sum_{k=1}^{n} A_k F_0^{\frac{1}{1+k_{\tau k}}}, \quad D = \sum_{k=1}^{n} A_k e^{\frac{\ln F_0/(1+k_{\tau k})}{1+q^2/(1+k_{\tau k})/2}}. \tag{8}$$

The quantities A_k and $k_{\tau k}$ are here equal to the corresponding quantities in (6), and $F_0 = exp(-q_0^2/2)$.

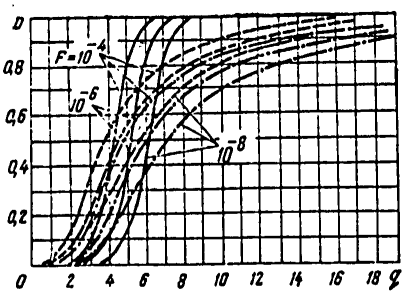

Figure 2.

The calculated detection curves are shown in Figure 2 for three cases: a) a signal with a random initial phase (solid line); b) a signal with a random initial phase and amplitude (dashed-dotted line); c) a signal with a random initial phase, amplitude and width (dashed line). The first two are taken from [1], while the third is plotted from (8) for the following initial data:

$$n = 2,\ k_{\tau 1} = 0{,}585,\ k_{\tau 2} = 3{,}414,\ A_1 = 0{,}853,\ A_2 = 0{,}146.$$

The precision in the calculation of D for n = 2 and n = 3 was compared for $F = 10^{-4}$ and q = 10. The quantities D do not differ by more than one in the third significant digit: D = 0.910 (n = 2), and D = 0.902 (n = 3). It follows from Figure 2 that in the region of large detection probabilities, the curves for a signal with random β, B and τ_c occupy an intermediate position with respect curves a and b. This attests to the fact that signal fading caused by fluctuations in amplitude is partially compensated by the increase in its energy due to the pulling of the width. For this reason, the specified detection probability are assured at a lower average

energy of the sounding signal. At low probabilities of correct detection, the fluctuations in the width and amplitude substantially improve the detection and the curves shifted considerably to the left. The advantages indicated here are assured by the more complex structure of the receive channel, for the design of which, it is necessary to know the probability density of the width of the useful signal.

BIBLIOGRAPHY

1. "Teoreticheskiye osnovy radiolokatsii" ["The Theoretical Principles of Radar"], Edited by Ya. D. Shirman, Moscow, Sovetskoye Radio Publishers, 1970.

2. V.V. Surnin, G.D. Filin, "Modeli fluktuatsiy dlitel'nosti gidroakusticheskogo ekho-signal" ["Models of the Variations in the Width of a Sonar Echo Signal"], Abstracts of the Reports of the First All-Union Conference on the Study and Utilization of the Resources of the Pacific Ocean, DVPI [Far Eastern Polytechnical Institute imeni V.V. Kuybyshev] Publishing House, Vladivostok, 1976.

3. V.I. Krylov, "Priblizhennoye vychisleniye integralov" ["The Approximation of Integrals"], Moscow, Nauka Publishing House, 1967.

8225
CSO:1870

ELECTRONICS AND ELECTRICAL ENGINEERING

UDC 519.17:621.391.26

THE APPLICATION OF THE METHODS OF GAMES THEORY TO THE RECOGNITION OF THE SIGNALS OF A SOURCE WHERE TRANSFORMING TYPE INTERFERENCE IS PRESENT IN THE CHANNEL

Mosocow RADIOTEKHNIKA in Russian No 11, Nov 78 pp 84-86

[Article by Yu.P. Kuznetsov, manuscript received 15 June, 1977]

[Text] The formulation of the problem consists in the following. There are two sources S_1 and S_2, each of which has a set of n different signals m_1, ..., m_n. The sources are turned on in random manner: S_1 is turned on with a probability p, while S_2, with (1 - p).

The source S_1 has different operational modes. In each mode, only two differe signals of the set of n signals, m_1, ..., m_n, are transmitted, for example, m_i and m_j in accordance with the law $\phi_{ij} = \{P(m_i) = q; P(m_j = 1 - q\}$, $i,j = 1,n$, $i \neq j$, where $P(m_i)$ and $P(m_j)$ are the a priori probabilities of the transmission of the signals m_i and m_j respectively, while q is a specified number, where $b \geq 1/2$. The total number of possible operational modes of source S_1 is equal to $n(n - 1)$.

The signals of the sources are transmitted using a multiposition symmetrical channel without a memory in the presence of transforming type interference. Such a channel is defined by the set of transition probabilities:

$$P(m_i/m_j) = \begin{cases} 1 - p_0, & i = j, \\ \dfrac{p_0}{n-1}, & i \neq j, \end{cases}$$

where p_0 is the probability of the conversion of a given signal into any other one, where $p_0 \leq (n - 1)/n$.

There is an observing system (SN) at the output of the channel, where this system should equate the receive signal with one of two signals transmitted by source S_1 in the given time interval, or consider it to be a signal of source S_2 without indicating the number of the signal. Let the source S_1 transmit the signals m_i and m_j in the given time interval. Then, the observation system should make one of three decisions based on the received signal: 1) the source S_1 sent the signal m_i; 2) the source S_1 sent the signal m_j; and 3) the signal was sent by the source S_2. We shall designate

these decisions wtih the symbols m_i, m_j and S_2 respectively. By virtue of the action of interference in the channel and the randomness of the triggering of the sources, the observation system can make both correct and incorrect decisions. Let $g > 0$ and $g' > 0$ mean the respective wins of the observation system for any correct or incorrect decision concerning the signals sent by the source S_1, while $h > 0$, and $h' > 0$ mean the corresponding wins of the observation system for any correct and incorrect decision concerning the presence of the source S_2, where $g,h > g',h'$.

There is an informational link between the cource S_1 and the observation system which consists in the fact that in each time interval of the observation system, the numbers of the signals and the law governing their transmission by the source S_1 are known. As regards the source S_2, it is assumed that it plays an ant gonistic game against the observation system, simulating the operation of source S_1. In this case, the operational modes of S_1 in different time intervals are not known to the source S_2. We shall adopt the win average of the observation system as an index of the outcomes in the game. The observer strives to maximize it, while the source S_2 strives to minimize it.

We shall enumerate the pure strategies of the players. The source S_2 has n strategies, where the i-th strategy consists in its transmitting the signal m_i $(i = \overline{1,n})$.

The strategies of the observation system are conditional [1], and they are represented in a more complex form than the strategies of the source S_2. In fact, since following the reception of any signal, the observation system should make one of three decisions, then the entire set of input signals $\{\mu\}$ should be broken down into three subsets, where a particular decision corresponds to each one of them. But with a sufficiently large n, the number of possible breakdowns, and consequently, the number of possible strategies for the observation system increase sharply. This complexity can be overcome by means of using one special breakdown of the set $\{\mu\}$, which is optimal for the solution of the entire problem as a whole and consists in the following [1].

Let the source S_1 transmit the signals m_i and m_j in the given time interval in accordance with the law ϕ_{ij}. We shall subdivide the set $\{\mu\}$ into three subsets: the first contains only the signal m_i, the second only the signal m_j, while the third, $\{m_{ij}\}$ contains all the remaining signals. It is convenient to break down all the possible strategies of the observation system into groups of $n(n-1)$ strategies each. The number of different groups of strategies of the observation system is 27. Of them, only five groups of strategies are the active ones:

$$I_1\left(\frac{m_i, m_j, \{m_{ij}\}}{\varphi_{ij}}\right) = [m_i, m_i, m_i], \quad i,j = \overline{1,n}, \ i \neq j;$$

$$I_1\left(\frac{m_i, m_j, (m_{ij})}{\varphi_{ij}}\right) = [m_i, m_j, m_i], \quad i, j = \overline{1,n}, \ i \neq j;$$
$$I_2\left(\frac{m_i, m_j, (m_{ij})}{\varphi_{ij}}\right) = [m_i, m_j, S_i], \quad i, j = \overline{1,n}, \ i \neq j;$$
$$I_3\left(\frac{m_i, m_j, (m_{ij})}{\varphi_{ij}}\right) = [m_i, S_i, S_i], \quad i, j = \overline{1,n}, \ i \neq j;$$
$$I_4\left(\frac{m_i, m_j, (m_{ij})}{\varphi_{ij}}\right) = [S_i, S_i, S_i], \quad i, j = \overline{1,n}, \ i \neq j.$$

The strategies written out here are read in the following manner. For example, the fourth group incorporates those n(n - 1) strategies such that if S_1 sends the signals m_i and m_j in accordance with the ϕ_{ij} law, then the decision is made that S_1 sent the signal m_i when m_i is received at the input of the observation system, and the decision that the signal was sent by the source S_2 when any other signal was received.

Calculations show that for the first, second, and fifth groups of strategies, the win average of the observation system does not depend on the operational mode of source S_1, while for the third and fourth groups of strategies, the win average of the observation system achieves the greatest value for the case of the equiprobable use of different operational modes by the source S_1. We shall designate the win average of the observation system when the i-th group of strategies is used as v_i $(i = \overline{1,5})$. The quantities v_i are equal to:

$$v_1 = pqg + p(1-q)g' + (1-p)h';$$
$$v_2 = pq\left(1 - \frac{p_0}{n-1}\right)g + pq\frac{p_0}{n-1}g' + p(1-q)(1-p_0)g + p(1-q)p_0g' + (1-p)h';$$
$$v_3 = p(1-p_0)g + pp_0g' + (1-p)h - \frac{2}{n}(1-p)(h-h');$$
$$v_4 = pq(1-p_0)g + pqp_0g' + p(1-q)g' + (1-p)h - \frac{1}{n}(1-p)(h-h');$$
$$v_5 = pg' + (1-p)h.$$

It can be seen from these expressions that the values of v_i depend on the relationship of the probabilities p, p and q, where one can segregate several ranges of linkages between them, in each of which, an optimal group of observation system strategies is easily found, as is the value of the game v which determines the maximum guaranteed win average of the observation system. Let:

$$0 < p < \frac{1}{1 + n(1-p_0)q\Delta} = p_1.$$

where $\Delta = (g - g')/(h - h')$. Then for any values of the parameters of the problem, the fifth group strategies dominates all the remaining ones, and consequently, is the optimal strategy. The value of the game is equal to $v = pg' + (1 - p)h$.

When $p \geq p_1$, the nature of the application of the observation system strategies depends on the ratio of the probability q and p_0. Here, one can segregate two cases of this linkage.

Case 1.

$$\frac{1}{1+\frac{p_0}{(n-1)(1-p_0)}} \leq q \leq 1. \tag{1}$$

Under condition (1), the useful groups are the first, third and fourth groups of strategies. Now let

$$p_1 = \frac{1}{1+n(1-p_0)q\Delta} \leq p \leq \frac{1}{1+\frac{n}{n-1}p_0q\Delta} = p_3. \tag{2}$$

In this case, the dominant group, and consequently, the optimal one is the fourth group. The value of the game is equal to:

$$v = pq(1-p_0)g + pqp_0g' + p(1-q)g' + (1-p)h - \frac{1}{n}(1-p)(h-h'). \tag{3}$$

Further let $p_4 = 1/\left(1+\frac{n}{n-1}p_0q\Delta\right) \leq p \leq 1$. Then the first group of strategies is dominant, and consequently, it is the optimal one. The value of the game is equal to $v = pqg + p(1-q)g' + (1-p)h'$.

Case 2.

$$\frac{1}{2} \leq q \leq \frac{1}{1+p_0(n-1)(1-p_0)}. \tag{4}$$

Under condition (4), the useful groups are the second, third and fourth groups of strategies. Now let

$$p_2 = \frac{1}{1+n(1-p_0)q\Delta} \leq p \leq \frac{1}{1+n(1-p_0)(1-q)\Delta} = p_3. \tag{5}$$

The fourth group of strategies is dominant here, and it is the optimal one. The value of the game in this case is defined by (3). Further let:

$$p_3 = \frac{1}{1+n(1-p_0)(1-q)\Delta} \leq p \leq \frac{1}{1+\frac{n}{n-1}p_0q\Delta} = p_4.$$

Then the dominant one, and consequently, the optimal group of the third group of strategies. The value of the game is equal to $v = p(1-p_0)g + pp_0g' +$ $+ (1-p)h - \frac{2}{n}(1-p)(h-h')$. . Finally, let $p_4 = 1/\left(1+\frac{n}{n-1}p_0q\Delta\right) \leq p \leq 1$.

In this case, the second group of strategies is dominant, which is the optimal one. The value of the game is equal to:

$$v = pq\left(1-\frac{p_0}{n-1}\right)g + pq\frac{p_0}{n-1}g' + p(1-q)(1-p_0)g +$$

$$+ p(1-q)p_0g' + (1-p)h'.$$

This completes the solution of the problem. We shall consider the results obtained. In the range of small values the probability p, where $p \in [0, p_1]$, the optimal strategies are those of the fifth group, which order the observation system to consider any received signal as a signal of the S_2 source with any operational mode of the source S_1. The indicator of the operational quality of the observation sytem v, does not depend on the probabilites p_0 and q, or on the number of signals n.

In the ranges $[p_1, p_2]$ under condition (1) and $[p_1, p_3]$ under condition (4), the optimal strategies are those of the fourth group which order the source S_1 to use all possible operational modes with equal probability, and the observation system to change the breakdown of the set of signals at the input each time there is a change in the operational mode of the source S_1. For a specific operational mode S_1, the optimum decision is that the signal of source S_1 is being transmitted with the greatest probability if the receive signal coincides with it, and the decision that S_2 is present in the contrary case. The operational quality indicator of the observational system in the ranges considered here depends on the probabilities p_0 and q, as well as on the number of signals n.

In the range $[p_3, p_4]$, under condition (4), the optimal strategies are those of the third group, which order the source S_1, and the observation system to take the same actions as the fourth group of strategies does. However, the character of the optimal behavior of the observation system in this case is different and consists in the following. If the received signal coincides with one of the signals of source S_1, then it is equated to the latter, otherwise, the received signal is considered to be a S_2 source signal. The operational quality indicator of the observation system in this range depends only on the probability p_0 and the number of signals n.

In the range $[p_4, 1]$ under condition (4), the optimum strategies are those of the second group, which for any operational modes of the cources S_1 and S_2 order the equating of the received signals only to the signals of the S_1 source according to the following rule: if the received signal coincides with the S_1 source signal, transmitted with the least probability, then it is equated to the latter, otherwise, the received signal is equated to the S_1 source signal, which is transmitted with the greatest probability. The operational quality indicator of the observation system in this range depends on the probabilities p_0 and q, as well as on the number of signals n.

In the range $[p_2, 1]$ under condition (1), the optimal strategies are those of the first group, which order the observation system to equate any received

signal to a signal of source S_1, transmitted with the greatest probability, and for the case of other operational modes, of the sources S_1 and S_2. The operational quality indicator of the observation system in this range depends only on the probability q.

With an increase in the number of signals n, the range of values of the probability q determined by inequality (4), expands, while range (1) contracts. In this case, the indicator of the operational quality of the observation system in all ranges of values of the probability p, where it depends on n, increases. Consequently, increasing the number of signals permits reducing to a certain extent both the harmful action of interference and the "interfering" action on the part of source S_2.

BIBLIOGRAPHY

1. V.F. Nesteruk, RADIOTEKHNIKA, 1969, Vol. 24, No. 5, 8, 9.

8225
CSO:1870

ELECTRONICS AND ELECTRICAL ENGINEERING

UDC 621.391:65.011.46

A QUANTITATIVE EVALUATION OF THE ECONOMIC ENGINEERING EFFICIENCY OF DISCONTINUOUS COMMUNICATIONS SERVICE

Moscow RADIOTEKHNIKA in Russian No 11, Nov 78 pp 97-100

[Article by F.F. Yurlov and L.A. Rozhdestvenskaya]

[Text] Discontinuous service is an effective means of transmitting information in channels with randomly changing parameters; it is employed in meteor scatter radio communications, as well as for combating fading in the VHF and UHF bands [1, 2]. Discontinuous communications permits increasing the information transmission rate by tens of times or reducing the transmitter power by the same amount at the requisite transmission rate for a specified noise immunity. However, the equipment is complicated in this case, something which is due to the presence of a feedback channel and storage devices with a large memory; this leads to additional economic expenditures. To justify them, it is necessary to compare discontinuous communications with continuous service based on economic engineering parameters.

Used as the criterion for evaluating the efficiency of the systems analyzed below are the expenditures referenced per unit of transmitted information at a specified information reproduction quality [3]. In the system being analyzed, the information is transmitted only in those time intervals when the signal/noise ratio at the input to the receiver exceeds a specified value. Under unfavorable reception conditions, the system is shifted over to a standby mode by means of a feedback channel, and the information at the transmit end of the communications channel is stored in a special store. At the receiving station, besides the detection of frequency telegraphy signals, the carrier level is also monitored. An analysis of the efficiency of discontinuous communications is made under the conditions that Rayleigh fading and fluctuating interference of the white noise type act in the channel.

Shortwave transmitters for trunk link communications were used as the transmitting devices. R-250M receivers were employed in the transmitting and receiving stations. It was also assumed that the narrow band feedback channel did not introduce any errors. The efficiency of the systems being compared is determined from the formula of [3]:

$$З_i' = \frac{З_i}{q_i} = \frac{E_i}{q_i} + E_н \frac{K_i}{q_i}, \quad (1)$$

where $З_i$ [Z_i] are the referenced annual expenditures for the i-th variant; q_i is the amount of information which is transmitted at a specified information reproduction quality; K_i are the capital investments for the i-th variant; $E_н$ is the normative efficiency coefficient; E_i are the annual operating expenses for the i-th system.

Since the systems being analyzed differ in terms of their noise immunity, transmission rate, communications range, etc., it is necessary to reduce them to a comparable form. Comparability in terms of noise immunity is accomplished when the following conditions is met:

$$P_{о.н} = P_{о.п} = P_{о.т}, \quad (2)$$

where $P_{О.Н}$, $P_{О.П}$ is the reception error probability for the case of continuous and discontinuous communications respectively; $P_{О.Т}$ is the requisite error probability based on the conditions of the problem.

Comparability as regards the communications range is relaized with the condition:

$$r_н = r_п = r_т, \quad (3)$$

[$r_Н$ = r continuous; $r_П$ = r discontinuous], where $r_Т$ is the requisite communications range.

The average error probability in a discontinuous communications system is:

$$\bar{P}_{оп}(S). = \frac{\int_{S_t}^{\infty} P_{оп}(S)\, w(S)\, dS}{\int_{S_t}^{\infty} w(S)\, dS},$$

where S_t is the threshold level of the signal/noise ratio; w(S) is the probability density of the signal/noise ratio at the input to the receiver.

For systems with an active pause with incoherent reception, the expressions for the average error probability in the discontinuous and continuous communications systems have the form [2]:

$$\bar{P}_{о.п}(S) = \frac{1}{2+S_*} e^{-\frac{S_t}{2}}; \quad \bar{P}_{о.н}(S) = \frac{1}{2+S_*}. \quad (4)$$

If (4) is used and conditions (2) and (3) are met, then one can determine the levels of the $S_{О.Н}$ and $S_{О.П}$ signal/noise ratios at the inputs to the receivers of the systems considered here, as well as the powers of the received signals:

$$N_{п.вх} = S_{о.п}\sigma_п; \quad N_{н.вх} = S_{о.н}\sigma_н,$$

[$N_{п.вх}$ = N discontinuous system, receiver input; $N_{н.вх}$ = N continuous system, receiver input], where $\sigma_п$ and $\sigma_н$ are the interfernce powers within the limits of the effective passband of the receivers.

After this, we find the necessary transmitters powers to assure a specified noise immunity and communications range r, i.e.:

$$N_п = \left(\frac{4\pi r_п}{\lambda_п F_п}\right)^2 \frac{N_{п.вх}}{G_{п1}G_{п2}}; \qquad N_н = \left(\frac{4\pi r_н}{\lambda_н F_н}\right)^2 \frac{N_{н.вх}}{G_{н1}G_{н2}},$$

where r, λ and F are the communcations range, wavelength and attenuation factors; G_1 and G_2 are the gains of the transmitting and receiving antennas respectively. The power gain using continuous communications is defined by the ratio $B = N_н/N_п$. By having available the capital investments and annual operational expenditures as a function of the power of the transmitters, one can determine the referenced expenditures needed to design and operate the transmitting devices. Having computed the referenced expenditures of the receivers, we shall determine the overall referenced annual outlays for the communications systems being compared.

To attain the requisite communications range, noise immunity and other parameters in a system with continuous information transmission, it is necessary to substantially increase the transmitter power, something which entails considerable additional outlays. The referenced annual expenditures for a continuous communications system are determined from the formula:

$$З_н = (K_н + \Delta K_н) E_н + E_н + \Delta E_н,$$

where $\Delta K_н$ are the additional capital outlays related to the increase in transmitter power; $\Delta E_н$ are the additional annual operational expenditures.

A discontinuous communications system includes a direct and a return channel, as well as devices for storing information as well as automatic start-up and shut-down equipment. This requires additional capital investments $\Delta K_п$ and operational expenditures $\Delta E_п$ (as compared to just a forward communications channel). The referenced annual outlays for the case of discontinuous information transmission are found from the expresssion:

$$З_п = (K_п + \Delta K_п) E_н + E_п + \Delta E_п.$$

The equipment cost was determined from price list 16-01 for products of the radio industry. The individual expenditures (for the installation of equipment, transportation, etc.) were calculated in a consolidated fashion in percent of the basic type of expenditure and were determined on the basis of experience in the project planning, construction and operation of communications installations. The cost of the transmitters were computed from the formula [4] $C = dN^m$, where n is the transmitter power in kilowatts;

m and d are constants. For automated transmitters, which operate in a telegraph mode, d = 10 [10^3 · rubles/KW]; m = 0.54. The operational expenses were computed taking into account the structure of the outlays and the relative share of the amortization deductions in the overall sum of the expenses indicated here. The amortization deductions were computed from the norms established for communcations and radio broadcast enterprises. The specific reference expenses were computed in accordance with (1). Using the procedure set forth here, the following functions were obtained:

$$1.\ \mathcal{Z}'_{\text{н}} = \varphi_1(S_t),\ S'_{\text{п}} = \varphi_1(S_t),\ P_0 = \text{const},\ r = \text{const};$$
$$2.\ \mathcal{Z}'_{\text{н}} = \psi_1(P_0),\ \mathcal{Z}'_{\text{п}} = \psi_1(P_0),\ S_t = \text{const},\ r = \text{const};$$
$$3.\ \mathcal{Z}'_{\text{н}} = f_1(r),\ \mathcal{Z}'_{\text{н}} = f_1(r),\ S_t = \text{const},\ P_0 = \text{const},$$

where the subscripts "н" and "п" characterize continuous and discontinuous communications respectively; $\mathcal{Z}^t_{\text{н}}$ [$Z^t_{\text{н}}$] and $\mathcal{Z}^t_{\text{п}}$ [$Z^t_{\text{п}}$] are the annual referenced expenditures per unit of transmitted information in the systems considered here; r is the communications range in kilometers.

The specific expenditures Z' are shown in Figure 1 as a function of the threshold level S_p, computed in the systems being compared for $P_0 = 10^{-4}$, $r = 2 \cdot 10^3$ km, $N^p_{\text{п}} = 3 \cdot 10^2$ KW and $N_{\text{п}} = 2$ KW [sic].

The specific expenditures increase sharply when $S_t < 2$ and $S_t > 12$, and moreover, there is a threshold at which the quantity Z' is minimal. The latter is explained by the fact that when S_t tends to zero, the noise immunity for discontinuous communications approaches the noise immunity of a discontinuous information transmission system, i.e., it is substantially reduced. Although in this case the volume of information being transmitted is increased, the transmitter power nonetheless significantly increases, something which causes a growth in the referenced annual outlays at low threshold levels. At large threshold levels, because of the increase in the noise immunity, the referenced expenditures fall off, but the average time and rate of traffic transmission are considerably reduced. At the limit when $S_t \to \infty$, the volume of transmitted information tends to zero. Correspondly, the expenditures referenced per unit of transmitted information increase considerably with a large threshold signal/noise ratio.

The most important parameters of the systems being compared are shown in Table 1 as a function of the reception error probability for a communications range of $r = 2 \cdot 10^3$ km and a threshold of $S_t = 10$; shown in Table 2 are the values obtained when $r = 1.5 \cdot 10^3$ km and $S_t = 10$; shown in Table 3 are the most important parameters as a function of the communications range r when $P_0 = 10^{-4}$ and $S_t = 10$. From the curves plotted in Figures 2 and 3 for the specific expenditures as a function of the reception error probability for the case of discontinuous and continuous communications service and ranges of $r_1 = 2 \cdot 10^3$ km and $r_2 = 1.5 \cdot 10^3$ km respectively, it is apparent that in the first case somewhat of an increase is observed in the expenditures

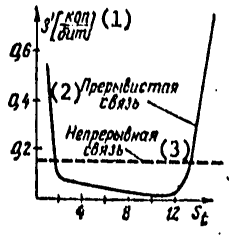

Figure 1.

Key: 1. Z' [kopecks/bit];
2. Discontinuous service;
3. Continuous service.

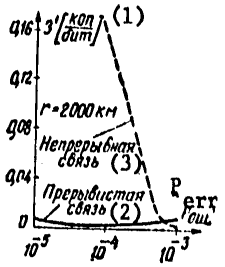

Figure 2.

Key: 1. Z' [kopecks/bit];
2. Discontinuous service;
3. Continuous service.

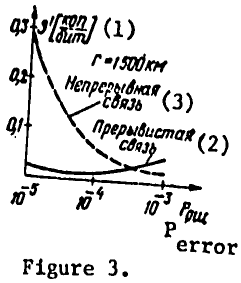

Figure 3.

Key: 1. Z' [kopecks/bit];
2. Discontinuous service;
3. Continuous service.

with a reduction in the reception error probability. This is explained by a decrease in the amount of correctly received information with a drop in the noise immunity. But the reduction in the absolute level of the outlays is poorly realized, since at low power levels of the transmitters, the major proportionate share in the outlays belongs to large capacity memories. An analysis of tables 1 and 2 shows that when $P_o < 10^{-3}$, discontinuous communications is significantly more efficient that continuous. For example, when $P_o = 10^{-4}$ and $r = 2 \cdot 10^3$ km, the annual savings which can be obtained when using discontinuous communications amounts to $S = [Z'_н - Z'_п]q_п = 67{,}500$ rubles. It follows from an analysis of table 3 that the efficiency of discontinuous communications increases with an increase in communications range. For example, when $r = 4.4 \cdot 10^3$ km, the specific expenditures for the systems being compared are:

$$Z'_н = 28.3 \text{ kopecks/bit};$$

$$Z'_п = 2.8 \cdot 10^{-2} \text{ kopecks/bit}.$$

It follows from Figure 4 and table 3 that with an increase in communications range, the rate of growth in the specific expenditures for the case of continuous transmission considerably leads the rate of growth in these expenditures for the case of discontinuous communications. In fact, when using continuous transmission, transmitter powers are required which are figured in

Table 1.

(A)	$P_{ош}$	10^{-3}	10^{-4}	10^{-5}
(B)	$P_{н}$, кВт	30	300	3000
(C)	$P_{п}$, кВт	0,15	2	20
(D)	$З_{н}$, тыс. руб./год	28	100	362
(E)	$З_{п}$, тыс. руб./год	18	21,5	52,8
(F)	$q_{н}\cdot 10^{-6}$, бит/год	162	67,2	$4,34\cdot 10^{-3}$
(G)	$q_{п}\cdot 10^{-6}$, бит/год	20,8	135	133
(H)	$З'_{н}\cdot 10^{2}$, коп./бит	1,73	15	$0,835\cdot 10^{3}$
(I)	$З'_{п}\cdot 10^{2}$, коп./бит	8,65	1,6	3,97

Table 2.

	$P_{ош}$	10^{-3}	10^{-4}	10^{-5}	(A)
	$P_{н}$, кВт	15	150	1500	(B)
	$P_{п}$, кВт	0,075	1	10	(C)
	$З_{н}$, тыс. руб./год	37,2	73,2	256	(D)
	$З_{п}$, тыс. руб./год	10,5	17,7	38,6	(E)
	$q_{н}\cdot 10^{-6}$, бит/год	172	115	0,89	(F)
	$q_{п}\cdot 10^{-6}$, бит/год	20,8	135	155	(G)
	$З'_{н}\cdot 10^{2}$, коп./бит	2,16	6,37	28,7	(H)
	$З'_{п}\cdot 10^{2}$, коп./бит	5,05	1,31	2,5	(I)

Key [for both tables]:

A. Error probability;
B. $P_{continuous}$, KW;
C. $P_{discontinuous}$, KW;
D. $Z_{Н}$, 10^3 rubles/year;
E. $Z_{П}$, 10^3 rubles/year;
F. $q_{Н} \cdot 10^{-6}$, bits/year;
G. $q_{П} \cdot 10^{-6}$, bits/year;
H. $Z'_{Н} \cdot 10^{2}$, kopecks/bit;
I. $Z'_{П} \cdot 10^{2}$, kopecks/bit.

hundreds of kilowatts. A change in the communications range of several times leads to a considerable increase in transmitter power, something which entails the necessity of large capital investments and current expenditures. The use of discontinuous communications requires the use of transmitting devices having a power of units of kilowatts. For this reason, for the case of a change in the communications range, the referenced annual expenditures also increase, but the rate of their growth is considerably less than for continuous communications.

Table 3.

	r, км / r, km	1500	2000	2400	2800	3100	3600	4400
(A)	$P_н$, кВт	150	300	450	600	750	1200	1500
(B)	$P_п$, кВт	1	2	3	4	5	8	10
(C)	$З_н$, $\frac{\text{тыс. руб.}}{\text{год}}$	73,2	100	129	155	174	218	256
(D)	$З_п$, $\frac{\text{тыс. руб.}}{\text{год}}$	17,7	21,5	24,5	27,1	29,4	33,2	38,6
(E)	$q_н \cdot 10^{-6}$, $\frac{\text{бит}}{\text{год}}$	118	69,5	49,9	23,1	16,2	2,8	0,93
(F)	$q_п \cdot 10^{-6}$, $\frac{\text{бит}}{\text{год}}$	137	137	137	137	137	137	137
(G)	$З'_н \cdot 10^2$, $\frac{\text{коп.}}{\text{бит}}$	5,9	14,4	26	64	108	906	2835
(H)	$З'_п \cdot 10^2$, $\frac{\text{коп.}}{\text{бит}}$	1,29	1,57	1,79	1,98	2,14	2,42	2,82

Key: A. $P_Н$, KW [continuous];
B. $P_П$, KW [discontinuous];
C. $Z_Н$, 10^3 rubles/year [continuous];
D. $Z_П$, 10^3 rubles/year [discontinuous];
E. $q_Н \cdot 10^{-6}$, bits/year;
F. $q_П \cdot 10^{-6}$, bits/year;
G. $Z'_Н \cdot 10^2$, kopecks/bit;
H. $Z'_П \cdot 10^2$, kopecks/bit.

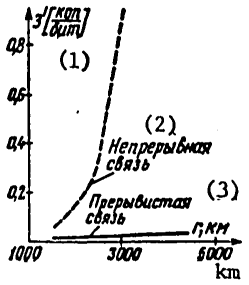

Figure 4.

Key: 1. Z' [kopecks/bit];
2. Continuous communications;
3. Discontinuous communications.

Conclusions. The comprehensive economic engineering analysis performed here has demonstrated the advantages of discontinuous communications over continuous service in a rather wide range of the main parameters (P_o, r, q).

BIBLIOGRAPHY

1. "Meteornaya radiosvyaz' na ul'trakorotkikh volnakh" ["Meteor Scatter Radio Communications at Ultrashortwave Frequencies"], Collection of articles edited by A.A. Kazantsev, Moscow, IIL Publishers, 1961.

2. A. G.Zyuko, "Pomekhoustoychivost' i effektivnost' sistem svyazi" ["Communications System Noise Immunity and Efficiency"], Moscow, Svyaz' Publishers, 1972.

3. F.F. Yurlov, "Otsenka effektivnosti sredstv svyazi s uchetom zatrat na ikh sozdaniye i ekspluatatsiyu" ["The Evaluation of the Effectiveness of Communications Equipment, Taking into Account the Expenditures for Its Desig and Operation"], The All-Union Scientific Session Devoted to Radio Day, Moscow, 1974.

4. "Ekonomicheskaya effektivnost' i stimulirovaniye sozdaniya i vnedreniya novoy tekhniki svyazi. Informatsionnyy sbornik" ["Economic Efficiency and Providing Incentives for the Design and Introduction of New Communications Equipment. Informational Collection"], Moscow, Svyaz' Publishers, 1969.

8225
CSO:1870

ELECTRONICS AND ELECTRICAL ENGINEERING

EQUIVALENT PARAMETERS OF GUNN DIODE IN TWO-FREQUENCY MODE

Moscow RADIOTEKHNIKA I ELEKTRONIKA in Russian No 10, 1978 pp 2208-2211

[Article by A. S. Kosov and I. A. Strukov]

[Text] Results are presented of the experimental investigation of a two-frequency oscillator generating signals at the basic frequency and the 2nd harmonic. The maximum generated power at the harmonic was 30% of the maximum power of the single-frequency oscillator. The mechanism of generation of the 2nd harmonic was investigated. It was shown that in the case studied, generation is basically parametric; that is, the negative conductivity introduced as a result of parametric coupling of signals considerably exceeded the intrinsic conductance of the diode at the 2nd harmonic. This makes it possible to increase by a factor of two the maximum frequency of Gunn oscillators. The effect of a reactive 2nd-harmonic load on the efficiency of the oscillator at the basic frequency was investigated. The possibility of increasing the efficiency by a factor of 1.5 in comparison with the case of single-frequency oscillation was demonstrated.

Introduction

Oscillators with output at the 2nd or higher harmonic may be used in systems in which synchronous oscillations are required at the basic frequency and at some harmonic, and also may be used to shift frequency into a region in which an instrument has no intrinsic negative resistance. As shown by calculations [1], at a frequency of 140 GHz the Gunn diode has no negative resistance. However, as the basic frequency is raised, the effect of the 2nd harmonic increases, and a two-frequency oscillator at a frequency of 140 GHz may be of comparable

efficiency with a single-frequency oscillator at 70 GHz. At the same time the power at the basic frequency of 70 GHz remains approximately at the maximum produced at this frequency in the single-frequency mode. Additionally, a reactive load at 140 GHz makes it possible to increase by a factor of 2 the maximum efficiency at 70 GHz in comparison with the single-frequency case. Thus, two-frequency oscillators using Gunn diodes may be widely applied in the mm-band and require detailed investigation and the choice of a system of basic parameters.

1. A system of equivalent parameters of a two-frequency oscillator

The approach used for analysis of a two-frequency oscillator is that of the authors of [2], applied by them to the analysis of an avalanche transit-time oscillator. The state of the oscillator is described by the amplitudes of the 1st and 2nd harmonics v_1 and v_2, their relative phase $\Phi=\phi_2-2\phi_1$, and the frequency ω_0. An active instrument is characterized in addition by the conductance matrix

$$\|Y\|(\omega_0, \Phi, v_1, v_2, x) = \left\| \begin{matrix} y_{11} & y_{12} \\ y_{21} & y_{22} \end{matrix} \right\|. \quad (1)$$

Here x signifies the bias, the temperature, and other parameters. The equivalent circuit of the active element is presented in fig. 1. The voltages of higher harmonics are assumed to be much smaller than those of the 1st and 2nd harmonics, justifying the representation of the instrument by a conductance matrix rather than by a total resistance matrix.

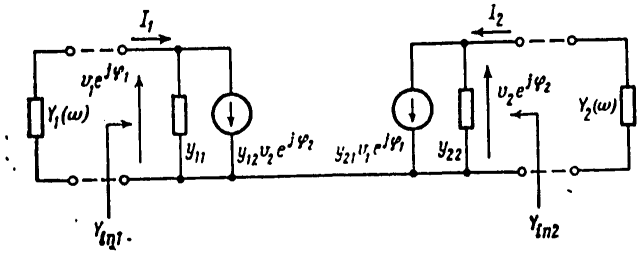

Fig. 1. Equivalent circuit of two-frequency oscillator.

The condition for free two-frequency oscillation may be written in the form

$$Y_1(\omega_0)+Y_{in1}=0,$$
$$Y_2(2\omega_0)+Y_{in2}=0,$$
$$Y=\left\| \begin{matrix} y_{11} & y_{12} \\ y_{21} & y_{22} \end{matrix} \right\|, \quad (2)$$

where

$$Y_{in1}=y_{11}+y_{12}\frac{v_2 e^{j(\varphi_2-\varphi_1)}}{v_1};$$
$$Y_{in2}=y_{22}+y_{21}\frac{v_1 e^{-j(\varphi_2-\varphi_1)}}{v_2}.$$

As shown by experiment, y_{12} and y_{21} have little dependence on ϕ_2 and v_2 and are proportional to v_1:

$$y_{12}\simeq k_1 v_1 e^{j(\varphi_1-\psi_1)},$$
$$y_{21}\simeq k_2 v_1 e^{j(\varphi_2+\psi_2)}. \quad (3)$$

Thus, in order to describe the active element in the two-frequency mode it is necessary to know the following equivalent parameters: y_{11}, the intrinsic conductance of the diode at the 1st harmonic, depending only on the amplitude of the 1st harmonic; y_{22}, the intrinsic conductance of the diode at the 2nd harmonic, depending on the amplitude of the 2nd harmonic; constants k_1 and ψ_1, determining the effect of the 2nd harmonic on the 1st; and constants k_2 and ψ_2, determining the effect of the 1st harmonic on the 2nd.

2. Design of a measuring cavity

The cavity of the two-frequency oscillator investigated is shown in fig. 2. To calculate the geometric dimensions of the diode holder, the method developed by Eisenhard and Khan was used [3]. Shown in fig. 3 are results of the calculation of the admittance of the load connected to terminals of the semiconductor structure with the geometric dimensions shown in fig. 2. A short circuit mode occurs for oscillations with a wavelength equal to $b_1/2n$, where n is a whole number, in the plane of the broader wall of the waveguide, where the contact pin 9 enters the coaxial portion.

As shown by calculations, with the design studied the magnitude of the impedance modulus of the load from the side of the waveguide for the basic frequency does not exceed 1 ohm in the region of 500 MHz, corresponding to the short circuit mode for the semiconductor instruments examined. Therefore, in order to decouple the oscillations, the height of the basic-frequency waveguide was chosen to be 8 mm, corresponding to a short circuit at a frequency of 18.8 GHz.

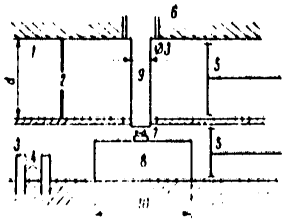

Fig. 2. Design of a two-frequency oscillator: 1 - waveguide 8x23; 2 - diaphragm; 3 - waveguide 5.5x11; 4 - three-pin transformer; 5 - shorting plunger; 6 - oxidized insert; 7 - Gunn diode; 8 - thick volume diaphragm; 9 - contact pin.

Fig. 2

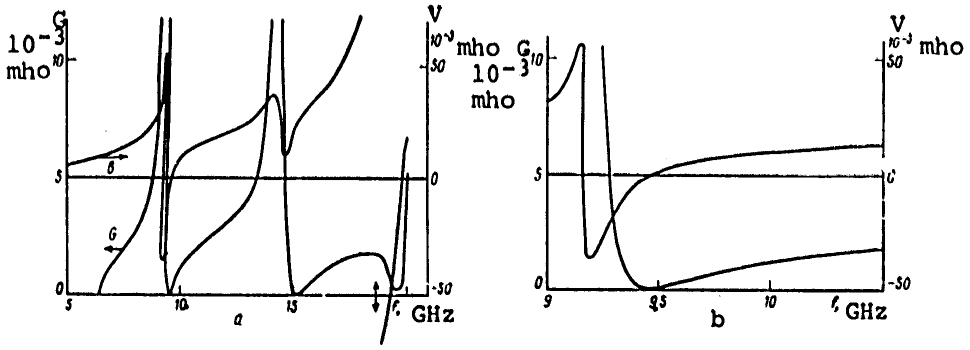

Fig. 3

Fig. 3. Calculation of load conductance: a - in the region 5-20 GHz; b - in the region 9-10 GHz.

The diameter of pin 9 was chosen to be 3 mm to achieve an active conductance for the first harmonic at the terminals of the semiconductor element on the order of 1/30 G_O, where G_O is the conductance of the diode at zero bias voltage. Diaphragm 2 served as an impedance transformer at the basic frequency.

A three-pin transformer was used to match impedance at the second harmonic. The bias was introduced through an oxidized aluminum insert.

3. Experimental results

Investigations were performed with an unencased Gunn diode. The doping profile was uniform. The dopant concentration was $(1-2)\cdot10^{15}$ cm^{-3}. The length of the active region was 10 μm. The threshold voltage U_T=3.5 V, and the threshold current I_T=0.5 A.

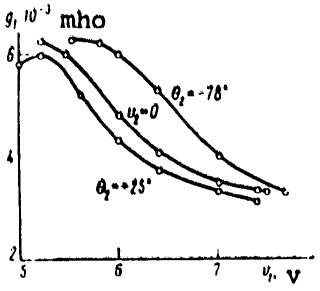

Fig. 4. Dependence of input conductance at the first harmonic on amplitude v_2 for various reactive loads at the 2nd harmonic.

The investigations were performed at a basic frequency of 9.4 GHz and a corresponding second harmonic of 18.8 GHz with a bias voltage of $2.5U_T$. Measurement of the oscillation parameters v_1, v_2, ω_o, and Φ, as well as the parameters of the instrument, was made according to the method discussed in [4].

The following results were obtained: v_1=5V, v_2=0.9V, Re y_{11}= $-6\cdot10^{-3}$mho, Im y_{11}=$+30\cdot10^{-3}$mho, Re y_{22}=$-1.5\cdot10^{-3}$mho, Im y_{22}= $+60\cdot10^{-3}$mho, k_1=$0.5\cdot10^{-3}$mho/V, ψ_1=+160°, k_2=0.8^{-3}mho/V, and ψ_2=-70°. The following were the load conductances:

$$Y_1(\omega_o)=(6-j30)\cdot10^{-3} \text{ mho},$$
$$Y_2(2\omega_o)=(30-j60)\cdot10^{-3} \text{ mho}.$$

It should be noted that Re $Y_2(2\omega_o)$>>Re y_{22}. This indicates that it is possible to form negative conductance at the second harmonic in Gunn diodes as a result of the parametric coupling y_{21}. The value of ψ_2=-70° shows the impossibility of describing an instrument with a volt-ampere characteristic having a segment with a negative resistance.

The case of a reactive load at the second harmonic, Re $Y_2(2\omega_o)$=0, was also studied. The input admittance at the first harmonic was measured for various amplitudes v_1, and the corresponding efficiency value for the first harmonic was calculated. Experimental results for three different modes at the second harmonic are presented in fig. 4. The parameter is the angle $\theta_2=\Phi-\psi_2$. The case θ_2=278° corresponds to a load at the second harmonic such that the maximum efficiency at the first harmonic is increased by 30% in comparison with the single-frequency case. The case θ_2=25° corresponds to the case in which the maximum efficiency is increased by 15%. Thus with an arbitrary reactive load at the second harmonic the maximum efficiency of the oscillator may vary by a factor of nearly 1.5.

Conclusion

Investigations of the two-frequency mode show that the negative conductance introduced as a result of coupling between ω_0 and $2\omega_0$ oscillations considerably exceeds the conductance of the instrument at the frequency $2\omega_0$ for $v_2=0$ in the instrument. This confirms the proposed possibility of using two-frequency Gunn oscillators at frequencies twice as high as those achievable in the single-frequency mode. The proposed measurement method makes it possible to give an adequate description of the instrument and may serve as the basis for the design of two-frequency oscillators.

References

1. W. R. Curtice, J. J. Purcell, IEEE TRANS., 1970, ED-17, 12, 1018.
2. C. A. Brackett, BELL SYSTEM TECHN. J., 1970, 49, October, 1777.
3. R. L. Eisenhard, P. J. Khan, IEEE TRANS., 1971, MTT-19, 8, 706.
4. D. F. Peterson, IEEE TRANS., 1974, MTT-22, 8, 784.

Received by editors 18 July 1977.

9187
CSO: 8144/0547

ELECTRONICS AND ELECTRICAL ENGINEERING

PRINCIPLES OF MINIATURIZATION OF PASSIVE MICROWAVE STRIP ELEMENTS

Moscow RADIOTEKHNIKA I ELEKTRONIKA in Russian No 10, Aug 78 pp 2216-2218

[Article by Ye. L. Bachinina, N. I. Prokhorova, and A. L. Fel'dshteyn]

[Text] The object of this article is to introduce criteria for the quality of bandpass filters taking into account all their basic parameters: passband (V_π,%), dissipative losses (b_Σ,db), volume (v,cm^3), and frequency selectivity (number of resonators n). The proposed criterion is of the form

$$\frac{b_\Sigma}{n} V_\pi \frac{v}{n} = G \geqslant \text{const.} \quad (1)$$

This relationship is based on the particular parametric relations given in [1-5]: between losses and passband for v/n=const. [1,2] and between losses and volume for V_π=const. [3-5].

Relationship (1) has a simple physical meaning. Since the quantity G is bounded below, the simultaneous improvement of all filter parameters is possible only up to a definite limit.

The dependence of achievable values of G on wavelength λ, determined by experimental methods, is presented in fig. 1. Data from the literature conform to the laws found; thus, a definite system is formed for evaluating and selecting materials from the literature.

The practical utility of the criterion G will be explained through examples.

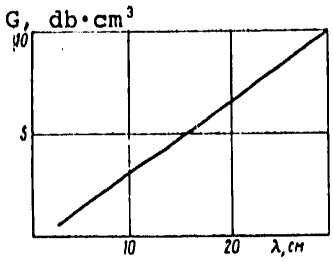

Fig. 1

Example 1. The following parameters are given for an opposing-stub bandpass filter: n=7, b_Σ=2.5db, V_π=2%, volume=60cm³. The quality criterion is to be determined. We find

$$\frac{b_\Sigma}{n} V_n \frac{v}{n} = \frac{2,5}{7} 2 \frac{60}{7}; \quad G = 0,12 \text{ db} \cdot \text{cm}^3.$$

Conclusion: the filter is poorly designed or constructed, since the average value of G in the 10-cm region is 3 (see graph in fig. 1).

Example 2. The following characteristics are given for a microstrip filter with parallel-coupled resonators: n=5, b_Σ=4.5 db, V_π=5%, v=4 cm³. We find the quality criterion

$$G = \frac{4.5}{5} 5 \frac{4}{5} = 3.6 \text{ db} \cdot \text{cm}^3.$$

Conclusion: the filter is well designed and constructed.

Some characteristics of the basic types of S-band bandpass filters are presented in the table. The filters are listed in order of increasing average thermal losses at the resonator for a 1% filter band. From the table it follows that the basic types of S-band bandpass filters all have G-values of approximately 3; that is, the reduction in resonator volume from type to type is accompanied by a proportionate increase in losses; new types of filters -- using supercritical waveguides, dielectric resonators, etc. -- may be evaluated using criterion (1); as demonstrated by experiment, the quantity G for these filters lies within the limits corresponding to the range of the graph in fig. 1; in wideband bandpass filters (passband not less than 5%) the limitations found are immaterial. This makes it possible to miniaturize them, in particular, in planar microstrip form.

The criterion shown above and the laws that follow from it are applicable not only to bandpass filters but to other passive microwave elements with resonant amplitude-frequency characteristics as well.

In conclusion we present an analytic proof of the connection between losses and passband (for a given type of filter). Previously this connection was found numerically [1].

We proceed from the known relationship [6]

$$b_{\text{э}} = 8{,}68\frac{\sum_{i=1}^{n} Q_i}{Q_0}, \tag{2}$$

where Q_0 is the intrinsic Q-factor of the resonator; Q_i is the Q-factor of the ith (ideal) resonator under load. Multiplying and dividing the right-hand part of (2) by the quantity S, where $S \approx 2\Delta f/f_0 = V_{\text{п}}$, we introduce the normalization in n:

$$\frac{b_{\text{э}}}{n} = \left\{\frac{8{,}68\sum_{i=1}^{n} Q_i S}{nQ_0}\right\}\frac{100}{V_{\text{п}}}, \tag{3}$$

where $V_{\text{п}}$ is in per cent and $V_{\text{п}} = S \cdot 100\%$.

This equation will be a hyperbola if the expression in braces (having the same meaning as the quantity a in [1]) is sufficiently unvarying. We will show that this is in fact the case.

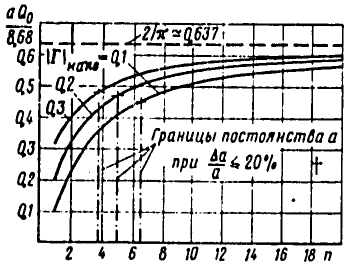

Fig. 2

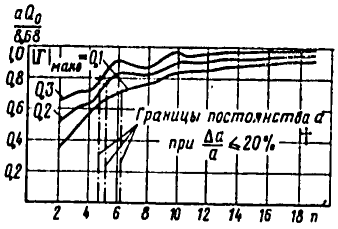

Fig. 3

† limits of constant value of a for $\Delta a/a \leq 20\%$

Fig. 2. Dependence of the hyperbolic coefficient a (normalized) on the number of resonators. The frequency characteristic of the filter is maximally flat.

Fig. 3. Dependence of hyperbolic coefficient a (normalized) on the number of resonators. The filter has a Chebyshev frequency characteristic.

We will introduce the normalized value $a_{\text{н}} = a(Q_0/8.68)$; then $a_{\text{э}} = (1/n)\sum_{i=1}^{n} Q_i S$. With a maximally flat amplitude-frequency characteristic

(4) $$\sum_{i=1}^{n} Q_i S = \sqrt[n]{h} \sum_{i=1}^{n} \sin(2i-1)\frac{\pi}{2n} = \frac{\sqrt[n]{h}}{\sin\frac{\pi}{2n}},$$

where $h = |\Gamma|_{макс} \Big/ \sqrt{1-|\Gamma|^2_{макс}}$; $|\Gamma|_{макс}$ is the allowance for mismatch in the passband. Hence

(5) $$a_n = \frac{\sqrt[n]{h}}{n\sin(\pi/2n)}.$$

Graphs of this function are given in fig. 2; they approach asymptotically the value $2/\pi$ as $n\to\infty$. The region over which a_n is relatively constant is marked on the graphs; it is bounded on the left by the values of n=4-7.

Parameters of basic types of S-band bandpass filters

	a) Тип полосно-пропускающего фильтра	Минимальная рекомендуемая полоса пропускания, $V_п$, % b)	Средние потери на резонатор при $V_п$=1 % b/n, дб c)	Собственная добротность резонатора, Q_0 d)	Габаритный индекс G, дб·см³ e)
f)	Волноводный фильтр с полуволновыми резонаторами	0,1	0,05–0,09	7000–9000	14,6
g)	Фильтр на запредельных волноводах	0,2	0,15	2000–5000	3–6
h)	Бочочный фильтр на симметричной полосковой линии с воздушным заполнением	0,3	0,22–0,36	2000–2500	2,2–2,6
i)	Встречно-стержневой фильтр на симметричной полосковой линии с воздушным заполнением	1	0,31–0,50	1000–1300	2,2–3,3
j)	Гребенчатый фильтр на симметричной воздушной полосковой линии	2	0,7	500–700	3–3,5
k)	Фильтр на печатной симметричной полосковой линии	3	1,47–2,33	200–300	7,5–8,1
l)	Фильтр на микрополосковой линии	5	2,40–3,80	150–250	3,0–3,6

a) Type of bandpass filter
b) Minimum recommended passband, $V_п$, %
c) Average losses at resonator for $V_п$=1% b/n, db
d) Intrinsic resonator Q-factor, Q_0
e) Dimensional index G, db·cm³
f) Waveguide filter with semiconductor resonators
g) Filter using supercritical waveguides
h) Bonochnyy filter using symmetrical strip line with air fill
i) Opposing-stub filter using symmetrical strip line with air fill
j) Comb filter using symmetrical air strip line
k) Filter using printed symmetrical strip line
l) Microstrip line filter

We will perform similar operations for a Chebyshev amplitude-frequency characteristic. The results are shown in fig. 3. In this case the asymptote has the value $a_H=1$. The fact that a_H is constant for both types of amplitude-frequency characteristic indicates that equation (3) is, in the asymptotic approximation, a hyperbola.

References

1. Ye. L. Bachinina, N. I. Prokhorova, A. L. Fel'dshteyn, RADIOTEKHNIKA, 1971, 26, 10, 46.
2. V. P. Leonchenko, A. L. Fel'dshteyn, L. A. Shepelyanskiy, Raschet poloskovykh fil'trov na vstrechnykh sterzhnyakh, ["Design of strip filters with opposing stubs"] (Handbook) IZD. SVYAZ', 1975.
3. V. M. Osipenkov, Ye. L. Bachinina, A. L. Fel'dshteyn, RADIOTEKHNIKA, 1973, 28, 5, 25.
4. Ye. D. Lotkova, Voprosy radioelektroniki ["Problems of radio electronics"], SER. TEKHNIKA RADIOSVYAZI, 1975, no. 4, 110.
5. A. V. Alekseyev, A. Ye. Znamenskiy, Ye. D. Lotkova, Elektricheskiye fil'try metrovogo i detsimetrovogo diapazonov ["Electrical filters for the meter and decimeter bands"], IZD. SVYAZ', 1976.
6. S. Kh. Kogan, RADIOTEKHNIKA I ELEKTRONIKA, 1962, 7, 8, 1316.

Received by editors 16 July 1976.

9187
CSO: 8144/0548

GEOPHYSICS, ASTRONOMY AND SPACE

UDC 551.46.083

FUNDAMENTALS OF THE THEORY AND TECHNIQUE FOR NEUTRON ACTIVATION ELEMENT AND SALT ANALYSIS OF SEA WATER UNDER FULL-SCALE CONDITIONS

Sevastopol' MORSKIYE GIDROFIZICHESKIYE ISSLEDOVANIYA in Russian No 1, 1978 pp 98-110

[Article by Ye. M. Filippov and I. A. Lamanova]

Abstract. Based on calculations it is shown that in measurements with neutron sources with output 10^8-10^{10} neutron/s one can define in sea water sodium, bromine and certain other chemical elements of saline composition. Data are given on the accuracy of determining the examined elements.

[Text] According to the change in concentration of salt-forming chemical elements in sea water one can solve a whole series of hydrophysical and oceanological problems associated with the processes of water mass transfer. Chemical methods are currently mainly used to determine the chemical elements of saline composition. These methods are generally very labor intensive and are carried out on ships and in shore laboratories. Using such methods it is impossible to rapidly solve the aforementioned problems. At the same time it is known that analysis of chemical elements can be solved rapidly with the help of the neutron activation method (NA) [8] which uses devices with radio isotope neutron sources (californium-252 and others), or with neutron tubes operating on the (d,t)-reaction principle [7,8]. Based on these and other sources of neutrons instruments can be created for full-scale hydrophysical studies. Besides this, to carry out NA under ship conditions laboratory neutron generators of the type NG-150I, NG-160 and others can be employed that have comparatively small dimensions but produce higher streams of neutrons [8].

We studied by calculation the possibility of using NA to analyze chemical elements of saline composition. These elements can be activated both under the influence of fast, and thermal neutrons. Fast neutrons are emitted directly from the source. In the (d,t)-reaction they have energy 14.6, and in californium-252 on the average 2.3 MeV. The thermal neutrons (0.025 eV) are obtained from fast neutrons during their moderation in water-containing

substances (water, paraffin, etc.). Sea water is a natural moderator of fast neutrons.

The NA techniques that can be realized based on fast and thermal neutrons are designated respectively NA-f and NA-t. By combining these techniques one can select the optimal pattern of irradiation and measurement of the induced activity of sea water as applied to the determination of each chemical element or their groups.

The number of impulses governed by gamma-radiation of radio isotopes emerging in a homogeneous unlimited medium, according to [7,8] will be defined by the following ratio:

$$N = iQ\varepsilon S \sum f(t) \int_V n_1(R_1) n_2(R_2) dV. \qquad (1)$$

Here i--number of gamma-quanta of certain energy emitted by radio isotope; Q--output of fast neutrons from source; ε--effectiveness of detector; S--effective surface of detector; Σ--macroscopic cross section of isotope activation; $n_1(R_1)$--function that describes the distribution of neutrons at distance R_1 from source; $n_2(R_2)$--function of distribution of gamma-quanta from the point of their emergence R_1 to the site of location of the detector R_2; V--volume of studied medium.

$$f(t) = \left(1 - e^{-\frac{0{,}693}{T} t_0}\right) \frac{T}{0{,}693} \left(e^{-\frac{0{,}693}{T} t_n} - e^{-\frac{0{,}693}{T} t}\right), \qquad (2)$$

where t_0, t_n and t--respectively the time of irradiation, pause, and measurement; T--half-life. If measurements begin immediately after the end of irradiation of the substance, then $t_n = 0$ and formula (2) adopts the appearance

$$f(t) = \left(1 - e^{-\frac{0{,}693}{T} t_0}\right) \frac{T}{0{,}693} \left(1 - e^{-\frac{0{,}693}{T} t}\right). \qquad (3)$$

In practice the time of irradiation and measurement are often selected as equal $t_0 = t$. In this case formula (3) is written as:

$$f(t) = \frac{T}{0{,}693} \left(1 - e^{-\frac{0{,}693}{T} t}\right)^2. \qquad (4)$$

In activation of the isotopes by fast neutrons of a spot source the function

$$n_1(R_1) = \frac{1}{4\pi R_1^2} e^{-R_1/\lambda}, \quad n/\text{см}^2 \cdot \text{s} \qquad (5)$$

where λ--mean path of fast neutrons in water. The distribution of gamma-quanta from a spot source without regard for the accumulation of scattered radiation is subject to the law

$$n_2(R_2) = \frac{1}{4\pi R_2^2} e^{-\tau_\gamma R_2}, \quad \gamma/\text{см}^2 \cdot \text{s} \qquad (6)$$

where τ_γ--linear coefficient of attenuation of gamma-quanta in water.

By substituting the given functions in expression (1) we obtain the formula for NA-f

$$N = \frac{iQ\varepsilon S \Sigma f(t)}{16\pi^2} \int_V e^{-R_1/\lambda - \tau_\gamma R_2} \frac{dv}{R_1^2 R_2^2}. \qquad (7)$$

The greatest number of radioactive isotopes is formed near the source. Therefore, where this is possible the measurements are made as follows: the studied medium is irradiated by neutrons, then the source is removed and in its place a radiation detector is installed. The calculations for such cases have the simplest form, since here the distances $R_1=R_2=R$. It is convenient in this case to compute the integral of expression (7) in a spherical system of coordinates, and formula (7) will adopt the following appearance:

$$N = Q_0 \int_a^\infty e^{-R(\lambda^{-1}+\tau_\gamma)} \frac{dR}{R^2}, \qquad (8)$$

where a--radius of spherical detector; $Q_0 = iQ\varepsilon S\Sigma f(t)/4\pi$. By integration we obtain

$$N = Q_0 \left[(\tau_\gamma + \lambda^{-1}) Ei\left[-a(\tau_\gamma+\lambda^{-1})\right] + \frac{1}{a} e^{-a(\tau_\gamma+\lambda^{-1})} \right]. \qquad (9)$$

By directing a to zero we have

$$N = Q_0 C \frac{1+\tau_\gamma \lambda}{\lambda}, \quad \text{imp} \qquad (10)$$

where C=0.5772--Euler's constant.

For convenience of calculating from this formula figure 1 presents the dependence of the values for the function $(1+\tau_\gamma\lambda)/\lambda$ on energy of the forming radio isotopes. The values of coefficients τ_γ are taken from reference book [6]. The amount λ in accordance with [7,8] equals 10.28 cm.

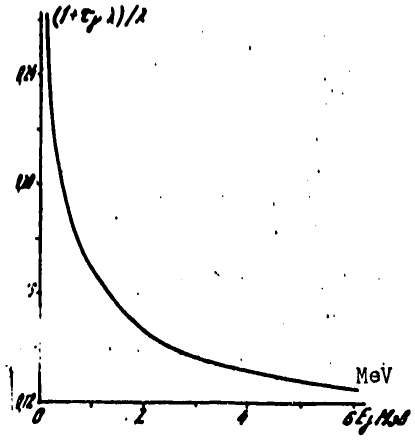

Figure 1. Function $(1+\tau_\gamma\lambda)/\lambda$

In practice the source and detector in a whole number of cases are placed a certain distance l from each other. Then the distances R_1 and R_2 are defined differently. Here it is more convenient to compute the integral (7) in a cylindrical system of coordinates. For NA-f it adopts the following appearance

$$N=\frac{Q_0}{l}\int_0^{\infty} r\,dr\int_{-\infty}^{\infty} e^{-R_1\lambda^{-1}-\tau_\gamma R_2}\frac{dz}{R_1^2R_2^2}, \quad (11)$$

$$R_1^2=r^2+z^2,\quad R_2^2=r^2+(l-z)^2.$$

A detailed computation of this integral is given in publication [11]. Therefore we will only given the final expression for the NA-f technique

$$N=\frac{Q_0}{l}\left\{\int_{-1}^{1}\frac{e^{\gamma l\alpha^{-1}}}{y}Ei\left[-\frac{l}{2}\left(\lambda^{-1}+\tau_\gamma\right)(u+y)\right]dy-\int_{-1}^{1}\frac{e^{-\gamma l\tau_\gamma}}{y}Ei\left[-\frac{l}{2}\left(\lambda^{-1}+\tau_\gamma\right)(u-y)\right]dy\right\}, \quad (12)$$

where $u=\sqrt{1+(d/l)^2}$; d - diameter of the instrument. The integral is computed numerically.

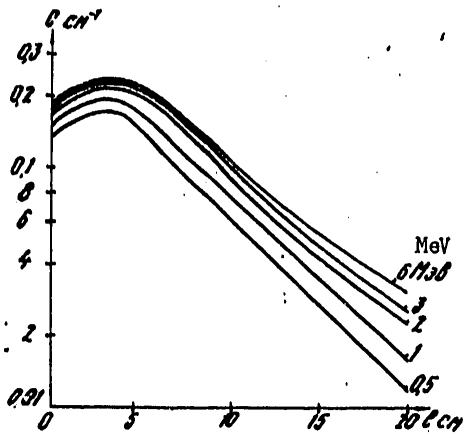

Figure 2. View of Functions $N/Q_0=f(l)$ in Activation of Chemical Elements by Fast Neutrons of (d,t)-Reactions

For convenience of caculations of this expression figure 2 presents the values for the functions $N/Q_0=f(l)$: the lower the energy of gamma-quanta, the faster the value of the functions f(l) drops with an increase in distance l.

We will now switch to derivation of formulas for calculations of NA-t.

The calculation of the moderation process of neutrons in water-containing media is a fairly complicated mathematical problem. To simplify it in this case often a one-group approximation is used [2]. The distribution of thermal neutrons with regard for diffusion will have the appearance [2]

$$n_t(R_t) = \frac{e^{-R_t/L_s} - e^{-R_t/L}}{4\pi R_t \Sigma_a (L_s^2 - L^2)}, \qquad n/см^2 \cdot s \qquad (13)$$

here L_s and L --respectively the length of moderation and diffusion of neutrons; Σ_a --macroscopic cross section of capture (absorption) of thermal neutrons in sea water.

The number of impulses governed by gamma-radiation of radio isotopes that emerge in sea water under the influence of thermal neutrons in a spherical system of coordinates will be determined from the following expression:

$$N = Q_t \int_a^\infty e^{-\tau_j R} \left(e^{-R/L_s} - e^{-R/L}\right) \frac{dR}{R}, \qquad (14)$$

where $Q_1 = iQe\delta\Sigma_f(t)/\sum_a \cdot 4\pi\left(L_s^2 - L^2\right)$.

Computation of the integrals produces

$$N = Q_1\left\{li\left[-a\left(\tau_y + L^{-1}\right)\right] - li\left[-a\left(\tau_y + L_s^{-1}\right)\right]\right\}. \qquad (15)$$

With a$\longrightarrow$0 we obtain

$$N = Q_1 \ln\left[\left(\tau_y + L^{-1}\right)\Big/\left(\tau_y + L_s^{-1}\right)\right]. \qquad (16)$$

For convenience of performing calculations by this formula figure 3 presents the dependence of values for logarithmic functions on the energy of gamma-quanta of emerging radio isotopes. The length of moderation of the neutrons L_s is estimated from the mean values for rise in neutrons [3]. For neutrons of (d,t)-reactions it is taken as equal to 12.69 cm, and for the californium source--5 cm. The sea water salinity is taken as equal to 32.5‰. The macroscopic cross section of thermal neutron capture Σ_a in accordance with [2,7,8] equals 0.0324 cm^{-1}, while the length of diffusion of thermal neutrons L =2.09 cm.

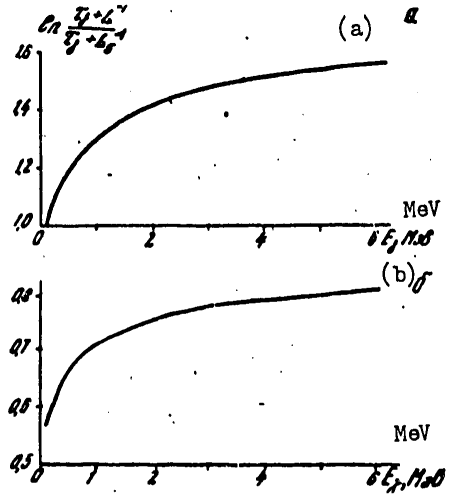

Figure 3. Dependences of Logarithmic Functions on Energy of Gamma-Quanta of Forming Radio Isotopes for Neutrons

Key:
a. (d,t)-reaction
b. californium source

In the case of NA-t the number of impulses recorded in a definite time interval will be determined by the following ratio:

$$N = \frac{Q_1}{2}\int_0^\infty r\,dr\left\{\int_0^\infty e^{-r_1/\Lambda_s - \tau_j r_2}\frac{dz}{r_1 r_2^3} - \int_{-\infty}^{\infty} e^{-r_1/\Lambda - \tau_j r_2}\frac{dz}{r_1 r_2^2}\right\}. \quad (17)$$

Computation of these integrals is given in publication [10]. In summary we write

$$N = Q_1\left(B_1 - B_2\right) = Q_1 f_1(l), \quad (18)$$

$$B_1 = \frac{\Lambda_s}{2l}\left\{e^{-l/\Lambda_s}\,Ei\left(-l\left(\tau_j - \Lambda_s^{-1}\right)\right) + \ln\frac{1+\tau_j\Lambda_s}{\left|1-\tau_j\Lambda_s\right|} - e^{l/\Lambda_s}\,Ei\left[-l\left(\tau_j + \Lambda_s^{-1}\right)\right]\right\},$$

B_2--the same when Λ_s is replaced by Λ.

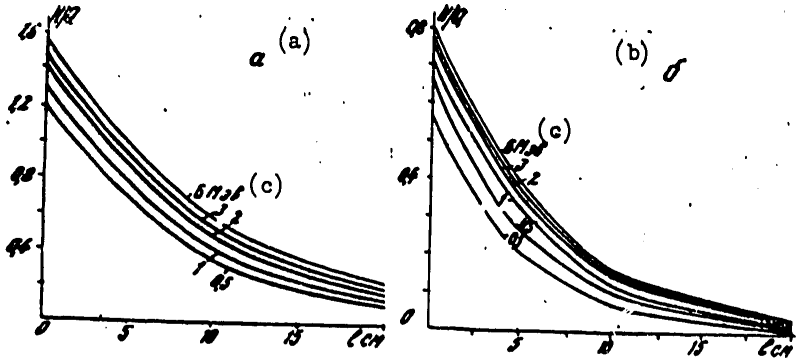

Figure 4. View of Functions $N/Q_1 = f_1(l)$ in Activation of Chemical Elements by Thermal Neutrons

Key:

a. on (d,t)-reactions
b. on californium source
c. MeV

The relationship $N/Q_1 = f_1(l)$ is depicted in figure 4 where the curves for the gamma-quanta of different energy decrease according to the same law.

We now switch to an estimate of the possibilities of using the NA method as applied to a determination of some of the most widespread chemical elements in sea water.

After examining the cross sections for the reaction and half-life of the forming isotopes [1], as well as their concentration in sea water [4, 12] we believe that the most suitable for NA are the following chemical elements (salinity, °/oo): oxygen (857), chlorine (19), sodium (10.5), magnesium (1.35), calcium (0.04) and bromine (0.065). The nuclear characteristics of isotopes that are the most suitable for measurements of NA-f and NA-t are given in table 1. The thresholds of the reactions of all isotopes that develop under the influence of fast neutrons are lower than 14.6 MeV, therefore these isotopes can be activated. If they are irradiated by neutrons of a californium sources $E_{n.cp}$=2.3 MeV, then only chlorine-37 will be noticeably activated. Therefore in the future calculations for NA-f will only be made for fast neutrons of (d,t)-reactions.

For spectrometry of gamma-radiation of induced isotope activity scintillation or semiconductor detectors can be used. The scintillation detectors are simple to handle and more efficient than the semiconductors which have a higher resolution, but can only operate at the temperature of liquid nitrogen. This complicates their operation. For protection from neutrons the indicated detectors can be screened by boron, lithium and cadmium. In the calculations of induced isotope activity we evaluate the possibility of using these and other detectors.

As a semiconductor detector in the calculations we take a germanium-lithium crystal 100 cm^3 in volume and effective area S=14.5 cm^2. Its effectiveness is evaluated according to [5,6]. From the scintillation detectors it is most convenient to use not sodium iodide activated by thallium and widely used in practice, but the crystal of cesium iodide also activated by thallium since otherwise the activation of sodium in the crystal will introduce additional errors to the analysis of sodium of sea water that has very high cross sections of activation by thermal neutrons (table 1). The diameter and thickness for cesium iodide are taken as 70 mm. For isotopes with complex spectrum we take the energy of gamma-quanta for the most intensive lines (in table 1 they are underlined).

The calculations in all cases are made for the stationary condition of the medium, i.e., we will assume that there is no water movement.

First we will study the possibility of using the NA method for the case l=0 (the detector is installed at the site of the source). We take the following time parameters: for NA-f t_0=t=60 s, t_n=2 s; for NA-t t_0=t=30 min, t_n=2 s. The calculation results are presented in table 2. For errors we adopt the designations: ΔN and SN--absolute and relative errors in the number of recorded impulses; ΔC--absolute error in determining the concentration of the element in water. Since the product εS for germanium-lithium detector is 20-30 times smaller than the analogous amount for cesium iodide, then also the induced activity measured with the help of the germanium-lithium detector will be the same amount lower than for CsI(Tl). Therefore in the case of semiconductor detectors to determine the elements with high accuracy comparable to the measurements for scintillation counters it is necessary to use a source with higher output of neutrons.

Table 1. Information on Nuclear Reactions and Composition of Emerging Gamma-Radiation of Chemical Elements of Sea Water

Type of reaction	Threshold of reaction, MeV	Cross sections		Half-life, T	Gamma-radiation of forming isotope, MeV (%)
		effective, mb	macroscopic, cm		
Fast neutrons of (d,t)-reaction					
$^{16}O(n,p)^{16}N$	10,0	90	0,0029	7,35 с (a)	7,1(11); 6,1(55)
$^{37}Cl(n,\alpha)^{34}P$	1,44	50	$3,86 \cdot 10^{-6}$	12,4 с (a)	2,13(25)
$^{23}Na(n,\alpha)^{20}F$	4,5	140	$3,85 \cdot 10^{-5}$	10,3 с (a)	1,63(100)
$^{25}Mg(n,p)^{25}Na$	3,0	50	$1,70 \cdot 10^{-7}$	1 мин (b)	1,61(5); 0,98(15); 0,58(15); 0,4(15)
Thermal neutrons					
$^{37}Cl(n,\gamma)^{38}Cl$	-	0,56	$4,24 \cdot 10^{-8}$	37,12 мин (b)	2,15(47); 1,60(31)
$^{23}Na(n,\gamma)^{24}Na$	-	14	$1,47 \cdot 10^{-4}$	15 ч (c)	2,75(100); 1,37(100); 3,85(9)
$^{26}Mg(n,\gamma)^{27}Mg$	-	27	$9,5 \cdot 10^{-8}$	10 мин (b)	1,013(30); 0,834(7)
$^{48}Ca(n,\gamma)^{49}Ca$	-	1100	$1,02 \cdot 10^{-8}$	8,75 мин (b)	4,68(3); 4,05(8); 3,1(89)
$^{79}Br(n,\gamma)^{80}Br$	-	8500	$2,12 \cdot 10^{-6}$	17,55 мин (b)	0,62(13); 0,511(6)

Key:
a. second
b. minute
c. hour

Table 2. Calculation Results from Determining Content of Certain Elements in Sea Water by NA Method with l=0

Element	Number of impulses N imp	Errors ΔN imp	δN%	C°/oo
Fast neutrons of (d,t)-reaction, $Q=10^{10}$ neutron/s, Ge(Li)				
Oxygen	668718	817	0,122	1,05
Chlorine	884	30	3,36	0,64
Sodium	3000	55	1,80	0,19
Magnesium	60	7,8	12,90	0,17
Fast neutrons of (d,t)- reaction $Q=10^{10}$ neutron/s, CsI(Tl)				
Oxygen	21134897	4597	0,0217	0,186
Chlorine	28661	169	0,617	0,116
Sodium	84930	291	0,343	0,036
Magnesium	1333	36,5	2,738	0,037
Thermal neutrons from (d,t)-reaction, $Q=10^{10}$ neutron/s, Ge(Li)				
Chlorine	2406	49	2,0	0,38
Sodium	1100707	1049	0,095	0,01
Magnesium	5591	75	1,34	0,02
Calcium	1119	33	3,0	0,012
Bromine	106383	326	0,3	$1,95 \cdot 10^{-4}$
Thermal neutrons from (d,t)-reaction, $Q=10^{8}$ neutron/s, CsI(Tl)				
Chlorine	729	27	3,7	0,70
Sodium	339458	583	0,17	0,018
Magnesium	1242	35	2,84	0,038
Calcium	190	14	7,26	0,029
Bromine	13604	117	0,86	$5,6 \cdot 10^{-4}$
Thermal neutrons from ^{252}Cf, $Q=10^{8}$ neutron/s, CsI(Tl)				
Chlorine	2927	54	1,85	0,35
Sodium	1346969	1161	0,086	0,009
Magnesium	5110	71,5	1,40	0,019
Calcium	753	27,4	3,64	0,015
Bromine	57000	239	0,42	$2,72 \cdot 10^{-4}$

After comparing the data obtained by the NA-f and NA-t methods (table 2) we see that with identical conditions the activation of chemical elements of a saline composition occurs more intensively under the influence of thermal neutrons. Sodium and bromine are activated here best of all, while by fast neutrons--oxygen. This phenomenon can be employed to investigate the rate of sea water movement [11].

Table 3. Calculation Results from Determining Content in Sea Water of Certain Elements by NA Method with l=10 cm

Element	Number of impulses N imp	Errors		
		ΔN imp	δN%	C°/oo
Fast neutrons of (d,t)-reaction, $Q=10^{10}$ neutron/s, Ge(Li)				
Oxygen	402850	634,7	0,156	1,35
Chlorine	260	16	6,2	1,18
Sodium	657	25,6	3,9	0,41
Magnesium	6,8	2,5	39,8	0,54
Fast neutrons of (d,t)-reaction, $Q=10^{10}$ neutron/s, CsI(Tl)				
Oxygen	12770345	3574	0,028	0,24
Chlorine	7998	89,4	1,118	0,212
Sodium	18600	136,4	0,733	0,077
Magnesium	140	11,8	8,45	0,114
Thermal neutrons from (d,t)-reaction, $Q=10^{10}$ neutron/s, Ge(Li)				
Chlorine	828	28,8	3,47	0,66
Sodium	390807	625	0,16	0,017
Magnesium	1789	42,3	2,36	0,032
Calcium	403	20,1	4,98	0,020
Bromine	81620	178	0,56	$3,64 \cdot 10^{-4}$
Thermal neutrons from (d,t)-reaction, $Q=10^{8}$ neutron/s, CsI(Tl)				
Chlorine	255	16	6,3	1,20
Sodium	120523	347	0,3	0,030
Magnesium	552	24	4,3	0,057
Calcium	124	11	9,0	0,036
Bromine	9752	98	1,0	0,00065
Thermal neutrons from ^{252}Cf, $Q=10^{8}$ neutron/s, CsI(Tl)				
Chlorine	145	12	8,3	1,6
Sodium	68274	261	0,38	0,04
Magnesium	221	15	6,7	0,09
Calcium	69	8	12	0,048
Bromine	2238	47	2,1	0,0014

In the transition from sources with output 10^{10} to sources with 10^{8} neutron/s with other conditions equal it should be kept in mind that measurement errors will rise by an order.

The calculation results for l=10 cm and $t_n=0$ are given in table 3: with an increase in the distance from l=0 to l=10 cm the measured amount of induced activity is reduced for each chemical element differently. This is linked exclusively to the amount of energy of gamma-radiation emitted by the isotopes.

With a further increase in the distance l to 20 cm the measured effect for NA-t is reduced roughly 3-fold in measurements with source of (d,t)-reaction, and 5-fold in measurements with a californium source.

Analysis of the data of tables 2 and 3 permits the conclusion to be drawn that of the chemical elements of saline composition chlorine is activated the worst of all. Therefore it is better to analyze it by NNM-t [9] or NGM [10]. In determining chlorine by NGM one can use the same detector as for NA; in the case of NNM-t it is necessary to include in the set of NA apparatus an additional plastic scintillation detector. The possibility of using a germanium-lithium detector in measurements by NGM is examined in publication [10]. Unfortunately there are no data on the use of scintillation detectors for these purposes.

Thus, in NA with sources 10^8-10^{10} neutron/s a number of chemical elements of sea water are activated (tables 2 and 3). For gamma-spectromet of the isotopes that emerge here it will be more convenient to use scintillation detectors of the type cesium iodide since in working with such crystals one can use sources of neutrons one-two orders lower than in measurements with a germanium-lithium detector. Therefore it is preferable to begin a check of the possibility of using NA with measurements with scintillation sources. In switching from sources with output 10^{10} to sources with 10^8 neutron/s with other conditions equal one should bear in mind that the measurement errors will increase by an order.

In analyzing the aforementioned one can draw the following conclusions: the methods of neutron activation analysis can be completely used for determining the change in content of chemical elements of a saline composition under full-scale conditions. Highly accurate determinations of chlorine in water can be simultaneously carried out here by the technique of NNM-t or NGM. If a stationary neutron generator with output to 10^{12} neutron/s [8] is installed aboard the oceanological ship then, by irradiating water samples of approximately 1 m^3 volume with other conditions equal from those examined the chemical elements of saline composition can be analyzed with even greater accuracy. In addition, with the help of such generators a whole series of other chemical elements that are contained in sea water in small quantities can also be analyzed.

BIBLIOGRAPHY

1. Aliyev, A. I., et al. "Yaderno-fizicheskiye konstanty dlya neutronnogo aktivatsionnogo analiza (spravochnik)" [Nuclear Physical Constants for Neutron Activation Analysis (Reference)], Moscow, Atomizdat, 1969.

2. Kozhevnkikov, D. A. "Neytronnyye kharakteristiki gornykh porod i ikh ispol'zovaniye v neftegazopromyslovoy geologii" [Neutron Characteristics of Rocks and Their Use in Oil and Gas Geology], Moscow, Nedra, 1974.

3. Kozhevnikov, D. A.; and Yudin, V. A. "Effect of Inelastic Scattering on Rise in Neutrons in Rocks," in "Novyye metody i apparatura yadernoy geofiziki i geokhimii" [Nuclear Methods and Apparatus of Nuclear Geo-Physics and Geochemistry], Moscow, ONTI VNIIYaGG, 1970.

4. Mero, Dzh. "Mineralnyye bogatstva okeana" ["Mineral Resources of the Ocean"], Moscow, Progress, 1969.

5. Reznikov, R. S.; and Sel'dyakov, Yu. P. "Promyshlennyye proluprovodnikovyye pribory" [Industrial Semiconducting Instruments], Moscow, Atomizdat, 1975.

6. Storm, E; and Israel', Kh. "Secheniya vzaimodeystviya gamma-izlucheniya (spravochnik)" [Cross Sections of Interaction of Gamma Radiation (Reference)], Moscow, Atomizdat, 1973.

7. Filippov, Ye. M. "Prikladnaya yadernaya geofizika" [Applied Nuclear Geophysics], Moscow, Izd-vo AN SSSR, 1962.

8. Filippov, Ye. M. "Yadernaya geofizika" [Nuclear Geophysics], Vol 1,2, Novosibirsk, 1973.

9. Filippov, Ye. M. "Possibility of Using Neutron Methods to Determine Chlorine Content of Ocean Water," MORSKIYE GIDROFIZICHESKIYE ISSLEDOVANIYA, Sevastopol', No 2, 1977.

10. Filippov, Ye. M. "Possibility of Using Gamma-Radiation of Radiation Capture of Neutrons to Determine Chlorine Content of Sea Water under Full-Scale Conditions," MORSKIYE GIDROFIZICHESKIYE ISSLEDOVANIYA, Sevastopol', No 3, 1977.

11. Filippov, Ye. M. "Study of Possibility of Using Neutron Activation Method to Study the Velocity of Sea Water Currents," Ibid.

12. Khorn, R. "Morskaya khimiya" [Marine Chemistry], Moscow, Mir, 1972.

Received 4 May 1977

9035
CSO: 1870

GEOPHYSICS, ASTRONOMY AND SPACE

UDC 551.463.1:621.039.8

POSSIBILITY OF DETERMINING SEA WATER SALINITY AND DENSITY FROM GAMMA-RADIATION ATTENUATION

Sevastopol' MORSKIYE GIDROFIZICHESKIYE ISSLEDOVANIYA in Russian No 1, 1978 pp 90-97

[Article by Ye. M. Filippov]

Abstract. Based on calculations it is shown that when measurements are made with the help of radio isotope sources that emit about 10^{10} photon/s, and the nanosecond technique the soft scattered radiation of 30-60 keV will carry information on sea water salinity with accuracy 0.01-0.03%, while the hard radiation over 80-100 keV--on sea water density with error about $3 \cdot 10^{5}$ g/cm^3.

[Text] Publication [8] has shown that the technique based on gamma-radiation absorption (GRA) can be used to determine sea water density. This same technique in recording soft scattered radiation in the range 30-60 keV can be used simultaneously to determine the sea water salinity.

To determine the density of different substances usually sources of gamma radiation are used below 1 MeV. The main effects of their interaction with the substance are Compton scattering and photoelectrical absorption. The summary coefficient of gamma-radiation attenuation will be formed from the coefficients

$$\tau = \tau_k + \tau_\varphi = \mu_k \rho + \mu_\varphi \rho \quad \text{см}^{-1}, \qquad (1)$$

that determine these two effects of interaction between the gamma quanta and the substance.

The coefficient for the Compton attenuation of gamma quanta is defined from the ratio

$$\tau_k = n_e \sigma_k = \frac{N_0 Z}{A} \rho \sigma_k = N_0 \beta \rho \sigma_k = \mu_k \rho. \qquad (2)$$

Here $n_e = \frac{N_0 Z}{A}\rho = N_0 \beta \rho$ --number of electrons in a unit of substance volume; N_0--Avogadro number; $\beta = Z/A$--ratio of atomic number of chemical element Z to its atomic weight A; σ_k--effective cross section of gamma quanta scattering [2,3,6,7].

The expression for the linear coefficient of gamma radiation attenuation due to the photoeffect is defined from the ratio

$$\tau_\varphi = \frac{N_0 Z^m}{A}\rho\sigma_\varphi = N_0 Z^{m-1}\beta\rho\sigma_\varphi = \mu_\varphi \rho, \qquad (3)$$

where σ_φ--amount of effective cross section of gamma quanta attenuation in the substance due to the photoeffect [2, 3, 6, 7]. The size of the exponential factor m for the gamma quanta with energy 0.1, 0.2, 0.3, 0.4, 0.5 and 1.0 MeV adopts respectively the following values: 4.04, 4.20, 4.27, 4.33, 4.36 and 4.47.

For media with complicated chemical composition instead of β β_{cp} is introduced, and instead of the atomic numbers of the chemical elements--the effective atomic number [9]

$$Z_{э\varphi} = \sqrt[3{,}1]{\frac{1}{\beta_{cp}}\sum_{i=1}^{n}\rho_i \beta_i Z_i^{3{,}1}}, \qquad (4)$$

where $\beta_{cp} = \sum_{i=1}^{n}\rho_i \beta_i$; P_i--weighted concentrations of i-th element in studied medium; $\beta_i = Z_i/A_i$--ratio of atomic number of i-th element to its atomic weight.

For fresh water $\beta_{cp} = 0.555$, and for sea water with salinity 17.5 and 35‰ respectively 0.553 and 0.551. The relative difference in values $\delta\beta_{cp} = \frac{1}{\beta_{cp}(0‰)}\left[\beta_{cp}(0‰) - \beta_{cp}(35‰)\right]100 = 0{,}721\%$. The effective atomic number for fresh water $L_{э\varphi} = 7.45$, while for water with salinity 17.5 and 35‰ respectively 7.72 and 8.00.

The values of the mass coefficients of gamma-radiation attenuation for fresh water taken from reference [4] and computed for ocean water with salinity 35‰ are given in table 1. It is apparent from it that with $E_\gamma \geq 100$ keV there is practically no influence of the photoeffect. With $E_\gamma = 80$ keV the relative difference in the coefficients of gamma-radiation attenuation in fresh and ocean water $\delta\mu = \frac{1}{\mu(35‰)}\left[\mu(35‰) - \mu(0‰)\right]\times 100 = 1.1\%$ (see table 2), i.e., is located on the level of change in the value β_{cp} for these media, but opposite in sign. It follows from this that if sea water is irradiated with streams of gamma quanta of 100 keV and over, then from the data of recording radiation of 80 keV and over one can judge the density of the sea water, and

Table 1. Mass Coefficients of Gamma-Radiation Attenuation in Water, cm^2/g

E_γ (1) кэВ	Пресная (2) вода (0°/oo)			Океаническая (3) вода (35°/oo)		
	$\mu_к$	$\mu_ф$	μ	$\mu_к$	$\mu_ф$	μ
20	0,178	0,499	0,676	0,1766	0,6596	0,8362
30	0,183	0,131	0,314	0,1817	0,1763	0,3580
40	0,183	0,0499	0,233	0,1818	0,0686	0,2504
50	0,180	0,0238	0,204	0,1800	0,0326	0,2126
60	0,177	0,0131	0,190	0,1772	0,0172	0,1942
80	0,170	0,00502	0,175	0,1691	0,0071	0,1762
100	0,163	0,00240	0,165	0,1622	0,0033	0,1655
150	0,147	0,00085	0,148	0,1463	0,00098	0,1473
200	0,135	0,000256	0,135	0,1345	0,00038	0,1349
300	0,118	0,000070	0,118	0,1175	0,000106	0,1176
400	0,106		0,106	0,1053		0,1053
500	0,0966		0,0966	0,0962		0,0962
600	0,0895		0,0895	0,0892		0,0892
800	0,0786		0,0786	0,0783		0,0783
1000	0,0707		0,0707	0,0704		0,0704
1500	0,0573		0,0574	0,0571		0,0572

Key:
1. keV
2. fresh water
3. ocean water

from recording radiation under 80 keV--the salinity of sea water and the amount $\beta_{ср}$.

In practice studies of sea water are usually carried out in specific regions in which the limit of change in salinity is known. For each such region the $\delta\beta_{ср}$ will be very small (close to zero), while $\beta_{ср}$ can always be computed. The amounts $\delta\mu$ for such regions will also be very small, while μ is computed in advance.

The distribution in water of the scattered gamma-radiation from sources with different energy obtained by calculation is given in publications [2,6]. Book [3] gives the spatial-energy distribution of the scattered radiation for a cesium source (E_γ=661 keV) obtained experimentally.

In his work V. I. Utkin [5] cites the calculated spectra of gamma-radiation for the range 0-200 keV obtained in an approximation of continuous losses for media with effective atomic numbers from 6 to 13. By using these data the spectra were computed for fresh water and water with salinity 17.5 and 35°/oo (fig 1).

Table 2. Contribution of Photoeffect (%) to Complete Coefficient of Gamma-Radiation Attenuation in Water

(1) E_γ кэВ	(2) Пресная вода (0‰)	(3) Океаническая вода (35‰)	(4) Разность значений σ_μ
40	21,5	27,4	5,9
50	11,7	15,3	3,6
60	6,8	8,8	1,9
80	2,9	4,0	1,1
100	1,4	2,0	0,6
150	0,44	0,65	0,21
200	0,19	0,28	0,09
300	0,06	0,10	0,04

Key:
1. keV
2. fresh water
3. ocean water
4. difference of values

It is apparent from the figure that the spectrum obtained in the approximation of continuous losses (solid curve 1) agrees welll with the spectrum computed from the method of moments (dotted curve 1) for $\tau r=5$ [2]. At such distances and over, as shown in publication [3] the spectrum becomes equilibrium and completely identical. Therefore in determining the salinity of sea water the indicated distance will be the optimal.

Publication [2] presents the spatial-energy distribution of gamma-radiation with starting energy 255 keV. For this radiation $\tau=0.125$ cm^{-1}(water). The size of the mean length of the primary radiation in water $\lambda=\tau^{-1}=8$ cm. From $\tau r=5$ we obtain $r=5\ \lambda=40$ cm. Consequently, in determining the salinity of sea water the distance between the source with $E_\gamma=255$ keV and detector should be selected as equal to 40 cm. From the sources put out by the all-union association "Izotop" selenium-75 approaches the closest to the indicated value (T=120.4 days, E_γ=400 (16%), 304 (1.5%), 279 (29%), 264.5 (71%), 199 (1.8%), 136 (61%), 121 (20%), 97 (3.9%) keV, and others). As we see its most intensive is radiation of 130, 264.5 and 279 keV.

From the spectral distributions of gamma-quanta(fig 1) it is apparent that to determine the salinity of sea water it is best of all to record the scattered radiation in the range 30-60 keV. According to the data of publication [2] the radiation intensity for one incident quanta will be $I_0=5.51\cdot10^{-7}$ photon/s. Further in the calculations we will start from the parameters of the selenium source. Currently the all-union association "Izotop" is supplying sources with exposure dose power $1.2\cdot10^{-5}$ R/cm which can be placed in a lead container weighing about 6 kg. Such a source in the range ~100-400 keV emits $2.2\cdot10^{10}$ photon/s and corresponds to

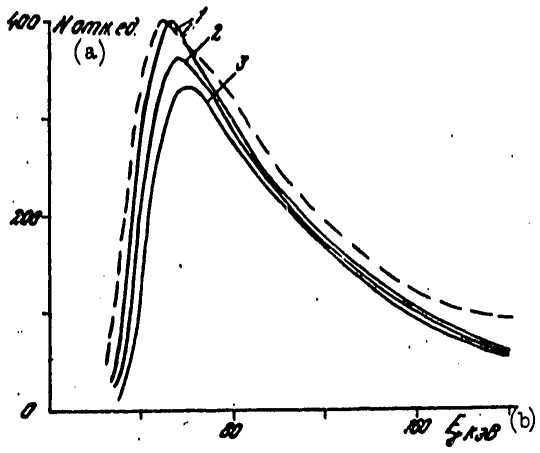

Figure 1. Spectra of Scattered Gamma-Radiation

Key:
1. for fresh water
2,3. for water with salinity 17.5 and 35‰
a. rel. unit
b. keV

51.5 mg·equiv Ra or 290 mCi. To record the radiation (in calculations) we use a plastic detector 40 mm in diameter and 100 mm high, i.e., the same as in publication [8]. The effectiveness of recording gamma quanta of 30-60 keV averages 0.5. As a result we obtain that with t=3 min the rate of calculation in fresh water will be $4.36 \cdot 10^7$ imp, in water with salinity 17.5‰ --$3.56 \cdot 10^7$ imp, and in water with salinity 35 ‰--$2.8 \cdot 10^7$ imp. Based on these data we obtain that salinity S=35‰ will be determined with error $\Delta S=0.00666$‰, $\Delta S_{пред}=3$, $\Delta S=0.020$‰, while salinity S=17.5‰--with errors $\Delta S=0.00294$‰, $\Delta S_{пред}=0.0088$‰. Calculation $3.04 \cdot 10^{10}$ imp with t=3 min will correspond to the energy range 80-255 keV. The error of determining the density is obtained from the ratio [8]

$$\Delta\rho = \frac{1}{\tau r\sqrt{N t A_y}} = \frac{1}{1 \cdot 1{,}745 \cdot 10^5 \cdot 0{,}65} = 8{,}85 \cdot 10^{-6}\ \text{g/см}^3 \quad (5)$$

From here $p_п=3 \cdot \Delta p=2.65 \cdot 10^{-5}$ g/cm^3. These amounts are obtained for r=λ= 8 cm, ε =0.43 P=40 cm^2 (2 detectors).

Thus, in creating an instrument with three scintillation gages the density of sea water can be determined with t=3 min with limit error $2.65 \cdot 10^{-5}$ g/cm^3, salinity--with limit errors 0.01-0.02 ‰. The density here is measured

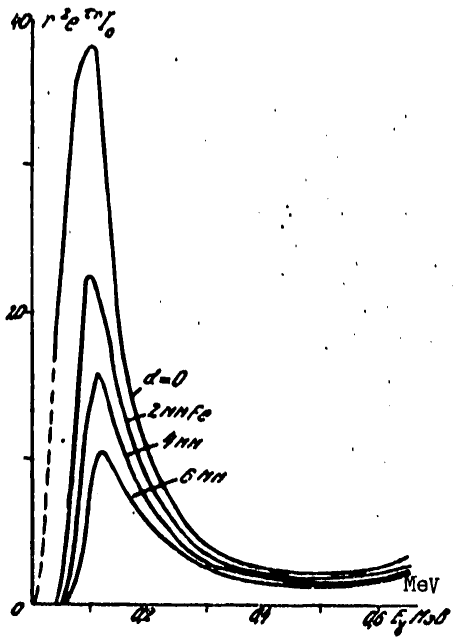

Figure 2. Spectrum of Cesium Source Recorded with Plastic Scintillator with Various Thicknesses of Steel (Iron) Housing

with the help of two scintillators placed at a distance of 8 cm from the source, and salinity--with the help of one detector placed at a distance of 40 cm. In measurements with cesium sources $8.77 \cdot 10^9$ photon/s (125 mg·equiv Ra) [8] with the help of a third detector set at r≈60 cm one can determine salinity with $\Delta S_{пред} = 0.014\text{-}0.032$ °/oo with t=3 min. The sea water density here is defined with $\rho_r = 3 \cdot 10^{-5}$ g/cm^3 with r=11.5 cm [8].

In the examined instruments in order to determine p and S highly stabilized systems are necessary with reference gamma radiators. A number of such works are described in publication [1]. In density measurements as a threshold system one can use the instrument housing. Figure 2 depicts the spectra of radiation that has passed through the housing of varying thickness. It is apparent that the intensity of the recordable radiation is reduced 10-fold as compared to the maximum for d=2 mm with E_γ=50 keV, for d=4 mm with E_γ = 65 keV and for d=6 mm with E_γ=70 keV. The indicated filters essentially do not distort the radiation in the hard section of the spectrum with $E_\gamma >$ 200 keV. Thus, in the densitometric gages the soft scattered radiation with $E_\gamma < 80$ keV can be suppressed by combining a metal filter (instrument housing) and electronic circuit. It is necessary to make the housing of the gages

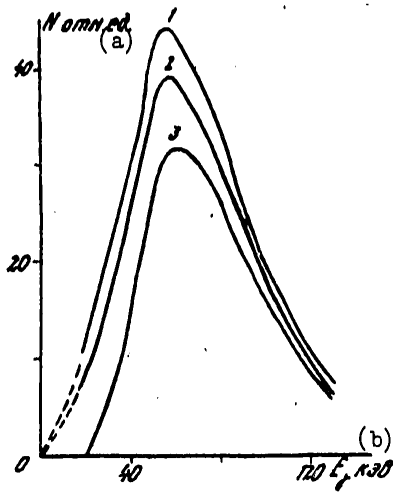

Figure 3. Equilibrium Spectrum of Scattered Gamma-Radiation

Key:

1. in water [3]
2,3. deformed by layers of absorber 5 mm thick made of plastic and duralumin
a. rel. unit
b. keV

for the "salinity" channel of light materials (fig 3) that are weak absorbers of soft radiation (plastic, duralumin, etc.). Measurements of the recordable radiation can be made with the help of intensimetric high-speed radiometers. In recording radiation with energy 30 keV and over a measurement will be made of the product of water salinity times density, while in recording hard radiation with energy $E_\gamma \geq 80$-100 keV--density. To exclude the effect of density on the channel of "salinity" one can use the approach of normalization for readings of the "density" channel $M = N_{сол}/N_{пл}$. Such approaches of measuring radiation are widely used in nuclear-geophysical studies and have shown good results [5,7]. The size of the ratio will depend only on the change in the salinity of water, i.e., $M = f(S)$. In relation to the fact that in the salinity channel rates of calculation are recorded on the order $2 \cdot 10^5$ imp/s, for measurement of such rates one can use inorganic scintillators of the type NaI(Tl) as well that have time of scintillation $2.5 \cdot 10^{-7}$ s. Here the radiation in the range 30-60 keV can be recorded with the help of a highly stabilized one-channel gamma-spectrometer, and in the density channel--with the help of a threshold highly stabilized nanosecond intensimeter.

BIBLIOGRAPHY

1. Gart, G. "Radioizotopnoye izmereniye plotnosti zhidkostey i binarnykh sistem" [Radio Isotope Measurement of Liquid Density and Binary Systems]. Moscow, Atomizdat, 1975.

2. Leupunskiy, O. I., et al. "Rasprostraneniye gamma-kvantov v veshchestv" [Spread of Gamma-Quanta in Substances], Moscow, Fizmatgiz, 1960.

3. Nelipa, N. F. "Vvedeniye v teoriyu mnogokratnogo rasseyaniya chastits" [Introduction to the Theory of Multiple Scattering of Particles], Moscow, Atomizdat, 1960.

4. Storm, E.; and Israel', Kh. "Secheniya vzaimodeystviya gamma-izlucheniya (spravochnik)" [Cross Sections of Interaction of Gamma-Radiation (Reference Book)], Moscow, Atomizdat, 1973.

5. Utkin, V. I. "Selektivnyy gamma-gamma-karotazh na ugol'nykh mestorozhdeniyakh" [Selective Gamma-Gamma-Logging on Coal Fields], Moscow, Nauka, 1975.

6. Filippov, Ye. M. "Prikladnaya yadernaya geofizika" [Applied Nuclear Geophysics], Moscow, Izd-vo AN SSSR, 1962.

7. Filippov, Ye. M."Yadernaya geofizika" [Nuclear Geophysics], Vol 1, Novosibirsk, Nauka, 1973.

8. Filippov, Ye. M, Lamanova, I. A.; and Doronin, I. F. "Question of Determining the Sea Water Density with Gamma-Radiation," MORSKIYE GIDROFIZICHESKIYE ISSLEDOVANIYA, Sevastopol', No 4, 1976.

9. Khaukovich, I. M., et al. "Effective Atomic Number of Inifinite Homogeneous Media with Sources of Gamma-Radiation," ATOMNAYA ENERGIYA, Vol 25, No 1, 1968.

Received 28 July 1977

9035
CSO: 1870

GEOPHYSICS, ASTRONOMY AND SPACE

UDC 621.317.725(088.8)

EXPERIMENTAL CHECK OF A BASELESS METHOD FOR MEASURING THE ELECTRICAL FIELD IN THE SEA

Sevastopol' MORSKIYE GIDROFIZICHESKIYE ISSLEDOVANIYA in Russian No 1, 1978 pp 157-163

[Article by Yu. P. Butrov, M. V.Panenko, Yu. L. Tsibul'skiy]

Abstract. Experiments with a baseless measuring system are described. It is shown that it is basically possible to eliminate the effect of an electrical field of induction while moving in a magnetic field. Causes for errors in the system operation are examined.

[Text] The method of measuring an electrical field in the sea with the help of spatially separated electrodes that form the base does not make it possible to exclude the electrical field of induction that is directed in the base conductor during its movement in the earth's geomagnetic field. Publications [1,2] theoretically substantiated the possibility of eliminating this deficiency if instead of a base the measuring system used a length of nonconducting surfaces (current fairings), while the electrodes were placed in the center of each side of the fairing. In such a measuring system the electrodes are geometrically superposed with accuracy to the thickness of the nonconducting surface, i.e., do not form a base, consequently, during the movement of the system in a geomagnetic field with the same accuracy the effect of the electrical field of induction is eliminated.

The purpose of the experiments was to investigate the effect on the measurement results of the movement of the system with current fairing in a geomagnetic field. For this a complex was set up (fig 1) to mechanically unite two measuring systems: polyethylene sheet fairing 1 with angular electrodes 3 symmetrically arranged on both of its sides, and control base 2 whose length corresponds to the size of the equivalent base of the fairing. The vertical position of the fairing is guaranteed with the help of float 5 and weight 4.

The synchronous realizations, one of which is illustrated in figure 2 present an idea of the reaction of each system to the rate of movement. On the recording obtained with the help of a base system the jump in voltage

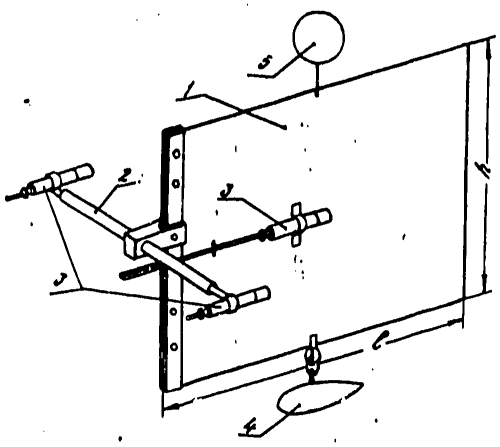

Figure 1. Complex for Comparative Study of the Effect of Velocity

is distinctly recorded when the towing velocity is included (fig 2,a) which indicates the application of electromotive force of induction in the base conductor when it intersects the magnetic force lines. In the measuring circuit with fairing there is practically no application of electromotive force of induction, and there are no jumps in voltage when the towing velocity is included in the recording. In individual cases an instability of the recording is observed, and the so-called aftereffect impulse of characteristic shape emerges (that shape as after the third engagement of towing on fig 2,b).

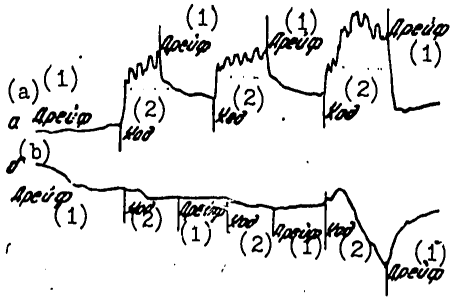

Figure 2. Model of Synchronous Recording of Voltage in Circuit

Key:

a. of electrodes of measuring base
b. of electrodes of fairing

1. Drift
2. Movement

The cited results confirm the basic possibility of excluding the electromotive force of induction with the use of lengths of a nonconducting surface instead of the base in a moving measuring system with electrodes.

Further a study was made without a control base. The towing of the system in different directions in calm weather and without currents made it possible to draw a conclusion on the independence of the recorded signal from a change in the course. In the presence of a current a signal was successfully modulated from an electrical field excited by the current and the movement of the measuring system in a circle. The amplitude of the obtained sinusoid is proportional to the horizontal component of the field intensity generated by the current. The latter confirms the possibility of using the rotating system with fairing to measure the intensity of the electrical field excited by the current, and consequently, to determine the current velocity. The creation of a measuring system that sinks with rotation would make it possible to determine the vertical epure of current velocities in the ocean.

The next experiments were directed towards revealing the different factors which could introduce errors into the operation of the system with fairing.

The dependence of the voltage in the circuit of the electrodes on their arrangement on the fairing was checked with the help of towing the fairing with the alternate advancing of each electrode. The asymmetry was ~25-30 cm. In a specific experiment of moving one of the electrodes ahead no anomalies were introduced into the recording. When another electrode was advanced an instability was observed in the recording each time towing was engaged: an impulse of aftereffect of characteristic shape developed as in figure 2,b. After the system stopped moving the electromotive force of the electrodes returned to the former value.

Thus, analogous impulses are observed under different experimental conditions. Therefore we should attempt to find the reasons for this phenomena.

We will examine the physicochemical processes that are possible here. When the nonconducting fairing is immersed in sea water, due to the adsorption of ions on each side of it a double electrical layer is formed, while in the adjacent liquid--a layer of free diffusion ions [3]. The average thickness of the ion-diffusion layer Δr and the contact voltage $\mathcal{E}_0$ depend on the water temperature and the concentration of substances dissolved in it, as well as on the material of the fairing (polar, neutral dielectric) whose electrochemical properties and surface condition can differ on two sides. Under such conditions even a strictly symmetrical arrangement of the electrodes does not guarantee the absolute identity of the electrical phenomena on both sides of the nonconducting surface.

The complete electrical charge of the ion-diffusion layer on one side with uniform distribution of the contact voltage $\mathcal{E}_{01}$ in accordance with [3] equals

$$e_1 = C_1 \mathcal{E}_{01} = \frac{\varepsilon S}{4\pi \Delta r_1} \mathcal{E}_{01}, \qquad (1)$$

c_1--capacitance; ε--electrical permeability of the liquid; S--area of one side of the fairing equal to $\ell \cdot h$ (figure 1). With the movement of the fairing relative to the stream of water with velocity V the diffusion layer is attracted by the moving liquid, a current of ions of one sign develops (for example, positive) J_+, proportional to velocity V. With regard for expression (1) the current J_+ can be written in the form

$$J_{+1} = \frac{e_1}{t} = \frac{chl}{4\pi\Delta r_1 t}\varepsilon_{01} = \frac{ch}{4\pi\Delta r_1} V\varepsilon_{01}, \qquad (2)$$

while the mean density of this current, depending on the width of fairing h and thickness of ion-diffusion layer Δr will equal

$$j_{+1} = \frac{J_{+1}}{h\Delta r_1} = \frac{ch}{h\Delta r_1 4\pi\Delta r_1} V\varepsilon_{01} = \frac{c}{4\pi\Delta r_1^2} V\varepsilon_{01}. \qquad (3)$$

On the other side of the fairing current J_{+2} with density j_{+2} correspondingly emerges. We present the fairing in a system of three mutually perpendicular planes P, Q and S. P--plane of the actual fairing; Q--plane passing through the center of the fairing and transverse to the stream of water during its horizontal movement; S--horizontal plane passing through the center of the fairing.

In the absence of symmetry of the adsorption processes on the two sides of the fairing relative to the plane P $J_{+1} \neq J_{+2}$ and $j_{+1} \neq j_{+2}$. Since the charges of one sign are carried away by water, on the front edge of the fairing a shortage of them develops and on the back edge--an excess, as a consequence of which a field of outside forces E is formed that is common to both sides. On each side it elicits equal inverse currents J_- with density

$$j_- = \gamma E, \qquad (4)$$

where γ--conductivity of sea water. The density of the inverse current

$$j_- = \frac{j_{+1} + j_{+2}}{2}.$$

By substituting this value in formula (4) and considering (3) we obtain

$$E = \frac{j_-}{\gamma}\left(\frac{eV\varepsilon_{01}}{2\cdot 4\pi\cdot\Delta r_1^2} + \frac{eV\varepsilon_{02}}{2\cdot 4\pi\Delta r_2^2}\right) = \frac{eV}{8\pi\gamma}\left(\frac{\varepsilon_{01}}{\Delta r_1^2} + \frac{\varepsilon_{02}}{\Delta r_2^2}\right). \qquad (5)$$

Thus the field E depends on the velocity V, the parameters of the current fairing and the sea water.

In the presence only of the indicated asymmetry the points of zero potential 01 and 02 are located in the center of each side of the sheet and the electrodes in them do not record the difference in potenitals.

With additional asymmetry relative to the plane P the points of zero potential are displaced realtive to the center different distances from plane Q, remaining in plane S. With the horizontal movement of such a nonconducting surface the electrodes arranged in the central points of the fairing sides record the difference in the potentials not equal to zero.

If there is asymmetry only in the planes P and S, then the points of zero potential 01 and 02 are displaced different distances from plane S, remaining in plane Q. Then the difference in the potentials of the electrodes with horizontal movement of the system equals zero, since in the field E the electrodes are located on the line of zero potential. Then the movement of the fairing along the vertical is accompanied by the emergence of a stationary field E_1 in which the difference in the potentials does not equal zero. Brief movement of the fairing along the vertical is possible at the initial moment of towing if there is a strong jerk.

With asymmetry in relation to three mutually perpendicular planes P, Q and S the difference φ_1 and φ_2 is recorded with horizontal movement, and $\varphi_1' - \varphi_2'$ with vertical (see figure 3).

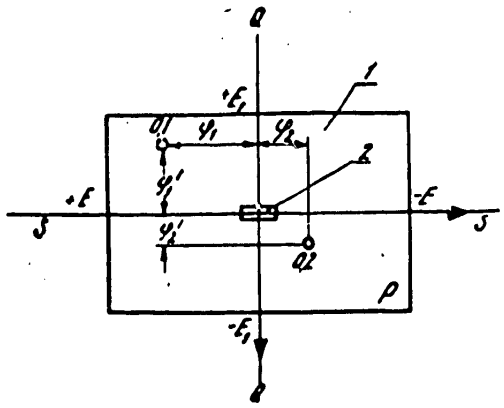

Figure 3. Example of Possible Arrangement of Points of Zero Potential on Two Sides of Fairing with Asymmetry of Adsorption Dynamics Relative to Planes P, Q and S

The advance of one of the electrodes in the aforementioned experiment artificially imitates the indicated asymmetry. The aftereffect impulse can be interpreted as a recording of the result of the summation of these differences $(\varphi_1 - \varphi_2) + (\varphi_1' - \varphi_2')$, which for the studied case had opposite signs. At the starting moment of movement when strong vertical jerks are possible, and the horizontal velocity has not yet reached a sufficient amount, and when the fields E and E_1 develop, according to the absolute value the second addend dominates (starting phase of the impulse). In the next period with

steady-state towing velocity and reduction in vertical jerks the first addend for the modulus rises, and the second is reduced. The top of the impulse--equality of two differences in potentials. In the absence of vertical jerks the field E_1, and consequently, the second addend $(\varphi_1' - \varphi_2')$ disappear, while the difference $(\varphi_1 - \varphi_2)$ continues to rise sometimes all the way until towing stops.

It would seem that with an increase by the water flow of all diffusion ions and the establishment of a stationary field E the indicated difference must be established on some definite level corresponding to the given towing velocity. Since sometimes this does not occur it is more likely to hypothesize that in the flowing water stream the properties of the surface of the nonconducting material are continuously altered. In any case the studies made show that the condition of dynamic equilibrium of adsorption during movement of the fairing in sea water is not always attained.

There can be other reasons for this phenomena, for example, the drop in temperature of the electrodes on different sides of the fairing. This will be discussed further.

Thus, the asymmetry of the adsorption processes significantly impairs the stability of recording and introduces great interferences. To diminish them it is necessary to make a fairing of neutral dielectrics that possess the maximum homogeneity of the adsorption processes over the entire surface, and high stability of the adsorption processes during the movement of the fairing at any velocity.

To select the material that possesses the listed properties to the greatest measure a number of tests were set up in which the behavior of different dielectrics in the role of current fairings was revealed. At the same time a check was made of the effect of the heterogeneity in the fairing materials and the electrode housings. Fairings were studied that were made of organic glass, polyethylene (neutral dielectric) and polyvinyl chloride plastic (polar dielectric) with electrodes in housings made of organic glass; in addition on the electrodes of the first two fairings polyethylene sleeves were applied. The indicated measuring systems were successively kept for a certain time in the sea with simultaneous recording of the voltage in the circuit of electrodes. The testing conditions were maintained as identical as possible for all the materials. In the beginning and end of each test the zero was recorded of the electrodes immersed in the vessel with sea water. The obtained realizations that are a recording of the change in the signal in time are reduced to the common level of zero of the electrodes. A comparative analysis of the curves shows that to make the fairing the most suitable material of the studied dielectrics is organic glass. The factor of the heterogeneity of the materials of the nonconducting surface and the electrode housings does not play an important role.

Thus, the key factor for the operation of the system is the material of which the fairing is made, and in the first place, the adsorption properties of this material.

A study of the effect of temperature on the system with fairing was made under laboratory conditions. Two electrodes separated by a thin nonconducting sheet were immersed into a vessel with sea water. The water was heated at first in turns at each electrode, then simultaneously at both electrodes. Continuous recording of the electromotive force of the electrodes in the process of the experiment made it possible to conclude that such heating does not influence the recorded voltage. With a sharp change in the water temperature at one electrode a jump in voltage is observed on the recording which is repeated with the opposite sign during analogous heating of the second electrode. A noticeable change in the voltage in the electrode circuit is observed already with a temperature difference on the order of 0.2-0.4°C. However it should be noted that when working with fairing under natural conditions the probability of any noticeable temperature drop in its electrodes is small. In such close points of the medium a difference in temperature is possible only with insufficient stabilization of the fairing along the vertical in the presence of a large vertical temperature gradient, which is possible, for example, in sunny weather in the near-surface water layer.

Based on the preliminary experimental studies it was confirmed that it is possible to exclude the effect of movement in a magnetic field of a system with current fairing on the measurement results of an electrical field in the sea obtained with the help of this system; the reasons were established for errors in the system operation with nonconducting fairing: asymmetry of the adsorption properties of the material on different sides of the fairing, a sharp rise in the instability of the adsorption properties of the fairing material in the flowing water stream, and drop in temperatures at the electrodes on different sides of the nonconducting surfaces; a conclusion was drawn on the possibility of using in subsequent experiments organic sheet glass that among the studie materials possesses the greatest stability of adsorption.

BIBLIOGRAPHY

1. Lopatnikov, V. I. "Problem of Measuring Electrical Field in the Ocean," MORSKIYE GIDROFIZICHESKIYE ISSLEDOVANIYA, Sevastopol', No 4, 1973.

2. Lopatnikov, V. I. "Parameters of Measuring Systems with Current Fairing," MORSKIYE GIDROFIZICHESKIYE ISSLEDOVANIYA, Sevastopol', No 2, 1974.

3. Krayev, A. P. "Osnovy geoelektriki" [Fundamentals of Geoelectrics], Moscow-Leningrad, Gostekhizdat, 1951.

Received 20 May 1977

9035
CSO: 1870

GEOPHYSICS, ASTRONOMY AND SPACE

UDC 551.46.08

CALCULATION OF AN EQUIVALENT BASE FOR A MEASURING SYSTEM WITH CURRENT FAIRING OF A RECTANGULAR FORM

Sevastopol' MORSKIYE GIDROFIZICHESKIYE ISSLEDOVANIYA in Russian No 1, 1978 pp 117-120

[Article by V. I. Lopatnikov, I. P. Stadnik, and A. S. Boguslavskiy]

Abstract. The theory and procedure for calculating the parameters of baseless measuring systems to investigate an electrical field in the sea are discussed. The algorithm and calculation results of the equivalent base for the system with rectangular current fairing are given. The calculation data can be used in the practice of hydrophysical research.

[Text] The problem of studying an electrical field in the sea with the help of instruments that drift together with the ship is solved on the basis of using baseless measurement fairing [1,2]. The most important parameters of the system with fairing of simple shape (circle, elliptical disk) are defined analytically [2]. When the indicated systems were put into practice it became necessary to employ fairings of diverse shape: in the form of a rectangle, piece of helicoid surface, etc. It is easy to see that the graduating operations to determine even individual parameters of such systems are very complicated, and in addition, inaccurate. The analytical methods are limited. Therefore in order to calculate the parameters of measuring systems with fairings of a certain shape it is expedient to involve numerical methods and modern computer technology.

Publication [3] presents a method of numerical solution for the general problem of fairing of a dielectrical sheet of arbitrary shape placed in a homogeneous current field. Based on this method we will examine the calculation of an equivalent base for a rectangular current fairing.

The boundary value problem for the potential φ that describes the fairing by the electrical current of nonconducting sheet S has the appearance

$$\begin{cases} \nabla^2\varphi = 0 & \text{outside S} \\ \dfrac{\partial\varphi}{\partial n} = 0 & \text{for S} \\ \varphi = \varphi_0 & \text{for} \end{cases} \qquad (1)$$

where φ_0--potential of homogeneous electrical field not excited by sheet S by which in the future will be meant rectangle with sides 2a and 2b.

We find the potential φ in the form of a sum of φ_0 and the potential of a double layer of density $\nu(P)$

$$\varphi(M) = \varphi_0(M) + \frac{1}{4\pi}\int_S \frac{\nu(P)(\vec{n}_P \vec{r}_{PM})}{r_{PM}^3} dS_P, \qquad (2)$$

where P--actual point of integration; M--point of observation; r_{pm}--distance between these points; $\vec{n}_p$--external perpendicular at point P to the surface of the rectangle. As shown in [3], the density of the double layer $\nu(P)$ is limited in all points of S.

We will break the integral in (2) into the following components:

$$\varphi(M) = \varphi_0(M) + \frac{\nu(Q)}{4\pi}\int_{\Delta S_Q} \frac{(\vec{n}_P \vec{r}_{PM})}{r_{PM}^3} dS_P + \frac{1}{4\pi}\int_{S-\Delta S_Q} \frac{\nu(P)(\vec{n}_P \vec{r}_{PM})}{r_{PM}^3} dS_P, \qquad (3)$$

where ΔS_Q--circle of small radius R with center at point Q on rectangle. In the first integral the amount $\nu(P)$ is taken out for the integral sign due to the insignificant amount of R and the limited nature of ν.

By differentiating (3) for the perpendicular to the rectangle and the limiting conversion with $M \to Q$ with regard for the second and third equalities in the system of boundary conditions (1) one can obtain an integral equation for the density of the double layer [3]

$$\nu(Q) = \frac{1}{2\pi}\int_{S-\Delta S_Q} \frac{\nu(P)}{r_{PQ}^3} dS_P + 2RE_{0z}. \qquad (4)$$

The solution to (4) can be obtained by the method of successive approximations. The convergence of the method for any small R is proved in [3].

By breaking the surface of the rectangle down into n squares from the side 2R we rewrite the integral in (4) in the form of a sum

$$\int\limits_{S-\Delta S_Q} \frac{\nu(P)}{r_{PQ}^3} dS_P = \sum_{i=1}^{i=n} \nu(P_i) \int\limits_{S_i} \frac{dS_P}{r_{PQ}^3} + \nu(Q) \int\limits_{S_Q-\Delta S_Q} \frac{dS_P}{r_{PQ}^3} . \qquad (5)$$

Here S_i--square with center at point $P_i\{x_i, y_i\}$. The index i traverses the values from 1 to n, with the exception of the number of point Q; $S_Q - \Delta S_Q$ -- area formed by the square S_Q with center at point $Q\{x_Q, y_Q\}$ minus the circle ΔS_Q. The integrals included in (5) permit the analytical expression

$$\int\limits_{S_i} \frac{dS_P}{r_{PQ}^3} = \frac{\sqrt{(x_i + R - x_Q)^2 + (y_i - R - y_Q)^2}}{(x_i + R - x_Q)(y_i - R - y_Q)} - \frac{\sqrt{(x_i + R - x_Q)^2 + (y_i + R - y_Q)^2}}{(x_i + R - x_Q)(y_i + R - y_Q)} +$$

$$+ \frac{\sqrt{(x_i - R - x_Q)^2 + (y_i + R - y_Q)^2}}{(x_i - R - x_Q)(y_i + R - y_Q)} - \frac{\sqrt{(x_i - R - x_Q)^2 + (y_i - R - y_Q)^2}}{(x_i - R - x_Q)(y_i - R - y_Q)};$$

$$\int\limits_{S-\Delta S_Q} \frac{dS_P}{r_{PQ}^3} = \frac{2(\pi - 2\sqrt{2})}{R}.$$

Thus, the integral equation (4) is replaced by a system of algebraic equations

$$\nu(Q_i) = \left(1 - \frac{2\sqrt{2}}{\pi}\right)\nu(Q) + \frac{R}{2\pi} \sum_{\substack{i=1 \\ i \neq i_Q}}^{i=n} \nu(P_i) \int\limits_{S_i} \frac{dS_P}{r_{PQ}^3} + 2R\ell_{0z} . \qquad (6)$$

Algorithm (6) is easily realized on a digital computer. The program of computations was compiled on the ALGOL-60 algorithmic language. Here mass values $\nu(P_i)$ were calculated for several rectangles with different ratio of sides and equivalent base $\ell_{экв}$ for current fairings of the same shape. The main property of the double layer potential

$$\varphi(Q) - \varphi(Q') = \nu(Q),$$

where points Q and Q' lie on different sides of the fairing plane produces a simple link between the size of the equivalent base and the density of this layer in the center of the fairing

$$\ell_{экв} = \frac{\varphi(Q) - \varphi(Q')}{\ell_{0z}} = \frac{\nu(Q_0)}{\ell_{0z}}.$$

The calculation results are expressed by curve 1 of the figure. Here along the x-axis the ratio is plotted for the sides of the rectangle $\frac{a}{b}$, and along

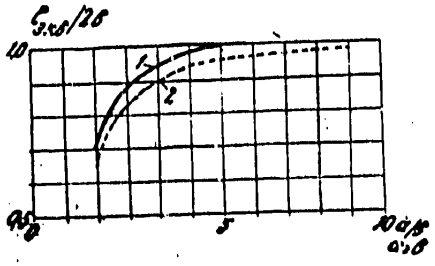

Figure. Dependence of Size of Relative Equivalent Base $\frac{\ell_{экв}}{2b}$ on Geometry of Fairing

Key:

1. For rectangle
2. For elliptical disk

the y-axis--the ratio of its equivalent base to the infinitely long band of width 2b. For comparison curve 2 is given which expresses the same relationship for fairings in the shape of an elliptical disk with semiaxes a and b. Curve 1 lies above curve 2, but does not intersect the straight line with ordinate 1 corresponding to the infinitely long band which expresses the direct dependence of the size of the equivalent base on the linear dimensions of the fairing.

From the value of the equivalent base one can determine also two other parameters in the system with current fairing: inner resistance and amplification factor for the current if the dimensions of the electrodes (size of the opening in the fairing in the case of a current system) are small as compared to the dimensions of the fairing [2].

The findings confirm the effectiveness of using numerical methods for calculating the parameters of measuring systems with current fairing, and can be used to put these systems into practice in measuring an electrical field in the sea. One should note however, that the convergence of the process of successive approximations for equations (4) and (6) is very delayed with a reduction in R. This results in an increase in machine time and is a shortcoming of the cited calculation method. The question of improving the convergence of the examined algorithm requires further studies.

BIBLIOGRAPHY

1. Lopatnikov, V. I. "Problem of Measuring an Electrical Field in the Ocean," MORSKIYE GIDROFIZICHESKIYE ISSLEDOVANIYA, Sevastopol', No 4, 1973.

2. Lopatnikov, V. I. "Parameters of Measuring Systems with Current Fairing," MORSKIYE GIDROFIZICHESKIYE ISSLEDOVANIYA, Sevastopol', No 2, 1974.

3. Stadnik, I. P. "Numerical Method for Solving the Problem of Fairing a Dielectrical Sheet by Direct Current," MAGNITNAYA GIDRODINAMIKA, No 2, 1977.

Received 7 September 1977

9035
CSO: 1870

PUBLICATIONS

INFORMATION NETWORKS AND THEIR ANALYSIS

Moscow INFORMATSIONNYYE SETI I IKH ANALIZ in Russian 1978 signed to press 7 Jun 78 pp 2, 213-220

[Annotation, table of contents and list of abstracts from book edited by A. D. Kharkevich and V. A. Germash, Izdatel'stvo "Nauka", 2,550 copies, 220 pp]

[Text] This collection deals with analysis and synthesis of information nets and individual elements. Questions of numerical analysis of certain queuing systems are discussed, and incomplete-access systems with a finite number of waiting positions and low load intensities are analyzed. The results of load measurements in rural communication networks are presented, the work of certain computer networks, particularly ring structures, are described, the synthesis of digital communication network structures is discussed, and the operation of information distribution devices, e.g. spatially rearrangeable switching networks with pulse time division of channels and with loop connections, nonordinary one-time [razovyy] switching systems and systems in homogeneous networks, are analyzed. Nodal switching systems are matrix switching units are discussed.

The collection is intended for specialists dealing with questions of the design of communications networks and switching units in information distribuyion systems and the operation of various types of queuing systems.

Contents Page

A. M. Gersht and A. B. Mitnitskiy. The Influence of Abrupt Changes in Input Flow Intensity on the Effectiveness of Tandem Operation..... 3

L. G. Ionin. Investigation of Irreversible States of Queuing Systems with Repeated Calling and a Finite Number of Sources..... 13

M. A. Shneps-Shneppe and S. N. Stepanov. Some Relationships for Systems with Repeated Call Attempts..... 26

Yu. M. Kornyshev and A. M. Zelinskiy. Analysis of the Status of Subscriber Lines..... 31

M. A. Shneps-Shneppe and A. V. Arutunyan. Optimal Incomplete-Access Systems with a Finite Number of Waiting Positions Under Minimal Load Intensities..... 37

A. I. Gromov and V. A. Naumov. An Approximate Method for Study of Multiphase Systems..... 46

S. N. Stepanov. Iteration Methods for Numerical Calculations on Queuing Systems..... 51

B. S. Tsybakov. Current Status and Prospects of Utilization of Computer Networks..... 57

L. V. Andreyev. Some Ring Data Transmission Networks..... 67

Ya. L. Shreyberg. Some Results of Statistical Analysis of the Operation of a Computer Center..... 76

N. P. Nikiforov and A. M. Svetlitskiy. A Method for Synthesis of the Optimal Structure of a Digital Interexchange Communication Network... 86

A. I. Krapiva. On Identification of Independent Trees of a Graph in Problems of Communications Network Viability..... 99

Ya. V. Fidlin and V. S. Shul'ga. Optimization of Spatially Rearrangeable Switching Networks with Pulse Time Division of Channels..... 105

G. G. Morozov and Ya. V. Fidlin. Digital Switching Networks with Loop Connections..... 110

M. P. Zyuz'ko and L. A. Shor. Nonblocking Systems for Nonordinary Switching..... 129

L. A. Shor. Nondisjoint Systems for Nonordinary One-Time Switching..... 132

N. I. Vitiska. Multistage Systems for One-Time and Nonordinary Switching with an Arbitrary Number of Disjoint Inputs and Outputs..... 135

V. A. Garmash and V. A. Shmelev. A Switching System with Unreliable Relays..... 140

Ye. O. Naumova. Iterative Construction of Nodal Switching Systems..... 144

Ye. O. Naumova. Estimation of the Blocking Probability of Some Nodal Switching Systems..... 148

A. P. Kiselev. A Method for Switching Two-Pole Elements in a Homogeneous Computer Medium..... 154

V. A. Shmelev, V. A. Garmash and V. D. Shershukov. A Matrix Unit for Contact Switching..... 162

N. I. Artyukhin. Control of One-Time Switching Systems with an Arbitrary Number of Arriving Demands..... 169

A. A. Podol'skiy and D. S. Shitova. The Question of Controlling Main Distribution Frame Switching..... 178

V. D. Vitchenko. Estimation of Relative Complexity of Integral Digital Communication Network Switching Nodes Constructed with Structurally Equivalent Switching Units..... 187

S. G. Sitnikov. On One-Time Switching Systems with Blocking..... 193

M. F. Shimko. Analysis of Characteristics of Aggregated States of a Group of Channels..... 198

Yu. A. Baklanov and A. D. Kharkevich. A Graphic Model of a System for Collection of Information on the Quality of Call Service in a Switching Center..... 202

Abstracts

A. M. Gersht and A. D. Mitnitskiy. The Influence of Abrupt Changes in Input Flow on the Effectiveness of Tandem Operation.

The question of determining effectiveness of tandem routes with a nonstationary (jump-type) flow is studied. The results are compared with the stationary case. Bibliography, 6 items.

G. L. Ionin. Investigation of Irreversible States of Queuing Systems with Repeated Calling and a Finite Number of Sources.

A theorem on the transition of the system described to an irreversible state in which service is impossible is proven. A method for calculating the average time for transition to the irreversible state is discussed and illustrated with examples. Tables, 4; illustrations, 5; bibliography, 4 items.

M. A. Shneps-Shneppe and S. N. Stepanov. Some Relationships for Systems with Repeated Call Attempts.

A model of a complete-access grading which gives the best approximation of subscriber behavior and leads to a system of equations which are easily solvable by computer is discussed, and relationships between the main probabilistic characteristics of the model are presented. Illustrations, 1; bibliography, 7 items.

Yu. N. Kornyshev and A. M. Zelinskiy. Analysis of the Status of Subscriber Lines.

A mathematical model describing the busy and no-answer conditions of a subscriber who is called is discussed. Formulas for the main service quality characteristics are derived and an analysis of measurement results is made. Tables, 2; bibliography, 4 items.

M. A. Shneps-Shneppe and A. V. Arutunyan. Optimal Incomplete-Access Systems with a Finite Number of Waiting Positions Under Minimum Load Intensities.

A theorem asserting that when load intensity tends to zero the optimal incomplete-access system in terms of loss probability, with a finite number of waiting positions, should contain the maximum number of individual lines is proven. Illustrations, 2; bibliography, 4 items.

A. I. Gromov and V. A. Naumov. An Approximate Method for Study of Multiphase Systems.

An approximate method for study of multiphase queuing systems which can be described by Markov processes with a finite number of states is proposed. The basis of the method of the method is expressions satisfying the stationary probabilities of states of two-phase systems. The precision of the method is illustrated for certain 3- and 5-phase queuing systems. Tables, 1; illustrations, 2; bibliography, 7 items.

S. N. Stepanov. Iteration Methods for Numerical Calculations on Queuing Systems.

The convergence of iteration methods for numerical solution of systems of equations for statistical equilibrium is discussed, the speed of convergence of the iteration process is studied, and practical methods of accelerating convergence are examined. Illustrations, 1; bibliography, 4 items.

V. S. Tsybakov. Current Status and Prospects of Utilization of Computer Networks.

The current status and trends in the development of computer networks in the West is discussed. The two most important network configurations are considered: the configuration with a centrally-located computer center and the configuration with a centrally-located trunk network. The hardware which made construction of the networks possible is described: high-speed communication and digital transmission lines, packet switching and adaptive route selection. Some existing networks and the tasks performed by them are described. In conclusion, the main stimuli to use of computer networks are identified. Illustrations, 5; bibliography, 15 items.

L. V. Andreyev. Some Ring Data Transmission Networks.

Mathematical models of ring-type data transmission networks are discussed. Such networks consist of a single central exchange and several terminals connected by a communication line. Data are brought from the terminals to the central exchange and from the central exchange to the terminals, with the first type of data having priority. Not more than a single message may be transmitted at one time on each section of the line. Accordingly, some data must be delayed at intermediate exchanges while more important messages pass through. The number of waiting positions for each exchange does not appear to be limited. Stationary queue length distributions are found for each exchange and for each message delay time in the network. Illustrations, 1; bibliography, 10 items.

Ya. L. Shreyberg. Some Results of Statistical Analysis of the Operation of a Computer Center.

On the basis of various statistical data that have been collected, the article analyzes the distribution of the incoming flow of orders reaching a specific computer center and the service time for random values. It is shown that the computer system in question can be studied as a queuing system with a recurrent input flow and an exponential service time. A number of other statistical results are obtained, and recommendations for organization and analysis of computer operations are given. Tables, 3; illustrations, 4; bibliography, 6 items.

N. V. Nikiforov and A. M. Svetlitskiy. A Method for Synthesis of the Optimal Structure of a Digital Interexchange Communication Network.

This article presents a method for synthesis of structures for digital interexchange communication networks which are optimal in terms of capital expenditures, based on transmissions with pulse code modulation which have been developed and put into use. Bibliography, 7 items.

A. I. Krapiva. On Identification of Independent Trees of a Graph in Problems of Communication Network Viability.

Machine algorithms for determining the number of k-dependent trees of a nonoriented graph are presented, along with a theorem on the maximum number of k-dependent trees of the graph and an algorithm for synthesis of graphs whose degree is not less than a value sepcified in advance. Bibliography, 5 items.

Ya. V. Fidlin and V. S. Shul'ga. Optimization of Spatially Rearrangeable Switching Networks with Pulse Time Division of Channels.

An algorithm for optimization of multistage spatially rearrangeable digital multiplexed and supermultiplexed switching systems for special optimization functions which are not necessary proportional to the number of switching points is given. Numerical results are given for specific equipment and cost functions. Tables, 1; illustrations, 2; bibliography, 2 items.

G. G. Morozov and Ya. V. Fidlin. Digital Switching Networks with Loop Connections.

Methods of using loop connections in digital switching sysetms both for the creation of bypass routes and for secondary multiplexing of the switching systems are discussed. A noniterative method for calculating loss probabilities which is suitable not only for space-time systems but also for nonmatrixed systems is discussed. A comparative analysis of a number of methods for calculating losses is made and the corresponding computational equations for a three-stage switching system with loop connections, variable delays and a space-time distribution of channels is given. Illustrations, 8; bibliography, 17 items.

M. P. Zyuz'ko and L. P. Shor. Nonblocking Systems for Nonordinary Switching.

The article discusses switching systems which allow, with identical making and breaking of connections, the connection of any specified input to several outputs. Structural parameters of such systems are optimized for limited quantities of simultaneous connections proceeding from a single input and for the total number of simultaneous connections. Bibliography, 3 items.

L. A. Shor. Nondisjoint Systems for Nonordinary One-Time Switching.

It is shown that if switching points are placed between two adjoining outputs in a disjoint system for ordinary one-time switching, and the inputs are considered as terminals, i.e. as both inputs and outputs, it is converted into a nondisjoint system for nonordinary one-time switching. Illustrations, 3; bibliography, 2 items.

N. I. Vitiska. Multistage Systems for One-Time and Nonordinary Switching with an Arbitrary Number of Disjoint Inputs and Outputs.

Methods for design of multistage systems working in the one-time switching mode and making possible any connection between one of 10 system inputs and an arbitrary subset of outputs without blocking are considered. The parameters which require a minimal number of switching elements for the one-time and nonordinary switching system structures which have been obtained are determined and formulas for estimation of expenditures on switching equipment are found. Illustrations, 4; bibliography, 4 items.

V. A. Garmash and V. A. Smelev. A Switching System with Unreliable Relays.

A method for designing a switching unit which is resistant to k-fold failures is described. The system has k/n times as many switching points as a system based on the Shannon-Moore method, where n is the number of switching network inputs and outputs. Illustrations, 4; bibliography, 2 items.

Ye. O. Naumova. Iterative Construction of Nodal Switching Systems.

The design of multilayer switching structures based on application of the iteration method to planar nodal switching circuits is described. Formulas for calculation of the main structural parameters of iteration systems are given. Illustrations, 2; bibliography, 2 items.

Ye. O. Naumova. Estimation of the Blocking Probability of Some Nodal Switching Systems.

A method for finding the upper and lower bound for determination of blocking probabilities of single-connection and k-connection planar non-disjoint nodal switching systems consisting of similar elements is given. Computational formulas are obtained by using the method of probability graphs. Illustrations, 8; bibliography, 3 items.

A. P. Kiselev. A Method for Switching Two-Terminal Elements in a Homogeneous Computer Medium.

It is proposed to use spatially staged switching systems to connect homogeneous two-terminal simulating computer elements of the medium among themselves. Estimates of the maximum recovery chain for the graph are made, and these are used to extablish a priority of two-terminal elements, making it possible to decrease switching unit size. Illustrations, 3; bibliography, 11 items.

V. A. Shemelev, V. A. Garmash and V. D. Shershukov. A Matrix Unit for Contact Switching.

Expressions for the ratio γ of noise to useful control signals in a two-dimensional matrix with multicoordinate control as a function of the number of groups of independent control windings and circuits operating the switched element are presented. The distribution of the magnetic field within a matrix with three-coordinate control is discussed, the nonuniformity of the magentic field within windings of various groups is determined, and a distribution of magnetic-controlled contact elements in the matrix is chosen. Formulas which make it possible to obtain the necessary relationships between currents in the windings for different coordinates so as to assure a specified value for γ and to estimate the deviation of the latter are presented. Illustrations, 3; bibliography, 5 items.

N. I. Artyukhin. Control of One-Time Switching Systems with an Arbitrary number of Arriving Demands.

Nonblocking algorithms for establishing connections in nonsymmetrical one-time switching circuits with truncated switching units in four-stage systems with limiting and with an arbitrary number of incoming demands are developed. Illustrations, 2; bibliography, 8 items.

A. A. Podolskiy and D. S. Shitova. The Question of Controlling Main Distribution Frame Switching.

The problems associated with control of main distribution frame switching systems are considered. A method for separate control of the capacity of groups of power lines within a branch and the establishment of bypass routes is proposed. Tracking of the number of free lines in the group is implemented in order to determine the necessity of reswitching power lines. Illustrations, 3; bibliography, 8 items.

V. D. Vitchenko. Estimation of Relative Complexity of Integral Digital Communication Network Switching Nodes Constructed with Structurally Equivalent Switching Units.

The design of a switching unit in a digital communication network using switching units constructed from non-controlled time-coordinate converters is discussed. An equation for the relative complexity of the switching system in question in comparison with switching systems constructed with switching units with controllable time-coordinate converters is obtained. An example of the comparison is given. Tables, 2; illustrations, 6; bibliography, 2 items.

S. G. Sitnikov. On One-Time Switching Systems with Blocking.

The causes of production of blocks in one-time switching systems with limitation and without limitation of the number of simultaneous connections are studied. Most detailed consideration is given to blocking resulting from the use of simplified algorithms and procedures for making connections. Illustrations, 3; bibliography, 14 items.

M. F. Shimko. Analysis of Characteristics of Aggregated States of a Group of Channels.

Possible methods of representing a group of channels in a network with dynamic control are discussed. The relationships between the length of time spent by groups of various capacity in aggregate states are given for a wide range of losses, along with expressions for the frequency of change of these states. An analysis of the results obtained is given. Illustrations, 4; bibliography, 4 items.

Yu. A. Baklanov and A. D. Kharkevich. A Graphic Model of a System for Collection of Information on the Quality of Call Service in a Switching Center.

The quality indicators for servicing of calls by switching center automated control equipment are studied. A graphic model of a system for collection

and analysis of information on the quality of servicing which is used to determine the required quality indicators is proposed. Tables, 3; illustrations, 3; bibliography, 3 items.

8480
CSO: 1870

PUBLICATIONS

LIST OF SOVIET ARTICLES DEALING WITH COMPOSITE MATERIALS

Moscow GOSUDARSTVENNYY KOMITET SOVETA MINISTROV SSSR PO NAUKE I TEKHNIKE. AKADEMIYA NAUK SSSR. SIGNAL'NAYA INFORMATSIYA. KOMPOZITSIONNYYE MATERIALY, Vol 3, No 21, 1978 pp 3-4

[Following is a listing of the Soviet entries from SIGNAL'NAYA INFORMATSIYA. KOMPOZITSIONNYYE MATERIALY (SIGNAL INFORMATION. COMPOSITE MATERIALS), a bibliographic publication of VINITI. This listing is from Vol 3, No 21, 1978]

[Excerpts]

1. Influence of annealing on the structure and compatibility of tungsten fluoride with structural graphite on a sublayer. Yemyashev, A. V., Slavgorodskaya, Z. V., Martynov, S. Z., "Konstrukts. materialy na osnove ugleroda" 1978, No 13, 70-78.

2. On the kinetics of phase growth in a diffusion layer between solid and molten metals. Pimenov, V. N., "Fiz. i khimiya obrabotki materialov," 1978, No 4, 58-63.

3. Influence that the strength of the bond between fiber and matrix has on the nature of destruction of a composite material reinforced with brittle boron fibers with a metal matrix of aluminum alloys. Shorshorov, M. Kh., Kolesnichenko, V. A., Yusupov, R. S., Ustinov, L. M., "Fiz. i khimiya obrabotki materialov," 1978, No 4, 117-123.

4. Investigation of the influence that processes of interaction of a melt with a substrate have on the kinetics of gallium flow over the surface of thin silver films. Grebennik, I. P., Langkhammer, Kh., Shipkova, I. G., "Fiz. i khimiya obrabotki materialov," 1978, No 4, 75-80.

5. A solder for diamonds, El'bor borazon material and other superhard materials. Naydich, Yu. V., Kolesnichenko, G. A., Zyukin, N. S., Kostyuk, B. D., "Svaroch. pro-vo," 1978, No 7, 21-23.

6. Determining temperature stresses in metal-plastic parts. Ushakov, B. N., "Sb. tr. MVTU im. N. E. Baumana," 1978, Vol 16, 3-11.

7. P. Joining dissimilar hard-to-weld materials. Dubovik, A. S., Osipov, A. A., USSR Author's Certificate (B 23 K 11/10), No 573293, filed 14 Apr 76, No 2348940, published 27 Oct 77.

8. Morphological stability of thin films on reinforcing fibers. Gol'diner, M. G., Mazur, V. A., Malinovskiy, T. I., Yagubets, A. N., "Fiz. i khimiya obrabotki materialov," 1978, No 4, 112-116.

9. Durability of AG-4s fiberglass plastic with bending in sulfuric acid. Shevchenko, A. A., Krasovitskiy, A. S., Starikov, V. P., "Fiz.-khim. mekh. materialov," 1978, Vol 14, No 4, 121-122.

10. On the influence that the geometry of initial mesh elements has on the properties of high-porosity fiber material. Zorin, V. A., "Polucheniye i issled. svoystv novykh materialov," Kiev, 1978, 153-156.

6610
CSO: 1870

PUBLICATIONS

LIST OF SOVIET ARTICLES DEALING WITH COMPOSITE MATERIALS

Moscow GOSUDARSTVENNYY KOMITET SOVETA MINISTROV SSSR PO NAUKE I TEKHNIKE. AKADEMIYA NAUK SSSR. SIGNAL'NAYA INFORMATSIYA. KOMPOZITSIONNYYE MATERIALY, Vol 3, No 23, 1978 pp 3-6

[Following is a listing of the Soviet entries from SIGNAL'NAYA INFORMATSIYA. KOMPOZITSIONNYYE MATERIALY (SIGNAL INFORMATION. COMPOSITE MATERIALS), a bibliographic publication of VINITI. This listing is from Vol 3, No 23, 1978]

[Excerpts]

1. On terminology and classification in the field of composite materials. Solomin, N. V., "Poroshk. metallurgiya," 1978, No 7, 102-103 (English abst.).

2. On the classification of composite materials. Pshanin, N. P., "Poroshk. metallurgiya," 1978, No 8, 102-103 (English abst.).

3. Interaction of tungsten fibers with cobalt-based matrices. Mirotvorskiy, V. S., Ol'shevskiy, A. A., "Poroshk. metallurgiya," 1978, No 7, 57-64 (English abst.).

4. Influence that surface treatment has on the properties of carbon fibers and plates based on them. Kobets, L. P., Polyakova, N. V., Kuznetsova, M. A., Kolyasinskaya, O. B., Samoylov, V. S., Bondarenko, N. V., "Mekh. polimerov," 1978, No 4, 579-582.

5. P. A method of butt-melt welding titanium and its alloys to high-temperature stainless steels and alloys. Poplavko-Mikhaylov, M. V., Strizhevskaya, L. G., Starova, L. L., Zhuravleva, L. B., Kulikov, F. R., Sorokin, S. Ya., Karev, V. F., Berlin, M. Ye., USSR Author's Certificate (B 23 K 35/32), No 280719, filed 28 Jul 69, No 352930, published 28 Oct 77.

6. Accounting for initial heat stresses in studying the energy capacity of flywheels made by winding composites. Portnov, G. G., Kulakov, V. L., "Mekh. polimerov," 1978, No 4, 615-620.

7. Inelastic properties of composite materials. Mechanics. "Novoye v zarubezh. nauke," 1978, No 16, 295 pp w/illus.

8. On the development of microinhomogeneous plastic deformation in laminar composites. Yavor, A. A., Mukhin, V. N., Abdrazakova, N. A., "Izv. AN SSSR. Metally," 1978, No 4, 157-160.

9. Fatigue fracture of a laminar composite. Anishchenkov, V. M., Mileyko, S. T., "Dokl. AN SSSR," 1978, Vol 241, No 5, 1068-1069.

10. Viscoelastic stresses of temperature shrinkage in linearly reinforced media. Popov, A. I., Kuznetsov, S. V., "Mekh. polimerov," 1978, No 4, 737-740.

11. Determination of characteristic volumes of regular composites by the method of photoelasticity. Kosheleva, A. A., "Vestn. LGU," 1978, No 13, 86-91 (English abst.).

12. Influence that the rate of heating has on thermal deformation of carbon-metal plates in different media. Tret'yachenko, G. N., Gracheva, L. I., "Probl. prochnosti," 1978, No 8, pp 68-71.

13. On the question of optimum arrangement of the reinforcing in plates. Nemirovskiy, Yu. V., "Mekh. polimerov," 1978, No 4, 675-682.

14. Investigation of the mechanical characteristics of a composite material with volumetric structure. Pichkhadze, G. P., "Mekh. polimerov," 1978, No 4, 621-624.

15. X-ray extinction determination of the diameter of silicon carbide whiskers. Shchetanov, B. V., Gorobets, B. R., Chernyak, A. I., Kondratenko, A. V., "Zavodsk. lab.," 1978, Vol 44, No 7, 827-828.

16. On the problem of studying the strength properties of carbon fibers based on polyacrylonitrile fibers by ultrasonic methods. Kotosonova, V. Ya., Perepenko, I. I., Frolov, V. I., "Mekh. polimerov," 1978, No 4, 724-728.

17. Influence that crystallization rate and heat treatment have on the structure and properties of eutectic Cu-Cu_2Zr composite. Somov, A. I., Sverdlov, V. Ya., Tikhonovskiy, M. A., Oleksiyenko, M. M., "Fiz. i khimiya obrabotki materialov," 1978, No 4, 124-129.

18. Investigation of the kinetics of crystallization of two contacting ingots. Solov'yev, V. V., Sokolov, L. A., "Izv. AN SSSR. Metally," No 4, 102-104.

19. P. A cladding layer plate for composite ingots. Shevbunov, E. V., Ovsyannikov, V. G., Butorin, V. I., Tokarenko, A. A., USSR Author's Certificate (B 22 D 17/20), No 579096, filed 22 Dec 75, No 2199935, published 20 Nov 77.

20. A device for making cylindrical sandwich specimens based on Syntact foam. Lipatov, Ye. A., Kanovich, M. Z., Levanova, T. A., "Zavodsk. lab.," 1978, Vol 44, No 7, 887-888.

21. On filtration of a polymer binder in the setting process. Murzakhanov, R. Kh., "Mekh. polimerov," 1978, No 4, 740-742.

22. Chemical heat treatment of two-layer nickel-chromium composite electrolytic coatings. Arkharov, V. I., Yar-Mukhamedov, Sh. Kh., "Fiz. tverd. tela (Kiev-Donetsk)," 1978, No 8, 66-70.

23. Low-cycle fatigue of a composite material with dispersed filler under cyclic compression. Filyanov, Ye. M., Shchedrov, A. K., "Mekh. polimerov," 1978, No 4, 653-657.

24. Particulars of tensile tests of high-strength unidirectional composites. Zhigun, I. G., Mikhaylov, V. V., "Mekh. polimerov," 1978, No 4, 717-723.

25. Determination of conditions of joint plastic deformation of the components of bimetallic wire with a soft coating. Tuktamyshev, I. Sh., Shchegolev, G. A., "Tekhn. progress v metizn. pr-ve (Moscow)" (formerly "Metizn. pr-vo"), 1978, No 17, 21-24.

26. K. Insoluble lead-based alloy anodes. Dunayev, Yu. D., Alma-Ata, Nauka, 1978, 316 pp, w/illus.

27. Electroslag surfacing of a small blast furnace bell with composition alloy. Shekhter, S. Ya., Reznitskiy, A. M., Lazarenko, Yu. N., Razinskiy, V. V., "Avtomat. svarka," 1978, No 8, 43-44, 47.

6610
CSO: 1870

END